Tohoku University's Chemistry Summer School 2013

August 28th -31st, Sendai, Japan

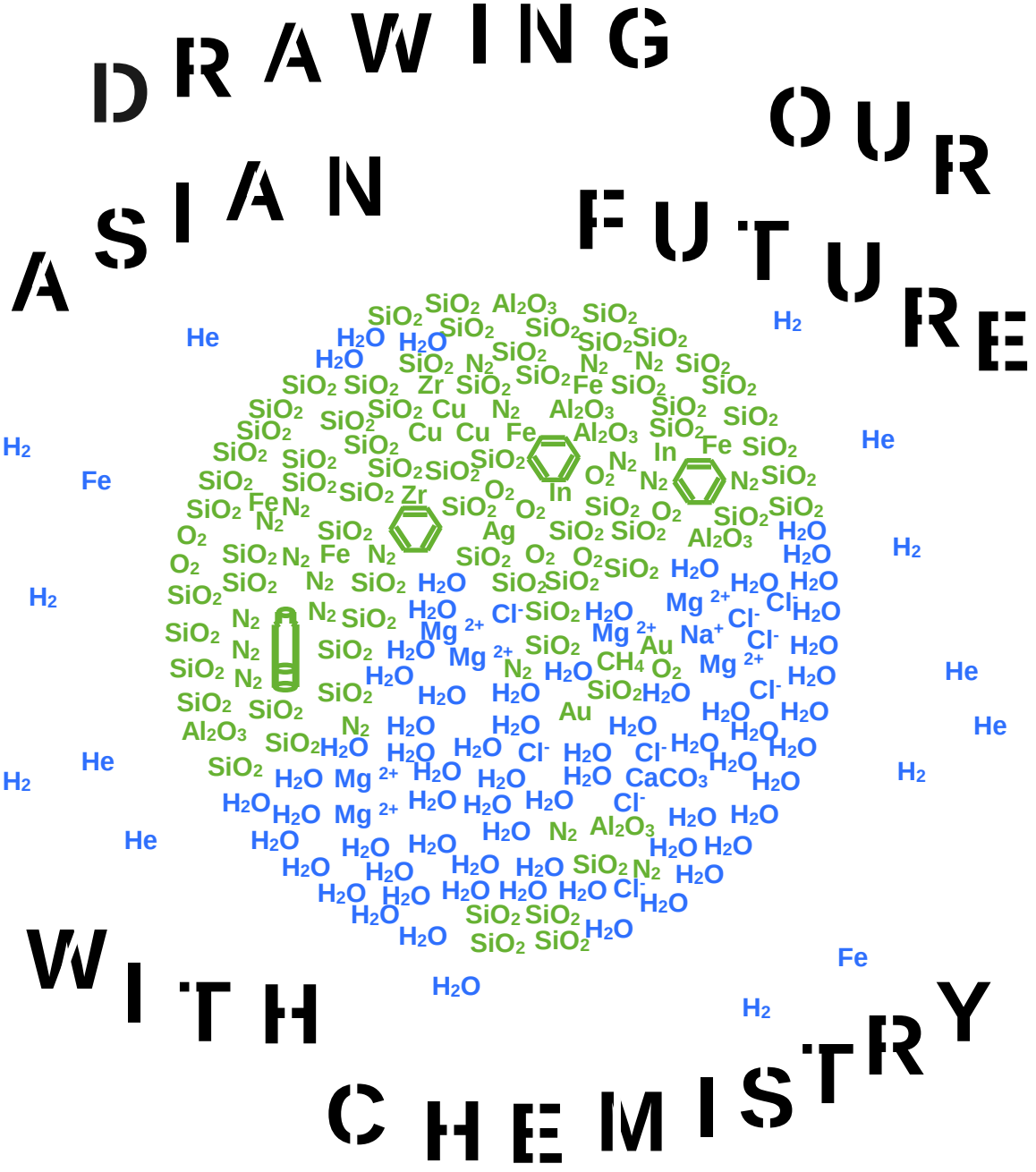

キャンパスアジア主催・分子科学会協賛

http://iremc.pharm.tohoku.ac.jp/~campusasia/SUSC.html

Introduction

Excellent human resources with a mind of wide international scope are quite precious in Japan and many other countries in the world. The role of higher education is to nurture students in such a way that they will be highly motivated to tackle and solve various complicated problems in the society using the knowledge and experience acquired during their university years. I believe that excellent opportunities of collaboration with international students should be quite valuable for the students to nurture such minds during their period spent in the university.

Tohoku University holds the International Summer School in the field of chemistry every year. This Summer School started in 2008 with the support of Global COE (Center Of Excellence) Project, and the CAMPUS ASIA Program succeeded to this summer school since 2012. The CAMPUS ASIA Program supports international student exchange among 6 universities, including Tohoku University, Nagoya University, Shanghai Jiao Tong University, Nanjing University, Seoul National University and POSTECH. This summer school invites students from many other universities beyond the CAMPUS ASIA members to encourage internationalization of education and research.

This Summer School is one of the important events in the schools and institutes related to chemistry in Tohoku University. We are happy to greet our guests from abroad, as well as encourage all Japanese participants to enjoy the atmosphere of free exchange of ideas and international cooperation. We would like to invite Japanese and overseas graduate students with energetic and highly motivated minds to participate in this Program as the first step towards becoming genuine leaders in society who can forge their countries' future. It should also be emphasized that we, all the faculty members involved in the Program would like to express our determination to ensure that all possible support will be provided for the young people in their efforts for becoming highly qualified specialists in their fields with invaluable experience of international cooperation.

Akihiro Morita

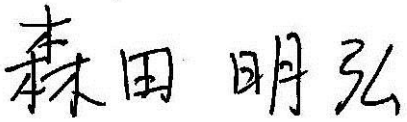

Program Leader, CAMPUS ASIA Project
Professor, Graduate School of Science, Tohoku University

Tohoku University's Chemistry Summer School 2013

Table of Contents

Summer School 2013 Schedule

Aug 28 (Wed) Laboratory tour in Tohoku University

13:30−	Laboratory tour
18:30−	Welcome Party

Aug 29 (Thu) Workshop

09:00−09:15	Opening Remarks
09:20−10:40	Oral Sessions
10:40−10:55	Coffee Break
10:55−12:15	Oral Sessions
12:15−13:15	Lunch Break
13:15−14:15	Poster Session (Odd Number)
14:15−15:15	Poster Session (Even Number)
15:30−17:00	Oral Sessions
17:00−17:15	Coffee Break
17:15−18:25	Oral Sessions
18:30−20:30	Banquet

Aug 30 (Fri) Workshop

09:00−10:30	Oral Sessions
10:30−10:45	Coffee Break
10:45−11:55	Oral Sessions
11:55−13:10	Lunch Break
13:10−14:20	Oral Sessions
14:20−14:35	Coffee Break
14:35−15:55	Oral Sessions
15:55−16:10	Coffee Break
16:10−18:00	Oral Sessions
18:00−18:10	Closing Remarks
19:30-	Farewell Party

Aug 31 (Sat) Excursion and discussion in each laboratory

10:30−/11:45−	Excursion
16:30−	Discussion

August 29, 2013 (Thursday)

Opening Remarks 09:00−09:15

9:00−9:05 Mr. Yuta Kudo (The Chairman of the Summer School)

9:05−9:15 Prof. Akihiro Morita(Campus Asia Program Leader)

Chairperson (Lecture 1, O-1−O-2): Takahiro Suzuki (Iwabuchi Lab.)

Lecture-1 09:20−10:00

Shigefumi Kuwahara, Masaru Enomoto, Akiko Asanuma

Total Synthesis of Indole Diterpenes

O-1 10:00−10:20

Akihiro Takada, Hiroaki Fujiwara, Kenji Sugimoto, Hirofumi Ueda, Hidetoshi Tokuyama

Synthetic Studies toward (–)-Isoschizogamine

O-2 10:20−10:40

Arisawa Mieko, Ichikawa Takuya, Yamaguchi Masahiko

Rhodium–Catalyzed Organosulfides Synthesis

10:40−10:55 Coffee Break

Chairperson (O-3−O-6): Yuichiro Inagawa (Iwamoto Lab.)

O-3 (I) 10:55−11:25

Janis Veliks, Jay S. Siegel

Linear Terpyridine: Versatile Building Block in Supramolecular Chemistry

O-4 11:25−11:45

Daiki Suzuoka, Shintaro Kimura, Hideaki Takahashi, Akihiro Morita

Computation of the solvation free energies due to the fluctuation of π-electrons in benzene in water utilizing the QM/MM simulations combined with perturbation theory

O-5 (I) 11:45−12:15

Philip J. Harford, Dr. Andrew E. H. Wheatley

New lithiocuprate bases for use as directed metallation agents

12:15−13:15　Lunch Break

13:15−14:15　Poster Session (Odd Number)

14:15−15:15　Poster Session (Even Number)

Chairperson (Lecture 2, O-6−O-7): Takatoshi Kasukabe (Kyotani Lab.)

Lecture-2　15:30−16:10

Itaru Honma

"Nanomaterials and Science"

for the next generation lithium ion battery technology

O-6 (I)　16:10−16:40

Benjamin Rausch, Dr. Mark D. Symes, Prof. Dr. Leroy Cronin

Decoupling Electrolytic Hydrogen and Oxygen Evolution at Scale Using an Electron-Coupled-Proton Buffer

O-7　16:40−17:00

Ming Zhao, Katsuhiro Abe, Shin-ichi Yamaura, Yoshinori Yamamoto, Naoki Asao

Chemical Fabrication of Pd-Ni-P Metallic Glass Nanoparticles and Their Application to Methanol Electro-oxidation as Highly Durable Catalysts.

17:00−17:15　Coffee Break

Chairperson (O-8−O-10): Qiang Chen (Asao Lab.)

O-8 (I)　17:15−17:45

Dongpo Xu, Shunai Che

Synthesis of lamellar mesostructured silica nanotube templated by bolaform surfactant

O-9　17:45−18:05

Yoshikazu Ikuta, Yoshitaka Koseki, Tsunenobu Onodera, Hitoshi Kasai, Tatsuya Murakami, Minoru Ueda, Hidetoshi Oikawa

Pure Nanodrugs : Synthesis, Fabrication and Anti-Cancer Properties

O-10 18:05−18:25

Ryo Nishida, Masafumi Nakaya, Atsushi Muramatsu

Passivation of α-Fe nanoparticles with oxide layer and their oxidation resistance

18:30−20:30 Workshop Banquet at Cafeteria

August 30, 2013 (Friday)

Chairperson (Lecture 3, O-11−O-12): Shuichi Toyouchi (Fukumura Lab.)

Lecture-3 09:00−09:40

Masaya Mitsuishi

Hybrid Polymer Nanoassemblies for Plasmonics Applications

O-11 (I) 09:40−10:10

Adam W Schuman

Investigations using Brewster Angle Microscopy: Micro-Separated Phases at the Liquid-Liquid Interface

O-12 10:10−10:30

Shu Ohmura, Takayuki Oyamada, Tsuyoshi Kato, Hirohiko Kono, Shiro Koseki

Molecular Orbital Analysis of Multi-Electron Dynamics Driven by an Intense Laser Field

10:30−10:45 Coffee Break

Chairperson (O-13−O-15): Gefei Li (Shoda Lab.)

O-13 (I) 10:45−11:15

Jeffrey C. Holder, Alexander N. Marziale, Michele Gatti, Kotaro Kikushima, Brian M. Stoltz.

The Development of a Palladium-Catalyzed Asymmetric Conjugate Addition of Arylboronic Acids to Cyclic Conjugate Acceptors.

O-14 11:15−11:35

Yuanyuan Liu, Ilya D. Gridnev, Masahiro Terada, Wanbin Zhang

Iridium-Catalyzed Asymmetric Hydrogenation with (a*S*)-Ir/^{i}Pr-BiphPHOX Catalyst and its Mechanistic Study by NMR and DFT Computational Analyses

O-15 11:35−11:55

Kengo Goto, Masafumi Oishi, Tadahiro Takeda, Azusa Kondoh, Masahiro Terada

Syntheses of Novel Helically Chiral Spirocyclic P3 Phosphazenium Salts

11:55−13:10　Lunch Break

Chairperson (O-16−O-18): Kiyonori Takahashi (Akutagawa Lab.)

O-16 (I)　13:10−13:40

Junying Chen, Yong-Min Lee, Katherine M. Davis, Mi Sook Seo, Kyung-Bin Cho, Young Jun Park, Shunichi Fukuzumi, Yulia N. Pushkar, Wonwoo Nam

Redox-Inactive Metal Ion Effect on the Reactivity of Mononuclear Non-Heme Manganese(IV)-Oxo Complex

O-17　13:40−14:00

Shohei Kumagai, Shinya Takaishi, Masahiro Yamashita

Charge-Density-Wave to Mott–Hubbard Phase Transition and Charge Dynamics in Bromide-Bridged Pd Chain Compounds

O-18　14:00−14:20

Min Xie, Yoshiyuki Matsuda, Tomoya Endo, Asuka Fujii

Infrared spectroscopy of cationic tetrahydrofuran(THF) and its dimer

14:20−14:35　Coffee Break

Chairperson (O-19−O-21): Huie Zhu (Mitsuishi Lab.)

O-19 (I)　14:35−15:05

Yern Seung Kim, Seung Jae Yang, Taehoon Kim, Kunsil Lee, Chong Rae Park

Practical Utilization of Boehm Titration for Surface Characterization of Carbon Nanomaterials

O-20　15:05−15:25

Yuki Sasaki, Ryo Kitaura, Yuta Yamamoto, Shigeo Arai, Hisanori Shinohara

Preparation and Observation Materials on Clean Graphene by Transmission Electron Microscope

O-21 (I) 15:25−15:55

Chi Cheng, Xiaowei Yang, Junwu Zhu, Dan Li

Multilayered graphene membrane: a novel porous carbon for capacitive energy storage

15:55−16:10 Coffee Break

Chairperson (Lecture 4, O-22−O-24): Ryohei Uematsu (Wada Lab.)

Lecture-4 16:10−16:50

Naoki Kanoh

Chemical Strategies for Discovering Unidentified Protein-Small Molecule Interactions

O-22 (I) 16:50−17:20

Jakob Franke, Keishi Ishida, Thorger Lincke, Swantje Behnken, Mie Ishida-Ito, Christian Hertweck

Genomics-Based Discovery of Secondary Metabolites from the Human Pathogenic *Burkholderia mallei* Family.

O-23 17:20−17:40

Ikuma Fujisawa, Yuanshu Zhou, Kosuke Ino, Hitoshi Shiku, Tomokazu Matsue

Single-Cell comprehensive gene expression analysis during cell differentiation

O-24 17:40−18:00

Takahiro Nakao, Takashi Fukushima, Hiroshi Nakajima, Yoshihito Watanabe

Controlled encapsulation and release of guest molecules from a caged protein, ferritin by an external stimulus

Closing Remarks 18:00−18:10

Program (Poster Session)

P-1
Yuta Ida, Shuhei Kusano, Shinya Hagihara, Fumi Nagatsugi
Design of the efficient cross-linking agent with the fixed conformation

P-2
Kaori Umetsu, Takahiro Maraoka, Kazushi Kinbara
Development of Membrane-Spanning Stimuli-Responsive Synthetic Molecules

P-3
Yusuke Miyauchi, Mihoko Ui, Makoto Murakami, Yasuyuki Araki, Takehiko Wada, Kazushi Kinbara
Creation of a Photoresponsive module based on the engineered PYP

P-4
Makoto Nishiguchi, Naoki Asao, Yoshinori Yamamoto, Tienan Jin
Nanoporous Gold for Heterogeneous Catalytic Reduction of Amides

P-5
Hirotaka Mutoh, Yoichi Takano, Naoki Asao
Synthesis of Rubrene Derivatives and Application for Organic Field-Effect Transistors

P-6
Tsubasa Hoshino, Naoki Asao
Synthesis of Deuterated Rubrene Derivatives for Organic Field-Effect Transistor

P-7
Ryuju Suzuki, Hiromi Noguchi, Tsunenobu Onodera, Hitoshi Kasai, Hidetoshi Oikawa
Fabrication of Fluorescent Copper Complex Nanoparticles and their Optical Properties

P-8
Akira Miura, Tsunenobu Onodera, Hitoshi Kasai, Takane Imaoka, Kimihisa Yamamoto, Hidetoshi Oikawa
Fabrication of Dendrimer Nanoparticles and their Complexation Behavior

P-9

Naoki Kashimoto, Satoru Tamura, Yasuhiro Ishimaru, Shin Hamamoto, Nobuyuki Uozumi, Minoru Ueda.

Interaction study between natural products and its targets in yeast

P-10

Ryo Tashita, Syusuke Egoshi, Minoru Ueda

Coronatine derivatives for bioorganic studies on stomatal opening

P-11

Naohiko Akasaka, Shintaro Ishida, Takeaki Iwamoto

Transformation of Molecular Silicon Clusters

P-12

Kenya Uchida, Shintaro Ishida, Takeaki Iwamoto

Cycloaddition of an Isolable Dialkylsilylene toward Various Aromatic Ketones

P-13

Minori Takiguchi, Shintaro Ishida, Takeaki Iwamoto

Synthesis, Structure and Dynamic Behavior of Tetraorganosilicates Having 9,10-Disilatriptycene Skeleton

P-14

Hiroki Shomura, Itaru Sato, Yujiro Hayashi

Asymmetric Mannich reaction of α-Ketoimines Catalyzed by Organocatalyst

P-15

Kei Yamada, Itaru Sato, Yujiro Hayashi, Masahiro Hirama

***p*-Benzyne Monochlorination Synthetic Study of Cyanosporasides A and B**

P-16

Daisuke Hayashi, Syuji Harada, Itaru Sato, Yujiro Hayashi, Masahiro Hirama

Total Synthesis of Ustiloxin D

P-17

Taku Hirama, Daichi Okamura, Itaru Sato, Yujiro Hayashi

Synthesis of Aziridine Containing Asymmetric Quaternary Carbon Center Catalyzed by Diphenylprolinol Silyl Ether

P-18

Takuya Koyama, Katsutoshi Takeuchi, Shuji Yamashita, Yujiro Hayashi, Masahiro Hirama

Study on Total Synthesis of Ciguatoxin CTX4B

P-19

Kanae Terayama, Eri Ozeki, Shuji Yamashita, Yujiro Hayashi, Masahiro Hirama

Synthetic Study of Presporolide

P-20

Kentaro Nishino, Itaru Sato, Yujiro Hayashi

Asymmetric formal [3+2] cycloaddition reaction of succinaldehyde via diarylprolinol-mediated domino aldol/acetalization reaction for the construction of tetrahydrofuran

P-21

Yuya Kawamoto, Daichi Okamura, Itaru Sato, Yujiro Hayashi

Organocatalytic asymmetric cyclopropanation of β-disubstituted *α*,β-unsaturated aldehydes

P-22

Yuta Kanda, Masahiro Kojima, Yusuke Yasui, Itaru Sato, Yujiro Hayashi

Asymmetric Aldol Reaction of Alkynyl Aldehyde Catalyzed by Diarylprolinol

P-23

Masataka Ikegami, Takasuke Mukaiyama, Itaru Sato, Yujiro Hayashi

Activity of Proline Type Organocatalyst Included Acidic Functional Group

P-24

Yuki Nakanishi, Itaru Sato, Yujiro Hayashi

Asymmetric Carbocyclization of Formyl Alkynes Catalyzed by Diphenylprolinol Silyl Ether and Palladium Dichloride

P-25

Keita Nakagawa, Kwon Eunsang, Kozo Toyota, Hiroyuki Sakaba

Substituent and Solvent Effects on the Reactions of Acetylide-Silylene Complexes with Acetone

P-26

Toshinari Honda, Kenji Omata, Kuninobu Kabuto, Kozo Toyota

A Chiral NMR shift Reagent Eu-pdta: Application to Determining Absolute Configurations of β-Amino Acids and β-Hydroxy Acids

P-27

Toshiki Onuma, Dong Zhang, Itaru Nakamura, Masahiro Terada

Synthesis of 1,6-Dihydropyrimidines by Copper-Catalyzed Intermolecular Cascade Reaction of *O*-Propargylic Oximes and Isocyanates.

P-28

Kyoko Kimura, Azusa Kondoh, Masahiro Terada

Asymmetric Intramolecular Cyclization of Alkynylesters Catalyzed by Brønsted Base

P-29

Takazumi Komuro, Yasunori Toda, Azusa Kondoh, Masahiro Terada

Chiral Phosphoric Acid Catalyzed Aza-Petasis-Ferrier Rearrangement for Construction of a Quaternary Stereogenic Center

P-30

Yoshinori Sato, Itaru Nakamura, Masahiro Terada

Construction of Nitrogen-Containing Medium Rings by Rhodium-Catalyzed 2,3-Rearrangement/Heterocyclization Cascade.

P-31

Kosuke Funayama, Norie Momiyama, Masahiro Terada

Design and Development of C_1 Symmetric Brønsted Acid Catalyst with Dynamic Axial Chirality

P-32

Sho Kamata, Taisuke Matsuno, Shunpei Hitosugi, Waka Nakanishi, Hiroyuki Isobe

Synthesis and Dynamic Behaviors of Cyclophanes: Silacyclophane and Cycloarylene

P-33

Yuta Nakamura, Jing Yang Xue, Waka Nakanishi, Daiki Tanimoto, Daisuke Hara, Hiroyuki Isobe

Synthesis and Properties of Substituted Naphthylene Macrocycle

P-34

Ai Hasome, Tomoko Fujino, Hiroyuki Isobe

Development of simplified and large scale synthesis of triazole-linked nucleic acids

P-35

Takashi Yamasaki, Shunpei Hitosugi, Ryosuke Iizuka, Hiroyuki Isobe

Molecular Bearing of Finite Carbon Nanotube and Fullerene in Ensemble Rolling Motion

P-36

Kiyonori Takahashi, Norihisa Hoshino, Shin-ichiro Noro, Takayoshi Nakamura, Tomoyuki Akutagawa

Structural Changes and Physical Properties of Copper(II) Complexes through Chemisorptions.

P-37

Masahiro Sato, Takashi Takeda, Norihisa Hoshino, Tomoyuki Akutagawa

Preparations, crystal structures, and electronic states of thiadiazole- and triazole-fused *p*-benzoquinones

P-38

Kawashima Masataka, Saito Yuko, Inomata Kyeong A, Kasuya Motohiro, Kurihara Kazue

Evaluation of pH at Alumina-Water by SFA Fluorescence Spectroscopy

P-39

Masataka Saito, Hsin-Liang Chen, Rita P.-Y. Chen, Kiyoto Kamagata, Hiroyuki Oikawa, Satoshi Takahashi

Microsecond dynamics of ubiquitin folding detected by single molecule fluorescence spectroscopy.

P-40

Agato Murata, Risa Kashima, Yuji Itoh, Takashi Tokino, Satoshi Takahashi, Kiyoto Kamagata

Direct observation of the multiple sliding modes of a tumor suppressor p53

P-41

Xiaoyong Wu, Qiang Dong, Shu Yin, Tsugio Sato

A high visible light induced NO_x gas destruction activity of carbon doped TiO_2

P-42

Yuta Ito, Misaki Okunishi, Kozo Shimada, Robert R. Lucchese, Toru Morishita, Kiyoshi Ueda

Extraction of electron-ion differential scattering cross sections from angle-resolved rescattering photoelectron spectra of C_2H_4 and C_2H_6 measured using IR laser pulses

P-43

Tetsuya Tachibana, Zoltan Jurek, Per.Johnsson, Hironobu Fukuzawa, Koji Motomura, Kiyonobu Nagaya, Marco Siano, Shin-ichi Wada, Subhendu Mondal, Miku Kimura, Yuta Ito, Tsukasa Sakai, Kenji Matsunami, Hironori Hayashita, Jumpei Kajikawa, XiaoJing Liu, Emmanuel Robert, Catalin Miron, Raimund Feifel, Jon Marangos, Kensuke Tono, Yuichi Inubushi, Takaki Hatsui, Makina Yabashi, Beata Ziaja, Sang-kil Son, Robin Santra, Makoto Yao, Kiyoshi Ueda

Multiphoton multiple ionization of Argon clusters by X-ray free electron laser

P-44

Akiyuki Yoshida, Yuuki Sato, Konosuke Hiramatsu, Teiko Yamada, Shigefumi Kuwahara, Hiromasa Kiyota

Synthetic studies of clionamines, autophagy-modulating amino steroids isolated from *Cliona celata*

P-45

Shigeki Tsuchiya, Yuko Cho, Keiichi Konoki, Kazuo Nagasawa, Yasukatsu Oshima, Mari Yotsu-Yamashita

Synthesis of putative biosynthetic intermediates in early stage for paralytic shellfish toxins, and their identification in toxin producing microorganisms

P-46

M. Kubouchi, K. Hayashi, Y. Miyazaki

Investigation on Amount of Interstitial Mg in Mg_2Si

P-47

Takuya Morioka, M. Takesue, H. Hayashi, R. L. Smith Jr.

Oxidative Stability of Copper Nanoparticles Produced by Supercritical Hydrothermal Synthesis

P-48

Yoshimasa Higashino, Masayuki Iguchi, Taku M. Aida, Masaru Watanabe, Richard Lee Smith Jr.

Effect of hydrothermal treatment on charcoal from waste wood in the absence and presence of additives

P-49

Masamichi Miyagawa, Masahiko Yamaguchi

Molecular Shape Recognition of Hetero-Double-Helix Ethynylhelicene Oligomers by Helicene-Grafted Chiral Silica Nanoparticles

P-50

Nozomi Saito, Ryo Terakawa, Masahiko Yamaguchi

Chiral recognition of hexadehydrotribenzo[12]annulene containing helicene

P-51

Masanori Shigeno, Yo Kushida, Masahiko Yamaguchi

Molecular Thermal Hysteresis in the Helix-dimer/random-coil Structural Change of Sulfonamidohelicene Oligomers in Solution

P-52

Ryusuke Doi, Masatoshi Shibuya, Yusuke Sasano, Yoshiharu Iwabuchi

DMN-AZADO : Development of a Highly Active Catalyst for Selective Oxidation of Primary Alcohols

P-53

Aki Kohyama, Shunsuke Sugiyama, Hiroyuki Yamakoshi, Naoki Kanoh, Yoshiharu Iwabuchi, Hiroyuki Shibata

Synthesis and cytotoxic activity of C_5-curcuminoid-thiol adducts

P-54

Ayano Kawamata, Yuta Miyazaki, Kenzo Yahata, Naoki Kanoh, Yoshiharu Iwabuchi

Synthetic Study of FD-891

P-55

Naoki Sekioka, Masahito Yoshida, Motoki Takagi, Miho Izumikawa, Kazuo Shin-ya, Takayuki Doi

Synthetic Study of Oligo-piperazic Acid-containing Natural Product Piperidamycin F

P-56

Koichi Fujiwara, Hirokazu Tsukamoto, Takayuki Doi

Synthetic study of JBIR-108

P-57

Atsushi Umehara, Hirofumi Ueda, Hidetoshi Tokuyama

Synthetic Studies on Leuconoxine.

P-58

Taichi Kurogi, Hideto Fujiwara, Shun Okaya, Kentaro Okano, Hidetoshi Tokuyama

Total Synthesis of (–)-Acetylaranotin

P-59

Kosuke Fujioka, Hiromasa Yokoe, Masahiro Yoshida, Kozo Shishido

Total syntheses of Penostatin B and E

P-60

Ayumi Irisawa, Yasushi Kino, Tsutomu Sekine

Radioactivity of wild mushrooms in Miyagi prefecture

P-61

Yosuke Sano, Yasushi Kino, Tsutomu Sekine, Toshitaka Oka

A Study of Ore Model Positronium Formation in Ar Gas.

P-62

Takashi Sugimoto, Ayumi Irisawa, Kazuma Koarai, Gohei Hayashi, Manabu Fukumoto, Yasushi Kino, Tutomu Sekine

Radioactive caesium contamination of soil in Fukushima and miyagi.

P-63

Shogo Nakamura, Yasushi Kino, Tsutomu Sekine, Toshitaka Oka

Binding Energy Analysis of Trapped Electrons in Organic Solids by Positron Annihilation Lifetime Spectroscopy

P-64

Yusuke Sato, Yushuang Zhang, Seiichi Nishizawa, Norio Teramae

Development of abasic site-containing DNA duplex-based aptamer for theophylline detection

P-65

Thiago Teixeira Tasso, Taniyuki Furuyama, Nagao Kobayashi

Synthesis and Photophysical Properties of Tetraphenylethylene-Substituted Porphyrazines

P-66

Akito Miura, Soji Shimizu, Nagao Kobayashi

Control of Alignment of Fullerenes Using Highly Deformed Phthalocyanines

P-67

Xu Liang, Soji Shimizu, Nagao Kobayashi

Push-Pull Subporphyrazines with Red-Shifted Absorptions

P-68

Kaoru Nakashima, Yukiyoshi Ohtsuki, Hirohiko Kono

Optimal control simulation of laser isotope separation utilizing molecular alignment

P-69

Nobuaki Kikkawa, Akihiro Morita

Theoretical analysis of ion transport through soft interfaces

P-70

Yuji Miki, Hideaki Takahashi, Akihiro Morita

Free energy analyses for ATP hydrolysis using quantum mechanical /molecular mechanical simulations combined with a theory of solutions.

P-71

Takashi Ishihara, Tatsuya Ishiyama, Akihiro Morita

Development of software “CALNOS” for Nonlinear spectroscopy calculation and its application to surface of water/methanol mixture

Oral Abstract

Lecture 1

Total Synthesis of Indole Diterpenes

Shigefumi Kuwahara, Masaru Enomoto, and Akiko Asanuma
Graduate School of Agricultural Science, Tohoku University, Tsutsumidori-Amamiyamachi, Aoba-ku, Sendai 981-8555, Japan
Email: skuwahar@biochem.tohoku.ac.jp
Key words: total synthesis, natural products, indole terpenoids

The indole diterpenoids constitute a large family of natural produts consisting of more than 100 members and exhibits a variety of intriguing biological properties such as tremorgenic, insecticidal, mito-inhibitory, and anti-MRSA activities. We have recently accomplished an efficient total synthesis of the tremorgenic indole diterpenes paspalinine (**1**) and paspaline (**2**) as well as the first synthesis of the indole sesquiterpene lecanindole D (**4**), a potent and selective progesterone receptor agonist, by using a Pd-mediated two-step indole ring formation as the key transformation.[1,2] In this lecture, we will talk aboout the total syntehsis **1**, **2**, and **4**, as well as our synthetic apporach to the DEF ring system of the insecticidal spirocyclic indole diterpene thiersinine B (**3**).[3]

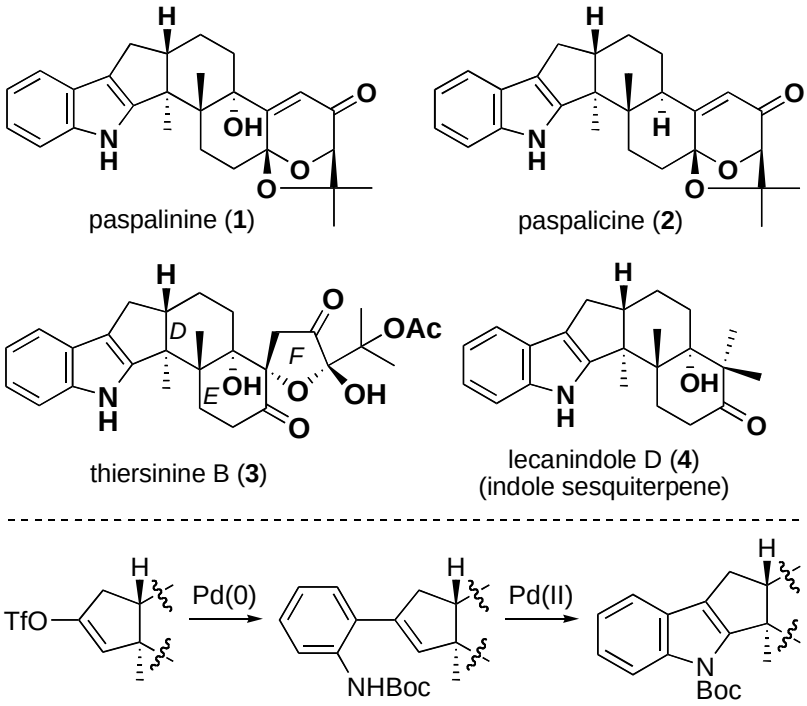

1) Enomoto, M.; Morita, A.; Kuwahara, S. *Angew. Chem. Int. Ed.* **2012**, *51*, 12833.
2) Asanuma, A.; Enomoto, M.; Nagasawa, Y.; Kuwahara, S. *Tetrahedron Lett.*, in press.
3) Enomoto, M.; Kuwahara, S. *J. Org. Chem.* **2010**, *75*, 6286.

Oral 1

Synthetic Studies toward (–)-Isoschizogamine

Akihiro Takada, Hiroaki Fujiwara, Kenji Sugimoto, Hirofumi Ueda, Hidetoshi Tokuyama
Graduate School of Pharmaceutical Sciences, Tohoku University, Sendai 980-8578, Japan
E-mail: B1YD1007@s.tohoku.ac.jp
Key words: C-H functionalization, aminal structure, natural product synthesis

Isoschizogamine (**1**), isolated from monotypic shrub *Schizozygia caffaeoides* by Renner and co-workers in 1963,[1] is an alkaloid which has polycyclic structure containing aminal functionality. Although a number of synthetic chemists have studied toward **1** due to it's unique structure, total synthesis of **1** have been reported only by Heathcook[2] and Fukuyama.[3] We report a racemic total synthesis of **1** utilizing late-stage C-H functionalization of tetracyclic lactam **3**.

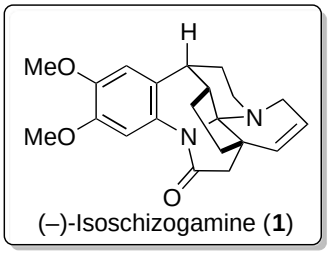

(–)-Isoschizogamine (**1**)

Compound **3**, a substrate for the C-H functionalization, was prepared from ketone **2** via diastereoselective introduction of the side chain possessing amino group. After extensive investigation, we found that control of electron density of the aromatic ring was critical for successful C-H functionalization. After removal of Boc group, aminal formation was performed to provide the desired aminal **5**. Following 5 steps conversion, we then conducted ring-closing metathesis to construct all core skeleton of **1**. A total synthesis of (±)-isoschizogamine (**1**) was accomplished after a four-step sequence including removal of silyloxy group and conversion of tosylate to methoxy group.

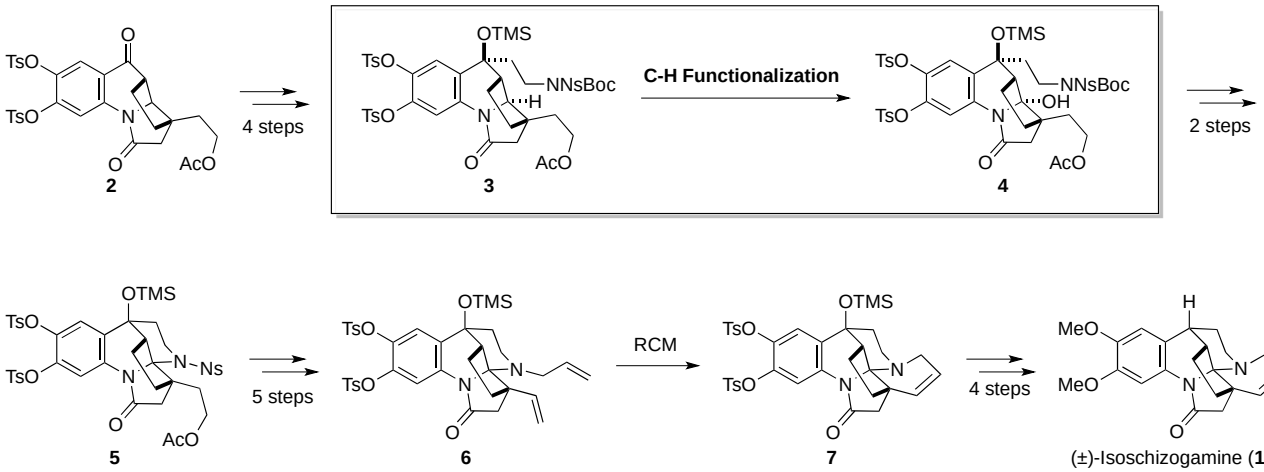

(1) (a) Renner, U. *et al*. *Experientia* **1963**, *19*, 244. (b) Renner, U. *Lloydia* **1964**, *27*, 406. (2) Heathcock, C. H. *et al*. *Org*. *Lett*. **1999**, *1*, 1315. (3) Fukuyama, T. *et al*. *J. Am. Chem. Soc.* **2012**, *134*, 11995.

Oral 2

Rhodium–Catalyzed Organosulfides Synthesis

Arisawa Mieko, Ichikawa Takuya, Yamaguchi Masahiko
Graduate School of Pharmaceutical Sciences, Tohoku University, Sendai, Japan
E-mail: b2yd1001@s.tohoku.ac.jp
Key words: rhodium catalyst, metathesis reaction, sulfur, C-S bond cleavage, aryl exchange

Organosulfides are used for drugs and materials, and development of efficient synthetic method is demanded. In general, they are synthesized using reactive sulfur reagents prepared from sulfur. Direct use of sulfur is attractive, although such synthesis is rare. In this study, rhodium-catalyzed syntheses of organosulfides using sulfur are described.

1. Rhodium-catalyzed synthesis of unsymmetrical diaryl sulfides

Our group studied rhodium-catalyzed synthesis of organosulfur compounds. Recently, a rhodium-catalyzed synthesis of diaryl sulfides was developed using aryl fluorides and sulfur.[1)] Rhodium catalyst activated the S-S bond of sulfur, and formed symmetrical diaryl sulfides. During this study, diaryl sulfides were found to react with aryl fluorides forming unsymmetrical diaryl sulfides via aryl exchange in the presence of rhodium catalyst. The results indicate that rhodium catalyst can be used for diaryl sulfide C-S bond formation and cleavage.[2)]

Symmetric Diaryl sulfide syntheis using sulfur[1)]

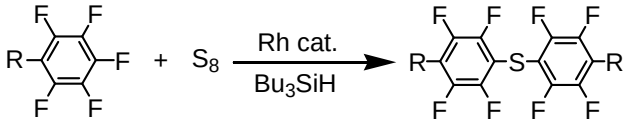

Unsymmetric diaryl sulfide synthesis via aryl C-S bond cleavage[2)]

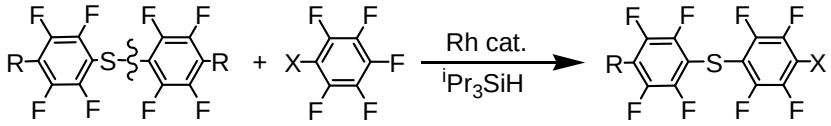

R or X = PhCO, MeCO, ArS, Ph_2N

2. Rodium-catalyzed sulfur addition reaction

Addition reaction of sulfur to unsaturated compounds has an advantage to synthesize organosulfides under high atom economical and environmental-friendly manner. In the presence of rhodium catalyst, benzonorbornene **1** and sulfur **2** (1.5 eq.) were reacted in reflux acetone, and exo-episulfide **3** (46%) was obtained.

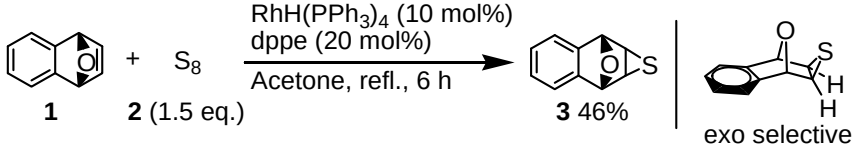

References: 1) Arisawa, M.; Ichikawa, T.; Yamaguchi, M. *Org. Lett.,* **2012**, *14*, 5318. 2) Arisawa, M.; Ichikawa, T.; Yamaguchi, M. *Tetrahedron Lett.*, **2013**, in press.

Oral 3 (Invited)

Linear Terpyridine: Versatile Building Block in Supramolecular Chemistry

Janis Veliks and Jay S. Siegel
Institute of Organic Chemistry, University of Zurich, Winterthurerstr. 190, 8057 Zurich, Switzerland

Email: jss@oci.uzh.ch, janis.veliks@uzh.ch
Key words: 2,2′:6′,2″-terpyridine, topology, supramolecular chemistry

The control over complex topology on molecular scale can be achieved by scrupulous engineering of building blocks that fulfill specific requirements of dimensions, stereochemistry and a pattern of supramolecular interactions.[1] Five-membered furan rings fused to tridentate 2,2′:6′,2″-terpyridine act as directing motifs to mimic the topology of bidentate 2,2′-bipyridine placing substituents perpendicular to the coordination site (Figure 1).[2] Fundamental building-blocks based on 2,2′:6′,2″-terpyridine with new topological features have various potential applications, for example, assembly of heterometallic molecular girds, synthesis of coordination polymers and metal-organic frameworks (MOFs). In addition, preliminary results show that these ligands have the right dimension and topology to advance the stepwise synthesis of the molecular Borromean link.

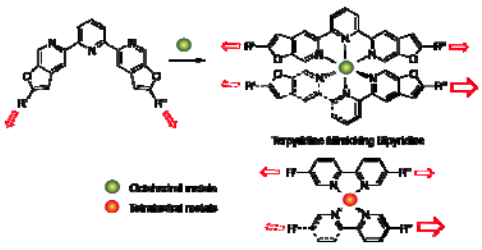

Fig.1 Linear terpyridine ligands mimicking topology of 2,2′-bipyridine.

Ref. [1] (a) J.-M. Lehn, *Supramolecular Chemistry-Concepts and Perspectives*, *VHC, Weinheim* **1995**. (b) J. C. Loren, M. Yoshizawa, R. F. Haldimann, A. Linden, J. S. Siegel, *Angew. Chem. Int. Ed.* **2003**, 42, 5702-5705. [2] J. Veliks, J.-C. Tseng, K. Arias, A. Linden, J. S. Siegel, *Manuscript in Preparation*.

Oral 4

Computation of the solvation free energies due to the fluctuation of π-electrons in benzene in water utilizing the QM/MM simulations combined with perturbation theory

Daiki Suzuoka, Shintaro Kimura, Hideaki Takahashi*, and Akihiro Morita
Graduate School of Science, Tohoku University Aoba 6-3, Aoba-ku, Sendai 980-8578, Japan.
Email: d_szok@s.tohoku.ac.jp

Key word: theory of solutions, energy representation, CH/π interaction, aromatic molecules

π electron is a fundamental building block of electronic structures in aromatic compounds and in biologically relevant molecules. An important attribute of the π electron is the spatial diffuseness and the softness of its electron density. This is considered as a major origin of the notable interaction referred to as σ-π interaction. However, the effect of the σ-π interactions on the hydration properties, in particular, on the thermodynamics of hydration is not investigated with quantitative basis. In the present paper, we address the issue of the hydration of benzene, which shows unexpectedly high solubility in water by utilizing the hybrid QM/MM simulation technique combined with a theory of solutions (QM/MM-ER). [1] The hydration free energy $\delta\mu$ due to the electron density fluctuation of benzene is decomposed into the contributions of σ and π electrons to elucidate the microscopic hydration mechanism of benzene.

In the QM/MM-ER method, solvation free energy $\Delta\mu$ of a solute is given by sum of the free energy $\Delta\bar{\mu}$ due to two-body solute-solvent interaction and residual many-body contribution $\delta\mu$, thus, $\Delta\mu = \Delta\bar{\mu} + \delta\mu$. We apply the perturbation theory in the present QM/MM simulation to realize the polarization of the solute. Then, $\delta\mu$ can be readily decomposed into the free energies $\delta\mu_\pi$ and $\delta\mu_\sigma$ due to the fluctuations of π and σ electrons, respectively, by virtue of the density functional theory of solutions.

Computed solvation free energies are presented in Table 1. The two-body contribution $\Delta\bar{\mu}$ was computed as 1.2 kcal/mol, indicating that benzene is not soluble in water without electron density fluctuation in solution. It was found, however, that inclusion of the free energy $\delta\mu_\pi$ due to many-body interaction leads a negative value (-0.3 kcal/mol) of the total solvation free energy. Further, the decomposition of the free energy $\delta\mu$ revealed that $\delta\mu$ gives the major contribution irrespective of the small number of the π electrons.

	$\Delta\bar{\mu}$	$\delta\mu_\pi$	$\delta\mu_\sigma$	$\Delta\mu$	$\Delta\mu_{\text{expt.}}$
Benzene	1.2	-0.9	-0.6	-0.3	-0.87

Table 1. Computed solvation free energy $\Delta\mu$ and its components for a benzene molecule in water solvent in units of kcal/mol. $\Delta\mu_{\text{expt.}}$ is the experimental value.

Ref. [1] H. Takahashi *et al.*, J. Chem. Phys. **136**, 214503 (2008).

Oral 5 (Invited)

New lithiocuprate bases for use as directed metallation agents

Philip J. Harford[1] and Dr. Andrew E. H. Wheatley[1]
[1]Department of Chemistry, University of Cambridge,
Lensfield Road, Cambridge, CB2 1EW, United Kingdom.
Email: ph313@cam.ac.uk
Key words: copper, lithium, directed metallation, solid-state structures

Two classes of lithium cuprates are described in the literature: Lower-order, or Gilman-type cuprates of the form [RCuR´Li]; and higher-order, or Lipshutz-type cuprates of the form [RCuR´Li_2X] (X = Cl, Br, I).[1] Here, a new class of lithium amidocuprate has been prepared and studied in the solid state (Fig. 1). We have focused on extending previous work with the sterically bulky amine ligand 2,2,6,6-tetramethylpiperidine (HTMP) to *cis*-2,6-dimethylpiperidine (HDMP) and investigating the steric effects of the amido ligand in directed *ortho* cupration (DoC). Employing HTMP and bulk Et_2O as the solvent led to the formation of the expected Lipshutz-type cuprates.[2] In contrast, using HDMP and varying amounts of Et_2O, dependent on the halide, the formation of lithium amidocuprates with an unprecedented structural motif was observed (e.g. Fig. 2). The new species contain a three-coordinate halide ion and are best viewed as being adducts between Gilman- and Lipshutz-type cuprates.[3] The aggregation behaviour and the DoC ability of the new cuprate adducts is being studied both experimentally and theoretically.

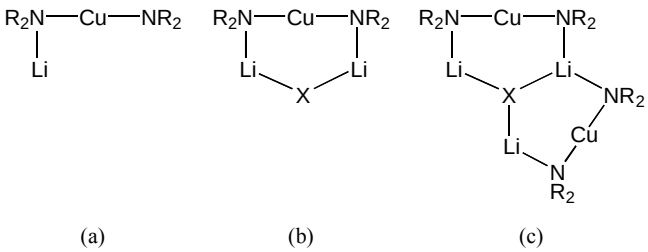

Fig. 1. *Cuprate structures (a) Gilman, (b) Lipshutz and (c) new Gilman-Lipshutz adduct. X = Cl, Br, I.*

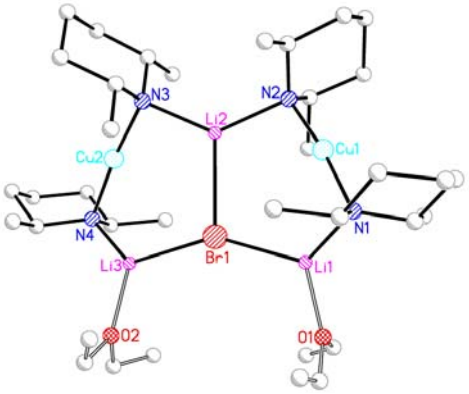

Fig. 2. *Crystal structure of the Gilman-Lipshutz adduct [(DMP)$_2$CuLi·OEt$_2$]$_2$LiBr*

Ref. [1] R. P. Davies, *Coord. Chem. Rev.*, 2011, **255**, 1226-1251.
Ref. [2] S. Komagawa, S. Usui, J. Haywood, P. J. Harford, A. E. H. Wheatley, Y. Matsumoto, K. Hirano, R. Takita, M. Uchiyama, *Angew. Chem. Int. Ed.*, 2012, **51**, 12081-12085.
Ref. [3] P. J. Harford, A. J. Peel, J. P. Taylor, S. Komagawa, P. R. Raithby, T. P. Robinson, M. Uchiyama, A. E. H. Wheatley, manuscript in preparation.

Lecture 2

"Nanomaterials and Science" for the next generation lithium ion battery technology

Itaru Honma

Institute of Multidisciplinary Research for Advanced Materials (IMRAM), Tohoku University Katahira 2-1-1, Aoba-ku, Sendai 980-8577, Japan.

Email: i.honma@tagen.tohoku.ac.jp

Key words: lithium ion battery, nanomaterials, organic electrodes

Recent surge in demands for large-scale batteries in electric vehicles and "smart grid" applications require development of lithium ion battery (LIB) materials that are low-cost, free of resource restrictions and environmentally friendly. The conventional metal oxide cathodes on the market today falls short for this purpose because they require "rare metals" such as Co, Ni, Mn and their preparation too, involves energy-intensive processes. On the contrary, organic compounds present promising possibilities because they are high energy density, primarily owing to their two-electron redox reactions, in spite of metal-free elements. Figure 1 shows examples of the candidate organic quinone molecules which, theoretically, possess higher specific capacities than that of inorganic cathodes such as $LiFePO_4$. However, they have not been actively pursued due to low cycleability, primarily owing to a dissolution into the electrolyte because discharge products of these organic molecules are highly soluble species of monoanion radical (-) and/or dianion (2-) states. But, we have successfully developed a high energy density all-solid state lithium battery cell with much better cycleability by suppressing the dissolution processes. A novel solid cell design is developed via application of quasi-solid electrolyte at the interface of organic crystalline cathodes, which successfully avoids dissolution of anionic molecular compounds. The cell features totally encapsulated cathode, PEO layer, quasi-solid electrolyte and controlled electrolyte- anode interface that accommodate soluble organic cathodes under charge/discharge cycles. Quasi-solid state electrolyte consists of silica nanoparticles and room temperature ionic liquid (RTIL) were used to stabilize organic cathode interfaces against dissolution. Molecular crystals of tetracyano quinodimethane (TCNQ) possesses two electron redox capacity equivalent of 262 mAh/g with first redox potential plateau at 3.2V (vs. Li/Li^+) and the second at 2.8V, providing apparent two step potential profile in fig.2. Many of such compounds shown in fig.1. have similarly two electron redox capacities exceeding 230 mAh/g; 2,3,5,6-tetrahydroxy benzoquinone (THBQ), 2,3-dichloro-5, 6-dicyano- benzoquinone (DDQ) and 2,5-dihydroxy benzoquinone (DHBQ) are intrinsically possessing higher energy density than that of $LiFePO_4$. The multi-electron capacity at high potential expected in the quinone family of organic cathodes may increase energy densities of the cell although no metallic elements are used in the active materials. If

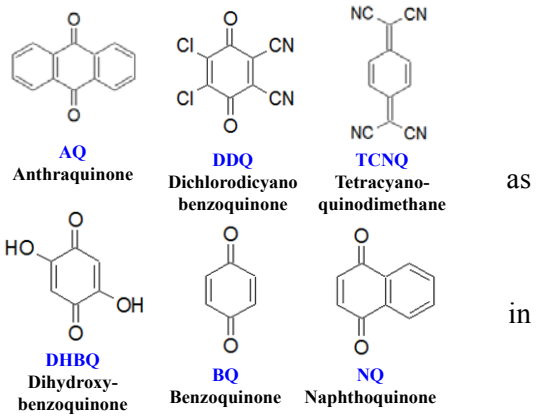

Figure 1.
Families of organic molecular active materials for high capacity electrodes

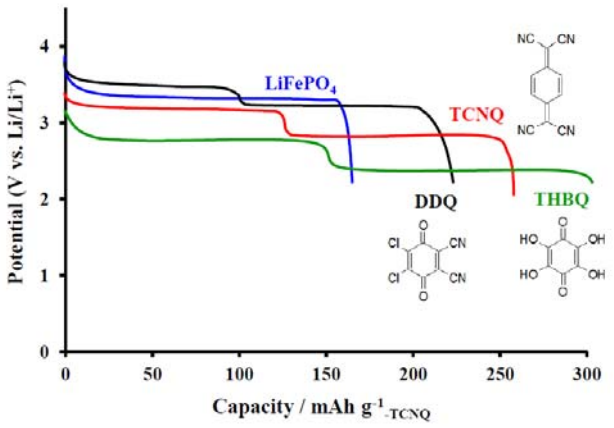

Figure 2.
Discharge profiles of several quinone molecular electrodes. The energy densities of these organic electrodes exceed that of inorganic one, $LiFePO_4$

these strategy are successfully implemented in the LIB device, significant reduction of the rare metals can be realized. Figure 3 shows the physical features of bulk organic all-solid lithium cell. A photograph of the actual pellet with a diameter of 10 mm and thickness ~ 1000 μm is shown and the TCNQ cathode paste in the insert. A large (~50 μm) TCNQ crystal is visible, while the solid state cathode contains TCNQ crystals, carbon current collector and room temperature ionic liquids (RTIL). Three layered electrolyte consisting of PEO membrane, silica-RTIL composite quasi-solid state electrolyte and artificial SEI separates the cathode from metallic lithium anode. Figure 4 shows cycle performances of the TCNQ cathodes and favourable capacity retention can be achieved, indicating that, by suppressing molecular dissolution into the electrolyte, organic materials can be used in the secondary battery electrodes under the solid state cell design. A cycleability of TCNQ using [BMP][Tf_2N] ionic liquid in the quasi-solid electrolytes at 0.2 C rate at room temperature has shown that, after extended charge-discharge cycles over 170 times, the capacity was still over 170 mAh/$g_{\text{-TCNQ}}$. The strategy of stabilizing electrode/ electrolyte interface of the organic cathodes have confirmed the possibilities of numerous molecularitic compounds dismissed before due to low cycleability would worth a re-visit under solid state design.

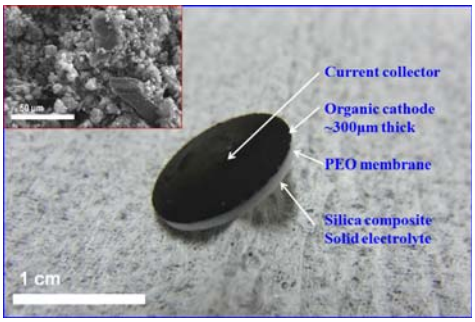

Figure 3.
Solid state lithium ion battery design employing TCNQ crystals (shown in the insert) as cathode enables higher energy storage density against present LIB cells

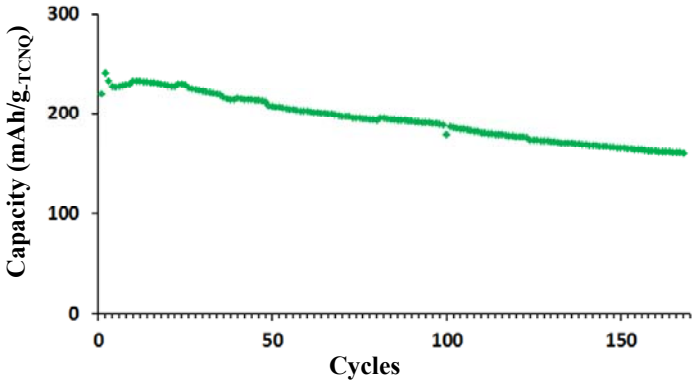

Figure 4.
Cyclic performance of TCNQ cathodes in the solid state cell over 170th times shows favourable capacity retention

References

1. M. Kempaiah Devaraju, Takaaki Tomai, Atsushi Unemoto and Itaru Honma: Novel processing of lithium manganese silicate nanomaterials for Li-ion battery applications. ***RSC Advances***, 3, 608 (2013)

2. Yuki Hanyu, Yoshiyuki Ganbe and Itaru Honma: Application of quinonic cathode compounds for quasi-solid lithium batteries. ***J. Power Sources***, *221*, 186-190 (2013)

3. Marappan Sathish, Satoshi Mitani, Takaaki Tomai and Itaru Honma: Ultra-thin SnS2 Nanoparticles on Graphene Nanosheets: Synthesis, Characterization and Li-ion Storage Applications, ***J. Physical Chemistry C*** 116, 12475 (2012)

4. M. Sathish, S. Mitani, T. Tomai and I. Honma: Graphene Anchored with Fe_3O_4 Nanoparticles as Anode for Enhanced Li-Ion Storage, ***J. Power Sources***, 217, 85 (2012)

5. Takaaki Tomai, Yuji Kawaguchi and Itaru Honma: Nanographene production from platelet carbon nanofiber by supercritical fluid exfoliation, ***Applied Physics Letters***, 100, 233110 (2012)

6. Yuki Hanyu and Itaru Honma: Rechargeable quasi-solid state lithium battery with organic crystalline cathode. ***Scientific Reports,*** *2*, 453 (2012).

7. Seitaro Ito, Atsushi Unemoto, Hideyuki Ogawa, Takaaki Tomai, and Itaru Honma: Application of quasi-solid-state silica nanoparticles- ionic liquid composite electrolytes to all-solid-state lithium secondary battery, ***J. Power Sources***, 208, 271 (2012)

8. Dinesh Rangappa, M. K. Devaraju, T. Tomai, Atsushi Unemoto and Itaru Honma: Ultra Thin Nanosheets of Li_2MSiO_4 (M= Fe, Mn) as High Capacity Li Ion Battery Electrodes, ***Nano Letters***, 12, 1146 (2012)

9. M.Okubo, Y.Mizuno, H.Yamada, J.-D.Kim, E.Hosono, H.S.Zhou, T.Kudo and I.Honma:

Fast Li-ion insertion into nanosized $LiMn_2O_4$ without domain boundaries, ***ACS nano***, 4, 741 (2010)

Oral 6 (Invited)

Decoupling Electrolytic Hydrogen and Oxygen Evolution at Scale Using an Electron-Coupled-Proton Buffer

Benjamin Rausch, Dr. Mark D. Symes, Prof. Dr. Leroy Cronin*
WestCHEM, School of Chemistry, The University of Glasgow, University Avenue, Glasgow, G12 8QQ, UK. Email: benra@chem.gla.ac.uk, lee.cronin@glasgow.ac.uk*, http://www.croninlab.com
Keywords: Electrochemistry, Water Splitting, Hydrogen Production, Electron Coupled Proton Buffer

Hydrogen is essential to several key industrial processes mainly for use in the manufacture of ammonia and in the petrochemical industries. Hydrogen also has great potential as a clean fuel, an energy storage medium and in the synthesis of liquid fuels *via* catalytic hydrogenation of suitable substrates, such as CO_2 in a future "hydrogen economy". While the demand on pure hydrogen will increase in the near future to replace fossil fuels, the majority of today's world hydrogen supply originates from the reformation of fossil fuels. Electrolytic hydrogen production from water, using renewably-generated power could generate H_2 without increasing the atmospheric CO_2 level. For renewable H_2 production to become more widespread, advances are required that could lead to much more economical electrolysers, and hence there exists a great need to develop new paradigms in electrolytic water splitting that could lead to new thinking, approaches, and electrolyser designs.

We present an alternative approach to water-splitting, whereby the electrons and protons generated during the oxidation of water to O_2 are taken up reversibly by an Electron-Coupled-Proton Buffer (ECPB) (Step 1 in Figure), rather than being used directly to make H_2. Subsequent re-oxidation of the ECPB releases these protons and electrons for hydrogen production (Step 2 in Figure). Hence the ECPB acts as a reversible electron and proton donor/acceptor, with a redox couple that is energetically intermediate between OER onset and HER onset. The overall result of using an ECPB is that H_2 and O_2 can be obtained from the electrolysis of water at completely different times, *i.e.* the OER is completely decoupled from the HER to produce O_2 that is essentially free of H_2, and H_2 that is essentially free of O_2. In this way, two smaller energy inputs are used to split water to give H_2 and O_2 at different times, as opposed to a single energy input which produces H_2 and O_2 simultaneously, which represents a potential safety hazard.[1]

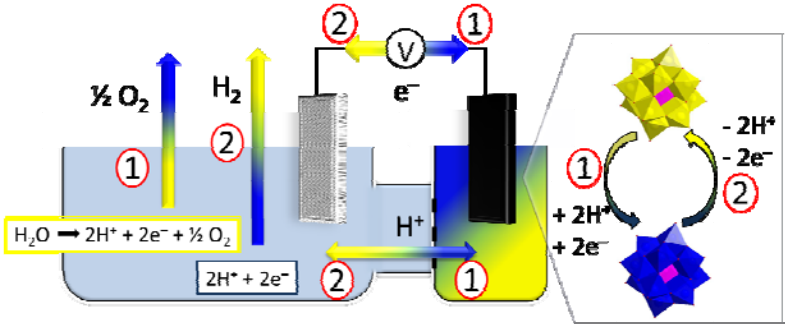

[1] M. D. Symes, L. Cronin, Nat Chem 2013, advance online publication.

Oral 7

Chemical Fabrication of Pd-Ni-P Metallic Glass Nanoparticles and Their Application to Methanol Electro-oxidation as Highly Durable Catalysts.

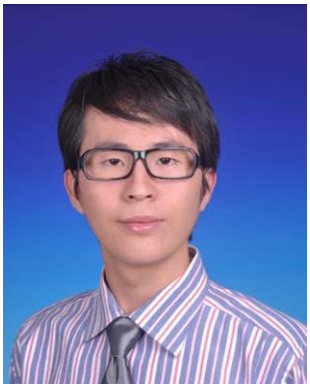

Ming Zhao,[1] Katsuhiro Abe,[2] Shin-ichi Yamaura,[2] Yoshinori Yamamoto,[1,3] and Naoki Asao[1]

[1] WPI-AIMR (WPI-Advanced Institute for Materials Research), Tohoku University, Sendai 980-8577, Japan.

[2] Institute for Materials Research, Tohoku University, Sendai 980-8577, Japan.

[3] State Key Laboratory of Fine Chemicals, Dalian University of Technology, Dalian 116012, China.

Email: mingzhao815@gmail.com

Key words: metallic glasses, palladium, methanol oxidation

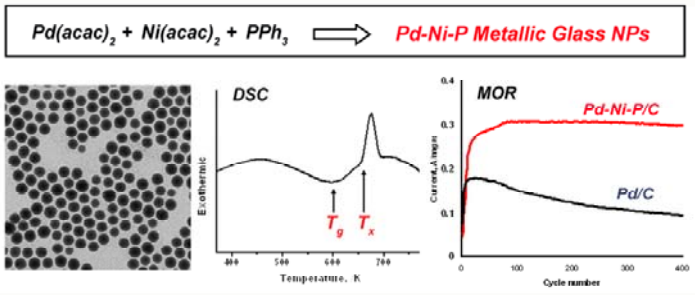

Metallic glasses show various distinctive chemical and physical properties compared with common crystalline alloys; however, their applications at nanoscales are very limited, and the physical fabrications of metallic glass nanomaterials were still restricted. In this work, the first chemical fabrication of metallic glass nanoparticles (MG-NPs) was presented. Reductions of readily commercially available Pd, Ni, and P-precursors by one-pot solvothermal synthesis proceeded smoothly to give small sizes of amorphous Pd-Ni-P NPs (6 nm, 8 nm, 11 nm, and 17 nm). The procedure was facile, ultra-highly reproducible, and mould-free. Differential scanning calorimetry (DSC) indentified the glass transition and wide supercooled liquid region (ranged from 602 K to 657 K) of the bare $Pd_{28}Ni_{43}P_{29}$ NPs, indicating their excellent metallic glass property. Furthermore, the deposited Pd-Ni-P NPs on activated carbon support exhibited remarkable catalytic durability in methanol electro-oxidation in alkaline medium compared with other Pd-based nanomaterials and more precious Pt-Pd bimetallic catalysts, identifying the MG-NPs inherited the characteristic of corrosion resistance from bulk metallic glasses.

Oral 8 (Invited)

Synthesis of lamellar mesostructured silica nanotube templated by bolaform surfactant

Dongpo Xu and Shunai Che*

School of Chemistry and Chemical Engineering
State Key Laboratory of Metal Matrix Composites
Shanghai Jiao Tong University
800 Dongchuan Road, Shanghai, 200240 (P.R. China)
*Email: chesa@sjtu.edu.cn
Key words: lamellar, silica nanotube, bolaform surfactant

The combination of mesostructure and one-dimensional silica nanotubes has attracted increasing research interests because of their hierarchical structures with at least three different length scales and well-defined macroscopic forms, which may lead to potential applications in drug delivery, separation and catalyst [1]. In order to control the morphology and structure of silica, soft-template methods were widely employed, which provides a simple and reliable synthetic tool to tailor well-defined materials. Up to now, several silica nanotubes with mesostructures inside of the wall have been synthesized by soft template method. However, construction mesostructures inner hollow side of the silica nanotubes is still a challenge.

Here we report the synthesis of an earthworm-like lamellar structure silica nanotube by using bolaamphiphiles surfactant, which possess hydrophilic carboxylic acid headgroups connected to a rigid hydrophobic part. The 3-aminopropyltrimethoxysilane (APS) has been used as the co-structure-directing agent (CSDA) interacting with carboxylic acid electrostatically. The powder X-ray diffraction (XRD) and transmission electron microscopy (TEM) show that the silica nanotube has lamellar structure with the *d*-spacing about 5.5 nm, which correspond to the length of rigid bolaamphiphiles surfactant. The lamellar structure of silica nanotubes resulted from lamellar arrangement of bolaamphiphiles surfactant with the single molecular layer. The average length of the tube is about 200 nm and the diameter about 50 nm.

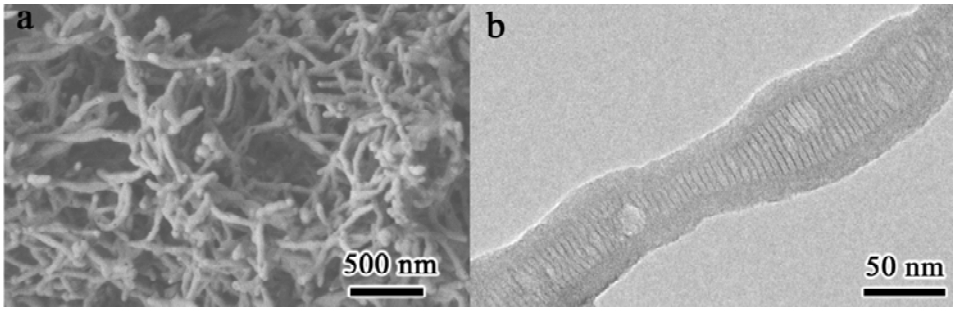

Fig.1 SEM (a) and TEM (b) image of the as-made lamellar mesoporous silica nanotube.

[1] L. Wang, Z. Shan, Z. Zhang, F. Wei, FJ. Xiao, Colloid Interface Sci. 2009 335,264.

Oral 9

Pure Nanodrugs : Synthesis, Fabrication and Anti-Cancer Properties

Yoshikazu Ikuta,[1] Yoshitaka Koseki,[1] Tsunenobu Onodera,[1] Hitoshi Kasai,[1] Tatsuya Murakami,[2] Minoru Ueda,[3] and Hidetoshi Oikawa[1]

[1]Institute of Multidisciplinary Research for Advanced Materials (IMRAM), Tohoku University, Aoba-ku, Sendai, 980-8577, Japan.

[2]Institute for Integrated Cell-Material Sciences (iCeMS), Kyoto University, Sakyo-ku, Kyoto, 606-8501, Japan.

[3]Graduate School of Science, Tohoku University, Aoba-ku, Sendai, 980-8579, Japan.

Email: y.ikuta@mail.tagen.tohoku.ac.jp

Key words: drug delivery systems, anti-cancer drug, reprecipitation method, pure nanodrugs

Due to poor solubility in a water, it is necessary to convert a number of physiological active agents by chemical modification for the purpose of increasing the water solubility. On the other hand, we have attempted to fabricate the nanoparticles by utilizing the water insolubility of drug compounds. The nanoparticles with 10 – 100 nm in size can be accumulated the tumor tissues by Enhanced Permeation and Retention (EPR) effect. As a result, it is expected to give a smaller dose of anti-cancer drug and to reduce the strong side effects. In the present study, we have selected SN-38 and podophyllotoxin (PPT), because they are known to be water insoluble and to have the so effective anti-cancer properties.

First, the dimeric forms of both SN-38 and PPT were synthesized to further reduce the water solubility, and then, the nanoparticles of SN-38 dimer (Fig. 1a) and PPT dimer (Fig. 1b) were succeeded in fabricating with approximately 50 nm in size by the reprecipitation method. Next, the resulting SN-38 dimer nanoparticles were added to cancer cell cultures. As a result, the nanoparticles of SN-38 dimer (■, ▲) could provide the highly cytotoxicity, compared with irinotecan (◆) , which is a water soluble prodrug of SN-38, (Fig. 1c)[1)]. Similarly, anti-cancer property of PPT dimer nanoparticles (●) was the higher than that of etoposide (×), which is a analog of PPT and soluble in the water (Fig. 1d)[2)].

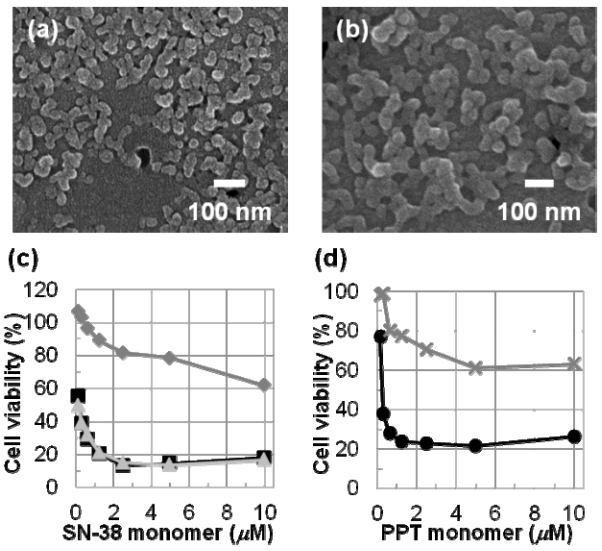

Fig. 1. SEM images of SN-38 dimer nanoparticles (a) and PPT dimer nanoparticles (b), and the results of their *in vitro* assay (SN-38 dimer: c, PPT dimer: d).

1) H. Kasai *et al*., *Angew. Chem. Int. Ed*. **2012**, *51*, 10315-10318.

2) Y. Ikuta et al., *Chem. Lett. in press.*

Oral 10

Passivation of α-Fe nanoparticles with oxide layer and their oxidation resistance

Ryo Nishida, Masafumi Nakaya, and Atsushi Muramatsu
Institute of Multidisciplinary Research for Advanced Materials (IMRAM), Tohoku University Katahira 2-1-1, Aoba-ku, Sendai 980-8577, Japan.
Email: ryo-24d@mail.tagen.tohoku.ac.jp
Key words: metal α-Fe nanoparticles, passivation, core-shell structure

Metal α-Fe nanoparticles have long been of scientific and technological interest because of its large magnetization (218 emu/g). However, it is difficult to keep the condition of α-Fe nanoparticles because α-Fe nanoparticles are easy to oxidize at the moment of exposure to the atmosphere. In order to make real metallic α-Fe nanoparticles for various applications such as biomedical imaging or sensing, the prevention of oxidation is indispensable. In this study, we intended to prepare surface-oxidized α-Fe nanoparticles by reduction of SiO_2 coated Fe_3O_4 nanoparticles and partial oxidation of their surfaces, and investigate its oxidation resistivity.

Fe_3O_4 nanoparticles were synthesized in oleic acid and oleylamine as solvent and surfactant. The obtained Fe_3O_4 nanoparticles were coated with SiO_2 shell (FIG.1(a)), and the resulting Fe_3O_4@ SiO_2 nanoparticles were treated to α-Fe@ SiO_2 nanoparticles under H_2 atmosphere at 500 ºC for 3 h (FIG.1(b)). And then the nanoparticles were partially oxidized to form the oxide layer under 2%-O_2/N_2 atmosphere at 300~400 ºC. The TEM image of partially oxidized nanoparticles, bright surface layer on dark core was observed (FIG.1(c)). The XRD pattern after reduction resulted in only the observation of α-Fe peaks. On the other hand, at 400 ºC partial oxidation treatment, the patterns of not only α-Fe but also Fe_3O_4 phase were observed. Judging from the TEM images and XRD pattern, α-Fe/ Fe_3O_4 core-shell structure could be formed by partial oxidation treatment. FIG.2 shows the change of saturation magnetization (M_s) with time. In the case of the α-Fe nanoparticles without surface oxidization, M_s was reduced by 40% after 1 day from the treatment. By contrast, in the case of the partially oxidized α-Fe nanoparticles, the large decrement of M_s was not observed even after 80 days. And the XRD pattern resulted in the observation of α-Fe phase after 80 days. These results show partial oxidation treatment must be effective to protect α-Fe phase from oxidization under atmosphere for long time.

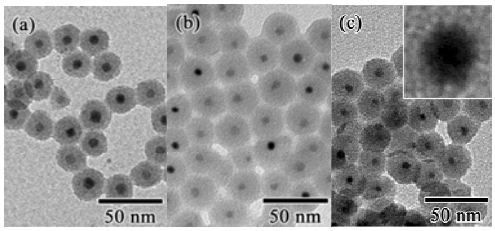

FIG. 1. TEM images of Fe_3O_4@SiO_2 nanoparticles: (a) as-synthesized, (b) after reduction, (c) after partial oxidation.

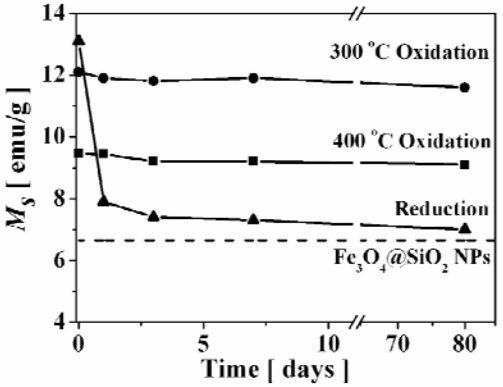

FIG. 2. The change of M_s with time. (M_s was estimated on the total mass including core and SiO_2 shell.)

Lecture 3

Hybrid Polymer Nanoassemblies for Plasmonics Applications

Masaya Mitsuishi
Institute of Multidisciplinary Research for Advanced Materials (IMRAM), Tohoku University, 2-1-1 Katahira, Aoba-ku, Sendai 980-8577, Japan.
Email: masaya@tagen.tohoku.ac.jp
Key words: Polymer, Surface Plasmon, Noble Metal, Nanophotonics

Bottom-up approaches such as layer-by-layer method and Langmuir-Blodgett technique allow us to assemble organic/inorganic hybrid nanomaterials at the nanometer scale. We have developed ultrathin polymer Langmuir-Blodgett films as a building block of hybrid polymer nanoassemblies. The monolayer of the polymer film has only 1.7 nm thickness. Inorganic nanoparticles such as noble metals and metal oxides can take a monolayer formation in the hybrid polymer nanoassemblies and the separation distance can be controlled with single nanometer precision. The advantage of the material involves flexible design of well-defined nanostructures. These assemblies offer a suitable model for elucidating light-matter interaction strongly related with nano-optics, e.g., localized surface plasmon, guided optical waves, quantum dot, and photofunctional molecules. Hybrid polymer nanoassemblies consisting of polymer nanosheets and metal nanoparticles confine far--field light effectively, and generate enhanced luminescence and photocurrent generation as well as second harmonic light. These events occurred at the visible light wavelength and needless to say are extendable to other wavelength region. We will discuss recent progress in our understanding of light-matter interaction occurred in hybrid polymer nanoassemblies in terms of structure-property relationship.

References

(1) Mitsuishi, M.; Ishifuji, M.; Endo, H.; Tanaka, H.; Miyashita, T. *Polym. J.* **2007**, *39*, 411-422.
(2) Tanaka, H.; Mitsuishi, M.; Miyashita, T. *Langmuir* **2003**, *19*, 3103-3105.
(3) Ishifuji, M.; Mitsuishi, M.; Miyashita, T. *Appl. Phys. Lett.* **2006**, *89*, 011903.
(4) Ishifuji, M.; Mitsuishi, M.; Miyashita, T. *J. Am. Chem. Soc.* **2009**, *131*, 4418-4424.
(5) Mitsuishi, M.; Tanaka, H.; Obata, M.; Miyashita, T. *Langmuir* **2010**, *26*, 15117-15120.
(6) Mitsuishi, M.; Morita, S.; Tawa, K.; Nishii, J.; Miyashita, T. *Langmuir* **2012**, *28*, 2313-2317.

Oral 11 (Invited)

Investigations using Brewster Angle Microscopy: Micro-Separated Phases at the Liquid-Liquid Interface

Adam W Schuman
Physics Department, University of Illinois at Chicago
845 West Taylor Street
Chicago, Illinois 60607
United States
Email: aschum3@uic.edu
Key Words: Brewster angle microscopy, microphase

Brewster angle microscopy (BAM) and quasi-elastic light scattering (QELS) are two well-developed techniques to investigate morphology and thermodynamic properties of liquid surfaces. In the physics department at the University of Illinois at Chicago, I have designed and constructed an in-house microscope to utilize these techniques to study temperature-controlled properties of liquid-liquid interfaces. In particular, we have observed the existence of periodic, micron sized structure in a state commonly referred to as a microphase for soluble surfactants near their transition temperatures. From BAM and in situ QELS surface tension measurements, I will present clear evidence of a microphase morphology at the interface between water and a solution of 1,1,2,2-tetrahydroperfluorododecanol (FC12OH) in hexane where the FC12OH self assembles at the hexane/water interface. A likely cause for the stability of the microphase is a short ranged attractive, long ranged repulsive pair potential generated by the surfactant. In virtue of this pair potential, microphases develop near the vapor-solid transition temperature of the monolayer. The full range of the interfacial structure is observed as the temperature is incrementally stepped through the vapor-solid transition including a microphase coexistence of clusters and stripes.

Oral 12

Molecular Orbital Analysis of Multi-Electron Dynamics Driven by an Intense Laser Field

Shu Ohmura,[1] Takayuki Oyamada,[2] Tsuyoshi Kato,[3] Hirohiko Kono,[1] Shiro Koseki[4]

[1]Graduate School of Science, Tohoku University Aoba 6-3, Aoba-ku, Sendai 980-8578, Japan.

[2]Graduate School of Nanobioscience, Yokohama City University, Seto 22-2, Kanazawa-ku, Yokohama 236-0027, Japan.

[3]School of Science, The University of Tokyo, Hongo 7-3-1, Bunkyo-ku, 113-0033, Japan.

[4]Graduate School of Science, Osaka Prefecture University, Gakuencho 1-1, Naka-ku, Sakai 599-8531, Japan.

Email: b2sm5017@s.tohoku.ac.jp

Key words: electron dynamics, intense laser field, tunnel ionization, multiconfiguration theory

Introduction Ultrashort (~ 1 fs = 10^{-15} s) intense (> 10^{12} W/cm^2) laser pulses have enabled us to induce and investigate attosecond (10^{-18} s) electron dynamics. The elucidation of the principles of such electron dynamics is one of the most fundamental and challenging subject for both physics and chemistry. We have developed time-dependent multiconfiguration theory based on the molecular orbital picture [1] to theoretically quantitate the electron dynamics driven by an intense laser field. Our method can simulate the dynamics of molecular orbitals including multi-electron correlation. We applied it to a LiH molecule (ground configuration: $1\sigma^2 2\sigma^2$).

Result and discussion Figure 1 shows the calculated dynamics of the 2σ orbital (HOMO). We assumed a two cycle pulse linearly polarized along the molecular axis. 2σ moves along the direction of the laser force during the initial few femtoseconds. In order to understand the mechanism of the dynamics within the molecular orbital picture, we introduced "chemical potential" of each molecular orbital and found that the HOMO strongly interacts with the inner shell orbital (1σ) which hardly responds to the laser field. The results indicate that the interaction between multiple orbitals beyond the conventional single-active-electron model plays a key role for understanding the electron dynamics.

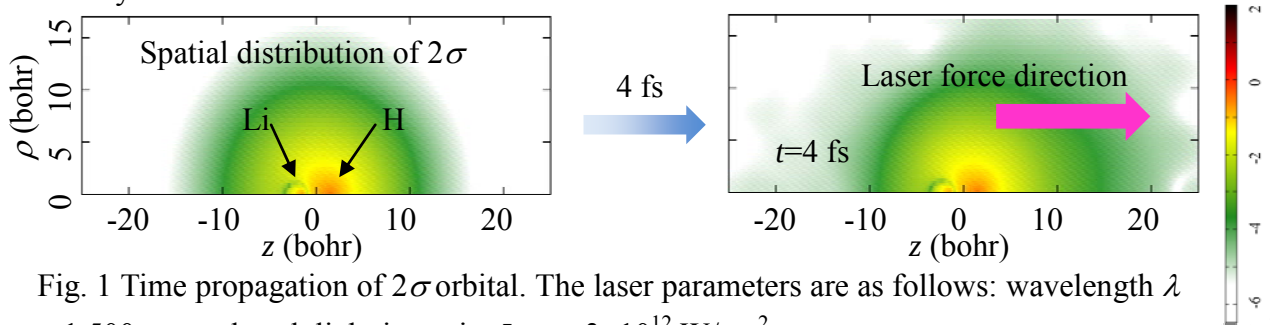

Fig. 1 Time propagation of 2σ orbital. The laser parameters are as follows: wavelength $\lambda \approx 1{,}500$ nm and peak light intensity $I_{peak} \approx 3\times10^{12}$ W/cm^2.

[1] T. Kato and H. Kono, *J. Chem. Phys.* **128**, 184102 (2008).

Oral 13 (Invited)

The Development of a Palladium-Catalyzed Asymmetric Conjugate Addition of Arylboronic Acids to Cyclic Conjugate Acceptors.

Jeffrey C. Holder,[1] Alexander N. Marziale,[1] Michele Gatti,[1] Kotaro Kikushima,[1] and Brian M. Stoltz.[1]

[1]Warren and Katharine Schlinger Laboratory for Chemistry and Chemical Engineering, Division of Chemistry and Chemical Engineering, California Institute of Technology, Pasadena, California 91125, United States of America.

Email: jholder@caltech.edu

Key words: asymmetric catalysis, conjugate addition, palladium catalysis

The first enantioselective palladium-catalyzed, asymmetric construction of all-carbon quaternary stereocenters via 1,4-addition of arylboronic acids to cyclic, β-substituted enones is reported.[1] A wide range of arylboronic acids and cyclic enones are reacted utilizing a catalyst prepared from $Pd(OCOCF_3)_2$ and a chiral pyridinooxazoline ligand to yield enantioenriched products bearing benzylic stereocenters. Notably, this transformation is insensitive to air or moisture, providing a practical and operationally simple method of synthesizing enantioenriched all-carbon quaternary stereocenters.

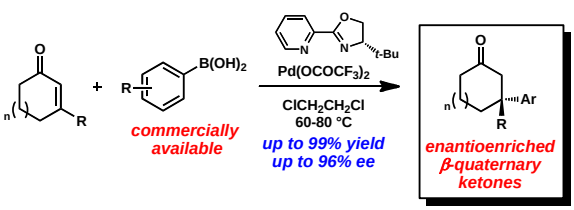

Fig. 1. Asymmetric conjugate addition of arylboronic acid to cyclic conjugate acceptor.

Ref. [1] Kikushima, K.; Holder, J. C.; Gatti, M.; Stoltz, B. M. *J. Am. Chem. Soc.* **2011**, *133*, 6902.

Oral 14

Iridium-Catalyzed Asymmetric Hydrogenation with (a*S*)-Ir/^{i}Pr-BiphPHOX Catalyst and its Mechanistic Study by NMR and DFT Computational Analyses

Yuanyuan Liu,[1,2] Ilya D. Gridnev,[2] Masahiro Terada,[2] and Wanbin Zhang[1]
[1]School of Chemistry and Chemical Engineering, Shanghai Jiao Tong University, 800 Dongchuan Road, Shanghai 200240, China.
[2]Graduate School of Science, Tohoku University, Aramaki 6-3, Aobaku, Sendai 980-8578, Japan.
Email: starskyyy@sjtu.edu.cn
Key words: iridium-catalyst, asymmetric hydrogenation, NMR study, DFT computation

Asymmetric hydrogenation by means of efficient chiral catalyst is one of the most important catalytic methods for the preparation of optically active compounds. In numerous catalyst system, iridium complexes with chiral P,N-ligands have attracted much attention because of their easy availability, high catalytic activity and enantioselectivity.[1] Recently, we have developed a novel class of P,N-ligand with an axis-unfixed biphenyl backbone, and applied them in iridium-catalyzed asymmetric hydrogenation of exocyclic α,β-unsaturated carbonyl compounds with high catalytic activity and good to excellent enantioselectivities.[2]

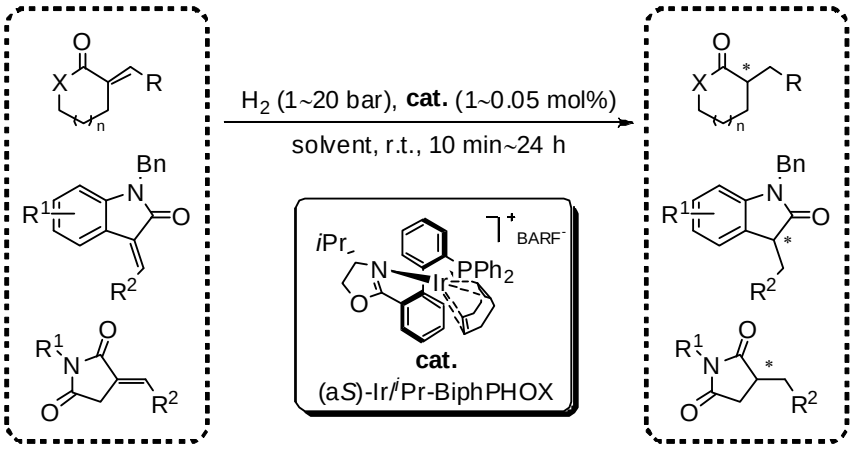

Fig.1 Ir-catalyzed asymmetric hydrogenation with (a*S*)-Ir/^{i}Pr-BiphPHOX

The mechanism of the Ir-catalyzed asymmetric hydrogenation has not been studied in sufficient details, especially with functionalized olefin substrates. In this talk we will present the mechanistic studies on asymmetric hydrogenation of representative prochiral α,β-unsaturated carbonyl compounds with (a*S*)-Ir/^{i}Pr-BiphPHOX catalyst on the basis of experimental and computational combined approaches.

Ref. [1] (a) Roseblade, S. J.; Pfaltz, A. *Acc. Chem. Res.* **2007**, *40*, 1402; (b) Xie, J.-H.; Zhu, S.-F.; Zhou, Q.-L. *Chem. Rev.* **2011**, *111*, 1713.

[2] (a) Liu, Y.; Zhang, W. *Angew. Chem. Int. Ed.* **2013**, *52*, 2203; (b) Yao, D.; Tian, F.; Zhang, W. *Chin. J. Org. Chem*. **2011**, *31*, 505; (c) Liu, Y.; Yao, D.; Li, K.; Tian, F.; Xie, F.; Zhang, W. *Tetrahedron* **2011**, *67*, 8445; (d) Tian, F.; Yao, D.; Liu, Y.; Zhang, W. *Adv. Synth. Catal.* **2010**, *352*, 1841.

Oral 15

Syntheses of Novel Helically Chiral Spirocyclic P3 Phosphazenium Salts

Kengo Goto,[1] Masafumi Oishi,[1] Tadahiro Takeda,[2] Azusa Kondoh,[1] and Masahiro Terada[1]

[1]Graduate School of Science, Tohoku University Aoba 6-3, Aoba-ku, Sendai 980-8578, Japan. [2]Daiichi Sankyo Co., LTD, Tokyo, Japan.

Email: phospohs@s.tohoku.ac.jp

Key words: anion recognition, helical chirality, phosphazenium salt

[Introduction] Anion recognition is rapidly developing field in organic synthesis as well as supramolecular chemistry. Since cinchona alkaloid derivatives were proven to be useful as anion recognition-type phase transfer catalysts in asymmetric synthesis,[1] a variety of anion recognition receptors have been synthesized so far and most of them are derived from quaternary ammonium. The guanidinium is also utilized as an efficient anion recognition moiety, which is a conjugate acid of a relatively strong organic base, guanidine. However the stability of the cationic guanidinium is still insufficient to recognize a variety of anionic species. Therefore, the development of novel chiral anion recognition receptors of stable cationic species is desirable and attractive. In this context, we envisioned that conjugate acids of strong organic superbases would serve as a novel "stable cation-based" chiral anion recognition receptors. To this end we focused on phosphazenium, which is a conjugate acid of organic superbase, as a synthetic target.

[Result and Discussion] Basicity of phosphazene increases with increasing the number of iminophosphorane units (**A**).[2] Meanwhile its conjugate acid, phosphazenium, becomes more stable. With this in mind, we designed a novel P3 phosphazenium salt **1**. This molecule bears helical chirality based on spirocyclic structure. In addition, when forming the contact ion pair between **1** and an anionic molecule, a double hydrogen bonding site introduced into the molecule would function as efficient recognition element in an enantioselective manner. In line with this molecular design, we achieved the syntheses of phosphazenium salt **1a-c** from commercially available sources in several steps. These molecules are expected to be useful as anion recognition receptors such as optical resolution reagents and chiral phase transfer catalysts.

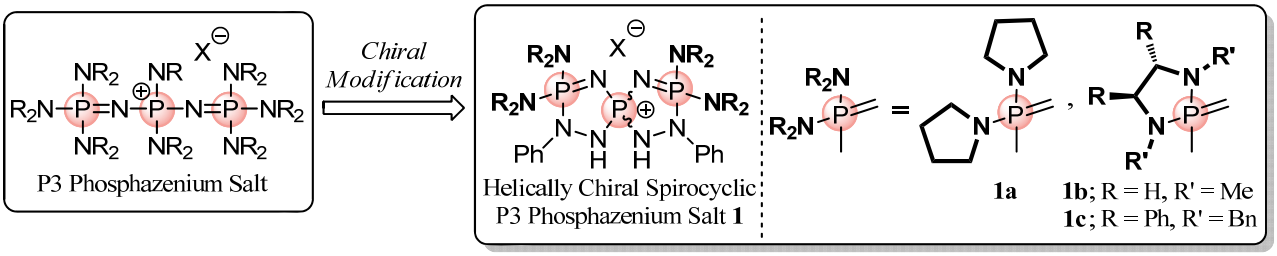

1) O'Donnell, M. J.; Bennett, W. D.; Wu, S. *J. Am. Chem. Soc.* **1989**, *111*, 2353.

2) Schwesinger, R. *Chimia* **1985**, *39*, 269.

Oral 16 (Invited)

Redox-Inactive Metal Ion Effect on the Reactivity of Mononuclear Non-Heme Manganese(IV)-Oxo Complex

Junying Chen,[1] Yong-Min Lee,[1] Katherine M. Davis,[2] Mi Sook Seo,[1] Kyung-Bin Cho,[1] Young Jun Park,[1] Shunichi Fukuzumi,*[,1,3] Yulia N. Pushkar,*,[2] and Wonwoo Nam*,[1]

[1]Department of Bioinspired Science, Chemistry and Nano Science, Ewha Womans University, Seoul 120-750, Korea

[2]Department of Physics, Purdue University, 525 Northwestern Avenue, West Lafayette, Indiana, 47907, USA

[3]Department of Material and Life Science, Graduate School of Engineering, Osaka University ALCA, Japan Science and Technology Agency (JST), Suita, Osaka 565-0871, Japan.

Email: chenjunying@ewhain.net

Key words: metal ion effect, oxygen atom transfer, hydrogen atom transfer

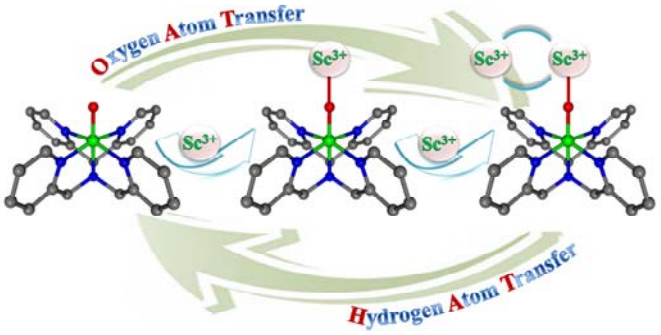

Redox-inactive metal ions play pivotal roles in regulating reactivities of high-valent metal-oxo species in a variety of enzymatic and chemical reactions. A mononuclear nonheme manganese(IV)-oxo complex bearing a pentadentate N5 ligand has been synthesized and used in the synthesis of a Mn(IV)-oxo complex binding scandium ions. The Mn(IV)-oxo complexes are characterized with various spectroscopic methods. The reactivities of the Mn(IV)-oxo complex are markedly influenced by binding Sc^{3+} ions in oxidation reactions, such as ~2200-fold increase in the oxidation of thioanisole (i.e., oxygen atom transfer) but ~180-fold decrease in the C-H bond activation of 1,4-cyclohexadiene (i.e., hydrogen atom transfer). The present results provide the first example of a nonheme Mn(IV)-oxo complex binding redox-inactive metal ions that shows a contrasting effect of redox-inactive metal ions on the reactivities of metal-oxo species in the oxygen atom transfer and hydrogen atom transfer reactions.

[1] S. Fukuzumi, Y. Morimoto, H. Kotani, P. Nammov, Y.-M. Lee, W. Nam, *Nature Chem.*, **2010**, *2*, 756-759.

[2] Y. Morimoto, H. Kotani, J. Park, Y.-M. Lee, W. Nam, S. Fukuzumi, *J. Am. Chem. Soc.*, **2011**, *133*, 403-405.

Oral 17

Charge-Density-Wave to Mott–Hubbard Phase Transition and Charge Dynamics in Bromide-Bridged Pd Chain Compounds

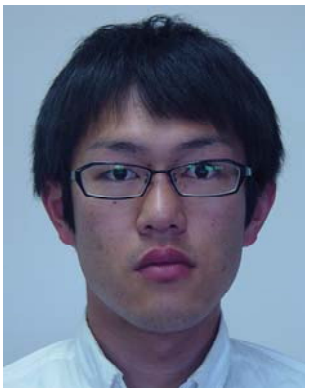

Shohei Kumagai,[1] Shinya Takaishi,[1] and Masahiro Yamashita[1]
[1]Graduate School of Science, Tohoku University Aramaki Aza-Aoba 6-3, Aoba-ku, Sendai 980-8578, Japan.
Email: s-kumagai@s.tohoku.ac.jp
Key words: one-dimensional material, phase transition, dielectric property

One-dimensional (1D) electronic materials are attractive because they have anisotropic optical and electronic properties and show anomalous physical properties such as metal–insulator transition. Quasi-1D halogen-bridged metal complexes (MX chains) are one of the 1D electronic materials, and have –M–X–M–X– (M: metal ions, X: halide ions) chain structures. So far, many interesting chemical and physical properties have been reported in MX chains, such as an intense and dichroic charge transfer band and gigantic third-order nonlinear optical susceptibility.

MX chains are composed of M (M = Ni, Pd or Pt), X (X = Cl, Br or I), in-plane ligands (L), and counterions (Y). By changing these components, MX chains alternatively have two electronic states In fact, Pd and Pt compounds form mixed valence states, represented as –M(IV)–X····M(II)····X–. This Peierls distorted 1D structure is also called charge-density-wave (CDW) state. On the other hand, Ni compounds form averaged-valence Mott–Hubbard (MH) state, represented as –M(III)–X–M(III)–. Although more than 300 MX chains have been synthesized, all of the Ni compounds, and Pd and Pt compounds had formed MH and CDW states, respectively, without exception.

However, we have synthesized and characterized Pd(III) MH state for the first time [1]. The counterions with long alkyl chains were introduced into bromide-bridged Pd compounds, $[Pd(en)_2Br](C_n\text{-}Y)_2(H_2O)$ (en = ethylenediamine; C_n-Y = dialkylsulfosuccinate; n = the number of carbon), to shorten neighboring Pd–Pd distance because MX chains in CDW states approach MH states as Pd ions come closer. Moreover, the compounds showed a phase transition from CDW to MH state as temperature decreased, for example, n = 5 transferred at 206 K, which is reverse to a normal Peierls transition. In order to observe the charge fluctuation upon the transition, the dielectric properties were measured along chain directions. An anomalous charge fluctuation was observed at the phase transition temperature as a clear rise of dielectric constant.

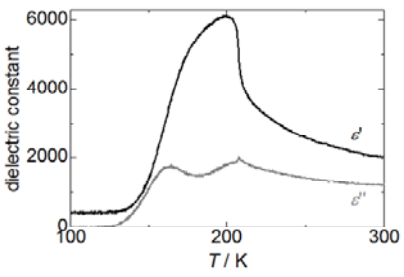

Fig 1. dielectric spectra of n = 5 (f = 10 kHz)

Ref. [1] S. Takaishi *et al.*, *J. Am. Chem. Soc.* **2008**, *130*, 12080

Oral 18

Infrared spectroscopy of cationic tetrahydrofuran(THF) and its dimer

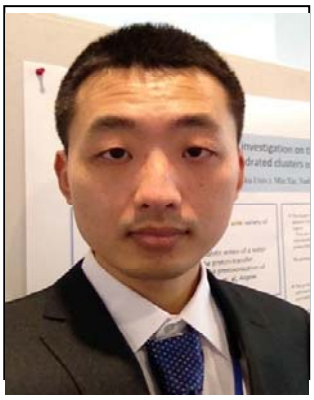

Min Xie, Yoshiyuki Matsuda, Tomoya Endo, Asuka Fujii
Graduate School of Science, Tohoku University, Aramaki-Aoba, Aoba-ku, Sendai, 980-8578, Japan.
Email: xiemin821@163.com
Key words: infrared spectroscopy, cation, proton transfer, CH bond

We have studied ionization dynamics of clusters with infrared (IR) predissociation spectroscopy based on the vacuum-ultraviolet (VUV) photoionization detection. [1] Upon the ionization of clusters of protic molecules such as methanol, ammonia, and acetic acid, the barrier-less proton-transfer reactions have been clarified from the OH and NH bonds. [1] These indicate high acidities of cationic OH and NH. Neutral CH is normally regarded as aprotic because of low acidities of the CH bonds. However, likewise cationic OH and NH, high acidities of CH may be expected in cationic states.

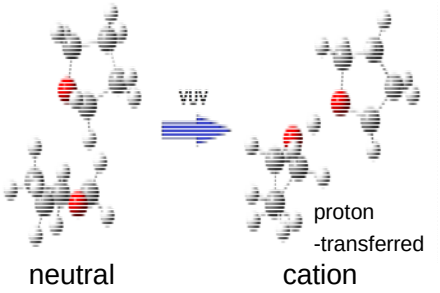

Fig. 1 Photoionization-induced isomerization of THF dimer

In this study, to investigate acidities of cationic CH, we have studied the cationic monomer and dimer of tetrahydrofuran (THF) with the IR spectroscopy and theoretical calculations. THF has the alkyl ring and the oxygen atom which acts the proton acceptor. Therefore, we can simply study the acidity of CH of the THF cation. The structures of the neutral and cationic THF were analyzed with the IR spectroscopy. The determined structures are depicted in Fig. 1. The THF dimer cation forms the proton-transferred structure which is formed through the proton-transfer reaction from CH after the photoionization. Fig. 2 shows the potential energy curve obtained by the intrinsic reaction coordinate (IRC) calculation from the vertically-ionized state. As seen in the plot, no effective energy barrier exists in the proton-transfer from CH in the ionized THF dimer. These results demonstrate that CH of cationic THF is acidic. We have also observed the intense stretch band of acidic CH of the bare THF cation out of normal CH stretch frequency region. We will discuss the acidity of the THF cation with the results of above-mentioned IR spectra of the cationic THF monomer and dimer.

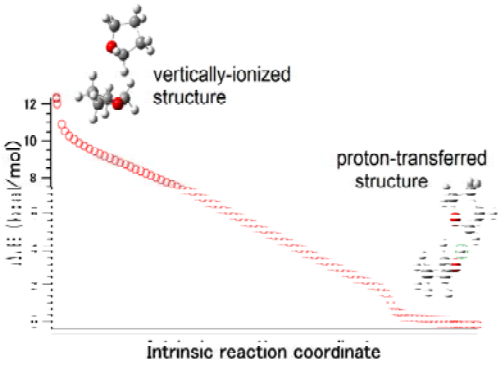

Fig.2 The intrinsic reaction coordinate (IRC) potential energy curve of THF dimer cation from the vertically-ionized structure to the proton-transferred structure

Ref. [1] Y. Matsuda, *Phys. Chem. Chem. Phys.*, **2009**, 11, 1279-1290.

Oral 19 (Invited)

Practical Utilization of Boehm Titration for Surface Characterization of Carbon Nanomaterials

Yern Seung Kim, Seung Jae Yang, Taehoon Kim, Kunsil Lee, and Chong Rae Park*

Carbon Nanomaterials Design Laboratory, Global Research Laboratory, Research Institute of Advanced Materials, and Department of Materials Science and Engineering, Seoul National University, Seoul 151-744, Korea

Email: nixenrpg@snu.ac.kr

Key words: Boehm Titration, Carbon Dioxide, Acidic Carbonaceous Compounds

For the surface characterization of carbonaceous materials, a number of research groups have adopted Boehm titration method which applies the selective neutralization of the surface functional groups (carboxylic, lactonic, and phenolic) with the different strength of base (NaOH, Na_2CO_3, and $NaHCO_3$) solutions called reaction bases [1].

However, Boehm titration involves a few sophisticated issues to be resolved for its easy utilization. One of the problems is dissolution of unexpected moieties including atmospheric carbon dioxide (CO_2) and acidic carbonaceous compounds (ACCs) into the reaction bases [2-4]. In addition, the experimental procedures, including reaction, filtration and titration, are rather complicated comparing to the other surface characterization methods.

To elucidate these problems in Boehm titration, we suggest a fundamental approach for analysis of Boehm titration results regardless of the dissolution of CO2 [3] or ACCs [4] in the reaction base. Furthermore, the alternative one-pot methodology for obtaining the Boehm titration results are developed adopting a direct titration method [5].

Ref.

[1] H. P. Boehm, *Carbon* **1998**, 32, 759.

[2] S. L. Goertzen et al., *Carbon* **2010**, 48, 759.

[3] Y. S. Kim et al., *Carbon* **2012**, 50, 1510.

[4] Y. S. Kim et al., *Carbon* **2012**, 50, 3315.

[5] T. J. Bandosz et al., *Carbon* **1993**, 31, 1193.

Oral 20

Preparation and Observation Materials on Clean Graphene by Transmission Electron Microscope

Yuki Sasaki[1], Ryo Kitaura[1], Yuta Yamamoto[2], Shigeo Arai[2],
Hisanori Shinohara[1]
[1] Department of chemistry and institute for advanced research,
Nagoya University, Nagoya, 464-8602, Japan
[2] High Voltage Electron Microscope Laboratory, Ecotopia Science Institute,
Nagoya University, Nagoya 464-8602, Japan
E-mail: sasaki.yuki@d.mbox.nagoya-u.ac.jp
Key words: graphene, TEM, gold, water liquid cell

High-resolution transmission electron microscopy (HRTEM) provides real-space and real-time information on structures of nanomaterials[1]. One of the most important issues for HRTEM observations of nanomaterials is the way to support samples. Due to the atomically thin structure and high electrical and thermal conductivity, graphene is the ideal support materials for HR-TEM observation [2]. In this work, we have developed a preparation method of clean free-standing graphene that is suitable to support various nanomaterials, and applied the graphene sample support to observe various nanostructures by aberration-corrected TEM.

Clean free-standing graphene was prepared by chemical vapor deposition and direct polymer-free transfer method[3]. Figure (a), (b) shows an example of HRTEM image after a deposition of Au, where an array of spot contrasts was clearly observed. The obtained structure possesses specific two-dimensional structure, which is significantly different from that of bulk Au crystal[4]. Furthermore, we have applied the free-standing graphene to observe water, and found a peculiar phase behavior. In this presentation, details of the sample preparation and structural analyses will be discussed.

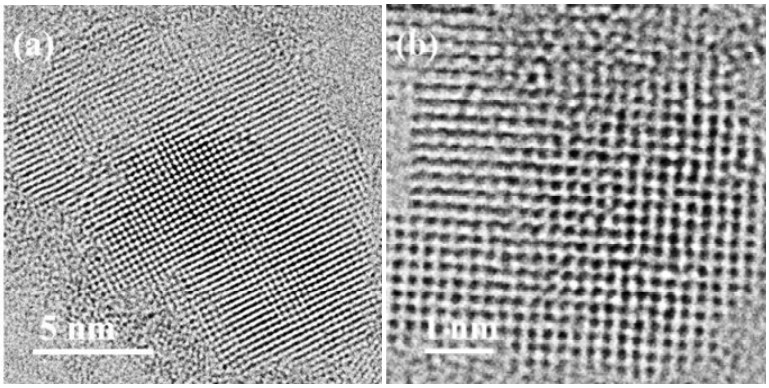

Figure (a) Typical HRTEM image of Au nanostructure on graphene at low magnification and (b) at high magnification.

Ref.[1] R. Kitaura, et.al., *Nano Lett.*, **2008**, 8, 693.
Ref.[2] A. W. Robertson, et.al., *ACSNano*, **2011**, 5, 6610.
Ref.[3] Y. Sasaki, et.al., *Appl. Phys. Express*, **2012**, 5, 065103.
Ref.[4] M. Schmidt, et.al., *Nature*, **1998**, 393, 238.

Oral 21 (Invited)

Multilayered graphene membrane: a novel porous carbon for capacitive energy storage

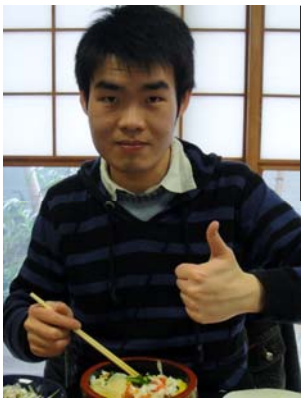

Chi Cheng,[1] Xiaowei Yang,[1] Junwu Zhu[1] and Dan Li[1]

[1]Department of Materials Engineering, Monash University, VIC 3800, Australia.

Email: david.cheng@monash.edu

Key words: chemically converted graphene, solution/colloid chemistry, porous carbon, capacitive energy storage

From a chemistry point of view, graphene is essentially a giant, two dimensional conductive macromolecule. It is also the fundamental building unit for carbon materials. As engineering carbon materials with desired properties comes down to judicious structural design at molecular scale, the ability of assembling graphene in a controlled, manipulable way is favorably demanded. Taking advantage of the intrinsic micro-corrugated two-dimensional configuration and the unique colloid chemistry of solvated graphene, we have successfully created in parallel a series of multilayered graphene assemblies (**Fig. 1**) with designable porous structure. Electrochemical capacitors based on these multilayered graphene membranes (MGMs) obtain specific energy (against active storage materials) approaching 120 Wh/kg. More importantly, the structurally designed MGMs represent themselves a novel platform that can be capitalized on towards researching fundamental problems relating to energy and nano-confined ionics.

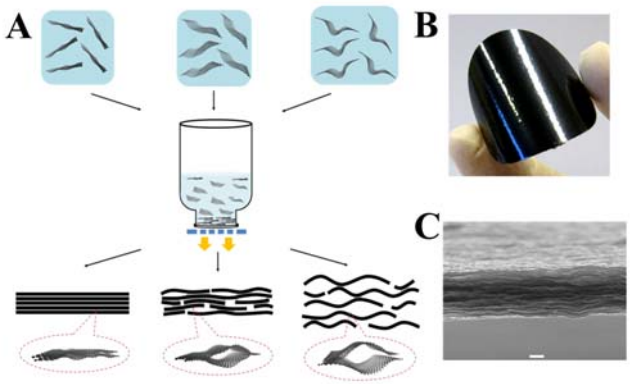

Fig. 1 Multilayered graphene membranes (MGMs) (A) Structural tuning of MGMs through control of the corrugation level of chemically converted graphene. (B) Image of an assembled MGM. (C) SEM image of the cross section of a MGM.

[1] D. Li et al., *Nat. Nanotechnol.* **2008**, 3, 101-105.

[2] X. Yang et al., *Angew. Chem. Int. Ed*. **2011**, 5, 7325-7328.

[3] C. Cheng et al., *Adv. Mater*. **2013**, 1, 13-30.

Lecture 4

Chemical Strategies for Discovering Unidentified Protein-Small Molecule Interactions

Naoki Kanoh
Graduate School of Pharmaceutical Sciences, Tohoku University, 6-3 Aza-Aoba, Aramaki, Aoba-ku, Sendai 980-8578, Japan.
Email: nkanoh@m.tohoku.ac.jp
Key words: chemical biology, protein-small molecule interaction, affinity purification, microarray, cytochrome P450

The discovery of unidentified interactions between cellular proteins and small organic molecules has been particularly important in the area of chemical biology. Historically, identification of cellular targets for bioactive small molecules has led to the discovery of novel functions of the target proteins and the signaling networks involving them. Also, discovery of small molecule ligands for proteins of interest has clarified our understanding of the protein's function in cells. Various technologies have been developed during the last several decades to facilitate the discovery process: however, this process is still a major bottleneck in chemical biology research, and technologies to solve this bottleneck are needed.

To this end, we have developed a unique "affinity purification" platform, in which small molecules are "photo-cross-linked" in a highly non-selective manner on affinity matrices [1] and in a miniaturized microarray format.[2] To the best of our knowledge, this sort of "random" chemistry has not previously been used to immobilize small molecules on a solid surface, but the resultant platforms have been found to be useful and are being utilized for the successful discovery of unidentified protein-small molecule interactions. The details of this method will be presented in the first part of my presentation.

In the second part of my talk, I will describe the screening platform to discover and identify substrates for cytochrome P450 enzymes.[3] P450 enzymes are widely found in nature and are distributed in most organisms. However, the functions of many of these enzymes are remain unclear because their substrates are unknown. We have recently developed a high-throughput fluorogenic screening method to identify P450 substrates from a library of small molecules. This platform is thought to be useful not only for screening substrates for orphan P450 enzymes, but also for determining substrate specificity for engineered P450s.

References

[1] *Angew. Chem. Int. Ed.* **2005**, *44*, 3559-3562; *Bioconjugate Chem.* **2010**, *21*, 182-186.
[2] *Chem. Asian J.* **2006**, *1*, 789-797.
[3] *ChemBioChem* **2011**, *12*, 2748-2752.

Oral 22 (Invited)

Genomics-Based Discovery of Secondary Metabolites from the Human Pathogenic *Burkholderia mallei* Family.

Jakob Franke,[1] Keishi Ishida,[1] Thorger Lincke,[1] Swantje Behnken,[1] Mie Ishida-Ito,[1] and Christian Hertweck[1]

[1] Leibniz Institute for Natural Product Research and Infection Biology, Hans-Knoell-Institute, Dept. Biomolecular Chemistry, Beutenbergstr. 11a, 07745 Jena, Germany.

Email: jakob.franke@hki-jena.de

Key words: *Burkholderia*, genome mining, polyketide, siderophore, virulence factor

Burkholderia mallei and *Burkholderia pseudomallei* are dangerous pathogenic bacteria that cause the diseases glanders and melioidosis, respectively, in humans and animals. Both species have been classified as biological warfare agents due to their high infectivity and mortality rates of up to 50%. Surprisingly, details about the infection process, especially regarding the role of small molecules, have remained obscure. To fill this gap, we investigated the least infective member of the *B. mallei* family, *Burkholderia thailandensis*. By exploiting genomic data we brought several natural products to light that have been either overlooked like thailandamide A (**1**),[1] neglected like malleobactin A (**2**)[2] or remained cryptic under normal culture conditions like burkholderic acid (**3**).[3,4]

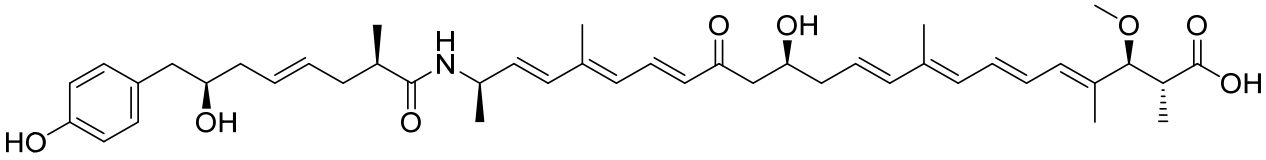

thailandamide A (**1**)

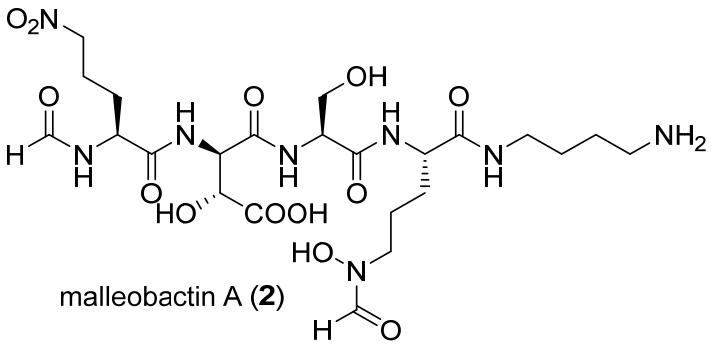

malleobactin A (**2**)

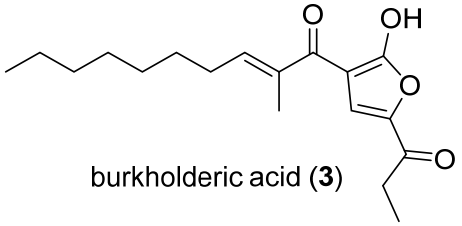

burkholderic acid (**3**)

Our studies are therefore important to support research on infections with *B. mallei*-like strains and contribute to the general methodology for finding novel secondary metabolites.

[1] T. Nguyen, K. Ishida, H. Jenke-Kodama, E. Dittmann, C. Gurgui, T. Hochmuth, S. Taudien, M. Platzer, C. Hertweck, J. Piel, *Nat. Biotechnol.* **2008**, *26*, 225–233.

[2] J. Franke, K. Ishida, M. Ishida-Ito, C. Hertweck, *Angew. Chem. Int. Ed.* **2013**, accepted.

[3] J. Franke, K. Ishida, C. Hertweck, *Angew. Chem. Int. Ed.* **2012**, *51*, 11611–11615.

[4] J. B. Biggins, M. A. Ternei, S. F. Brady, *J. Am. Chem. Soc.* **2012**, *134*, 13192–13195.

Oral 23

Single-Cell comprehensive gene expression analysis during cell differentiation

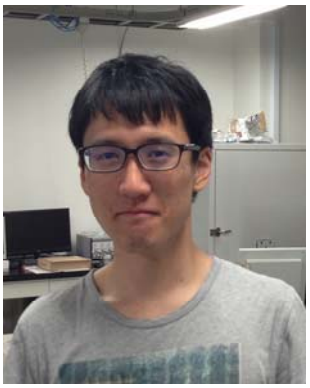

Ikuma Fujisawa[1], Yuanshu Zhou[1], Kosuke Ino[1], Hitoshi Shiku[1], Tomokazu Matsue[1,2]

[1]Graduate School of Environmental Studies, Tohoku University, Aoba 6-6-11-604, Aoba-ku, Sendai 980-8579, Japan.

[2]World Premier International Advanced Institute for Materials (WPI-AIMR), Tohoku University Katahira 2-1-1, Aoba-ku, Sendai 980-8577, Japan.

Email: fujisawa@bioinfo.che.tohoku.ac.jp

Key words: single cell, gene expression, cell differentiation

Gene expression has highly variable mRNA levels between individual cells, even in a seemingly homogeneous cell population. Access to fundamental information about cellular mechanisms, such as correlated gene expression, motivates measurements of multiple genes in individual cells. Since there must be some relationship between heterogeneity and cell differentiation, we quantified the number of mRNA of differentiated culture HL-60 cells (human Leukemia cell line) at single cell level using high throughput single-cell measurement systems combined with FACS (Fluorescence-activated cell sorting) and comprehensive Real-Time PCR.

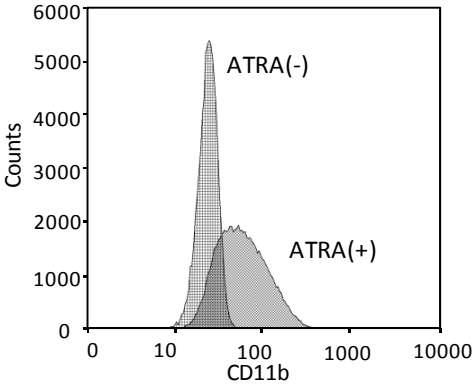

Fig.1. Expression of CD11b analyzed by FACS

To differentiate cell to the granulocyte-like cells, the cells were incubated with 1 μM All-trance retinoic acid (ATRA) for 4 days. We collected single cells and detected the granulocyte marker CD11b expression by using FACS. Then the RT reaction was carried out to synthesize the first-stand cDNA. Finally, the Real-Time PCR was performed by the microfluidic dynamic arrays system (Fluidigm).

FACS data and cell viability late showed that approximately 50% cells were induced to granulocyte-like cells by ATRA. Although absolute gene expression of *GAPDH* was same level between single-cell and multi-cell, *GAPDH* relative expression indicated distinct large variation in single cell level. This behavior seemed to derive from the heterogeneity of the individual single-cell Now we investigate other gene expression levels and their distributions.

Oral 24

Controlled encapsulation and release of guest molecules from a caged protein, ferritin by an external stimulus

Takahiro Nakao,[1] Takashi Fukushima,[3] Hiroshi Nakajima[1] and Yoshihito Watanabe[1, 2]

[1]Department of Chemistry, Graduate School of Science, Nagoya University Furo-cho, Chikusa-ku, Nagoya 464-8602, Japan.

[2]Reserch Center for Materilas Science (RCMS), Nagoya University Furo-cho, Chikusa-ku, Nagoya 464-8602, Japan

[3]Institute for Integrated Cell-Material Sciences (iCeMS), Kyoto University Yosida Ushinomiya-cho, Sakyo-ku, Kyoto 606-8501, Japan

Email: nakao.takahiro@h.mbox.nagoya-.ac.jp

Key words: drug delivery system, caged protein, ferritin, iron release

Ferritin is an iron strage protein with spherical structure, composed of 24 subunits (Fig.1 a). There are eight channels around the 3-fold axes, which is assumed that the 3-fold channels function as both entry and exit routes for iron ions or small organic molecules. The spherical structure of ferritin has attracted much attention as a carrier for drug delivery system (DDS). In recent studies, encapsulation of drug molecules into the ferritin cavity was achieved by dissociation and reassembly of ferritin subunits. However encapsulated drug molecules couldn't be released from the ferritin at target site. It is necessary to control encapsulation and release for efficient DDS. In this study, at the first step for control of encapsulation and release of guest molecules from ferritin cavity, simplified mechanism was designed, in which molecular flow through the 3-fold channels is inhibited by introduction of alkyl chains around the 3-fold channels.

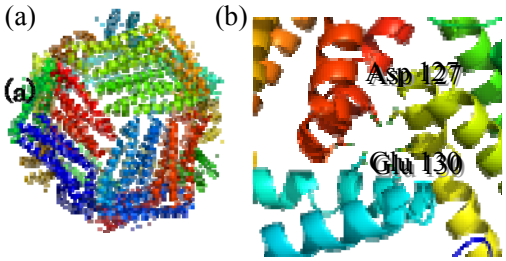

Fig. 1 crystal structure of ferritin
(a) overview (b) 3-fold channel

Iron release from the ferritin including oxide iron core was triggered by reduction of Fe(III) with flavin mononucleotide (FMN). Initial rate of iron release from ferritin cavity decreased with elongation of alkyl chains (Fig.2). I suggested that flow of FMN though the 3-fold channel is inhibited by alkyl chains. Furthermore, in order to close the 3-fold channel, I introduced pyridine near the 3-fold channels and a metal complex is formed between cap molecule and pyridine modified ferritin. I measured molecular pass of pyridine modified ferritin with binding cap molecules onto 3-fold channel.

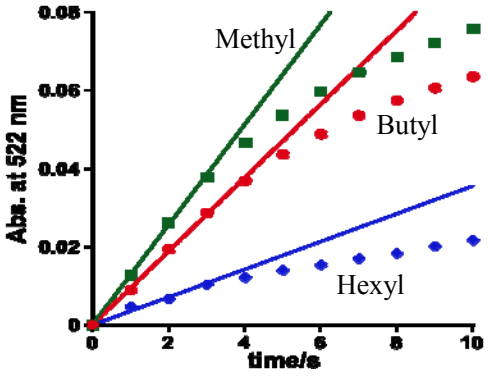

Fig. 2 Iron release rate. Decreasing of iron release rate with elongation of alkyl chain, Methyl-, Butyl-, Hexyl modified ferritin

Poster Abstract

Poster 1

Design of the efficient cross-linking agent with the fixed conformation

Yuta Ida,[1] Shuhei Kusano,[1] Shinya Hagihara,[1,2] and Fumi Nagatsugi[1,2]
[1]Graduate School of Science, Tohoku University, Sendai, Japan
[2]Institute of Multidisciplinary Research for Advanced Materials, Tohoku University, Sendai, Japan
Email: y-ida@mail.tagen.tohoku.ac.jp
Key words: RNA; cross-link; antisense; oligonucleotide; fixed conformation

[**Introduction**] The artificial control of gene expression by synthetic oligonucleotide (ONs) has been the subject of considerable interest. In particular, crosslink forming oligonucleotides (CFOs) have been expected to enhance the inhibitory effect. Recently, we have developed 2-amino-6-vinylpurine (AVP) as a crosslinking nucleobase that reacts selectively with uridine residue in RNA. However, the slow reaction rate of AVP with the target uracil is one of obstacle for in-cell crosslinking. The vinyl group of AVP can adopt two conformations, s-cis and s-trans, as shown in Fig.1 and AVP with s-trans conformation does not undergo the cross-linking reaction to uridine. We assumed that the slow reaction rate of AVP can be attributed to the equilibrium between two conformations. Thus, we designed the novel AVP analog (**1**) and (**2**), which were expected to be fixed the s-cis conformation with favorable for the crosslinking reaction. In this presentation, we report the synthesis of CFO containing (**1**) and (**2**), and the evaluation of these reactivity.

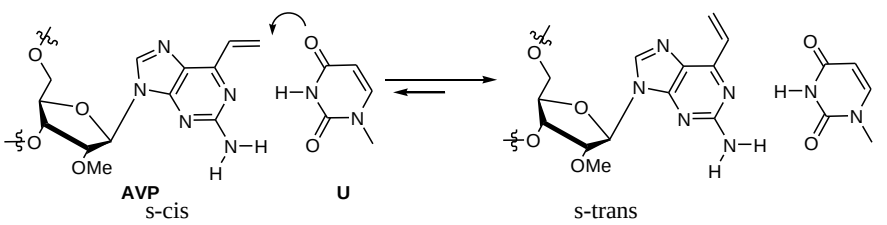

Fig.1. The equilibrium between two conformations of 2-AVP

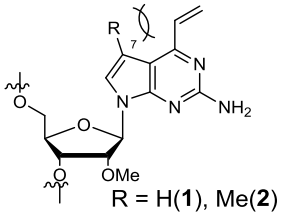

Fig.2. Structure of the novel cross-linking

[Result and discussion] 2'-OMe RNA oligonucleotide containing **3** was synthesized with DNA automatic synthesizer. The sulfide-protected 2'-OMe RNA oligonucleotide was smoothly converted to **4** by oxidation with magnesium monoperphthalate (MMPP) following an alkaline condition. The cross-linking reaction was investigated with **4** to a target RNA. CFO **4** reacted to a uracil base on the target position of RNA with highly selective and in good yields under neutral conditions. It is notable that the deaza derivative (**1**) with more electron rich than 2-AVP showed the similar reactivity to that of 2-AVP. Now, we investigate the synthesis of CFO containing **2** and we would like to present the reactivity of the synthesized these CFOs in detail.

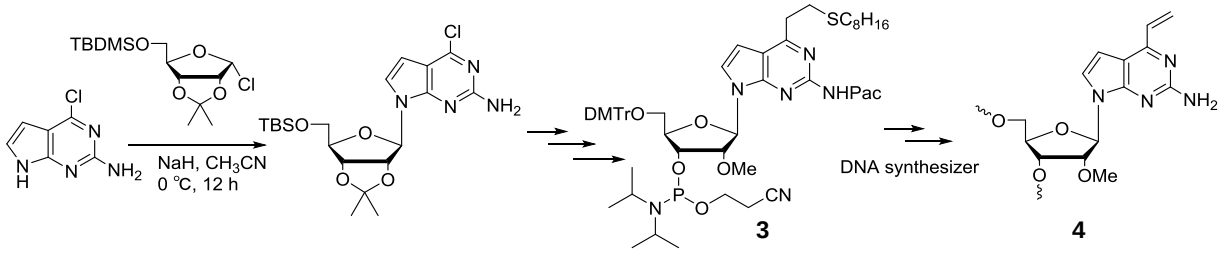

Poster 2

Development of Membrane-Spanning Stimuli-Responsive Synthetic Molecules

Kaori Umetsu,[1] Takahiro Maraoka,[1] and Kazushi Kinbara[1]
[1]Institute of Multidisciplinary Research for Advanced Materials (IMRAM), Tohoku University Katahira 2-1-1, Aoba-ku, Sendai 980-8577, Japan.
Email: k-umetsu@mail.tagen.tohoku.ac.jp
Key words: multipass transmembrane protein, amphiphile, stimuli responsiveness

Membrane proteins play important vital roles such as transport of substances and information across a cytoplasmic membrane. Among various membrane proteins, multipass transmembrane proteins are intriguing research targets because of their dynamic features in response to external stimuli. Multipass transmembrane proteins are composed of alternating hydrophobic and hydrophilic components, where the hydrophobic components span the membrane and the hydrophilic ones are exposed to aqueous media to fold into the multipass transmembrane conformation. Triggered by an external stimulus such as ligand-docking, or thermal, electrochemical, photochemical and mechanochemical input, the conformation and/or orientation of the membrane-spanning hydrophobic components changes. For instance, rhodopsin in the retina is a photoresponsive multipass transmembrane protein in which a photochemical reaction of the retinal cofactor triggers a conformational change of opsin to initiate a signal transduction cascade. Another example includes mechanosensitive ion channels in the inner ear, which bare membrane proteins capable of responding to mechanical stress such as tension in the surrounding lipid bilayer to regulate the gating of ion transportation.

Inspired by these abundant examples seen in nature, we have been developing synthetic mimics of stimulus-responsive transmembrane proteins, and already reported the synthetic multipass transmembrane molecules which allow ion transportation across a phospholipid bilayer.[1],[2] Synthetic details and spectroscopic characterization of the synthetic stimulus-responsive transmembrane molecules will be presented.

[1] T. Muraoka *et al.*, *Chem. Commun.* **2011**, *47*, 194–196 (Hot Article).
[2] T. Muraoka *et al.*, *J. Am. Chem. Soc.* **2012**, *134*, 19788–19794.

Poster 3

Creation of a Photoresponsive module based on the engineered PYP

Yusuke Miyauchi, Mihoko Ui, Makoto Murakami, Yasuyuki Araki, Takehiko Wada, and Kazushi Kinbara
Institute of Multidisciplinary Research for Advanced Materials (IMRAM), Tohoku University Katahira 2-1-1, Aoba-ku, Sendai 980-8577, Japan.
Email: y.m@mail.tagen.tohoku.ac.jp
Key words: Photoactive Yellow Protein, Photoresponsivity, Homopropargylglycine, Huisgen cycloaddition reaction, Photoresponsive biodevice

Photoactive Yellow Protein (PYP) is known as a photoreceptor and exhibits the photocycle as shown in Fig. 1(a).[1] PYP contains *p*-coumaric acid chromophore linked covalently to Cys69 via a thioester bond. The chromophore undergoes *trans*-to-*cis* photoisomerization by irradiation with 446 nm light, which causes unfolding of the higher-order structure, followed by thermal *cis*-to-*trans* isomerization to recover the initial *trans* configuration. PYP has a potential for application as a photoresponsive device, of which properties can be controlled by light due to its remarkable structural change caused by light irradiation. Here, we tried to construct a photoresponsive module that can be attached selectively to a target molecule at the appropriate site. Homopropargylglycine (Hpg), that was a synthetic amino acid bearing an alkyne group, was incorporated into PYP molecule instead of the methionine by using *E. coli* B834(DE3) expression system. The UV-vis absorption spectroscopy in the dark and under light irradiation showed that Hpg-incorporated PYP had the almost same photocycle as that of wild-type PYP except for the elongated lifetime of the transition from I_2' to P. The mass spectroscopy and SDS-PAGE analysis suggested that Hpg-incorporated PYP could bind to a target molecule bearing azide groups via Huisgen cycroaddition reaction that enabled site-specific modification of a target molecule with PYP. We will report the preparation and characteristics of Hpg-modified PYP in detail.

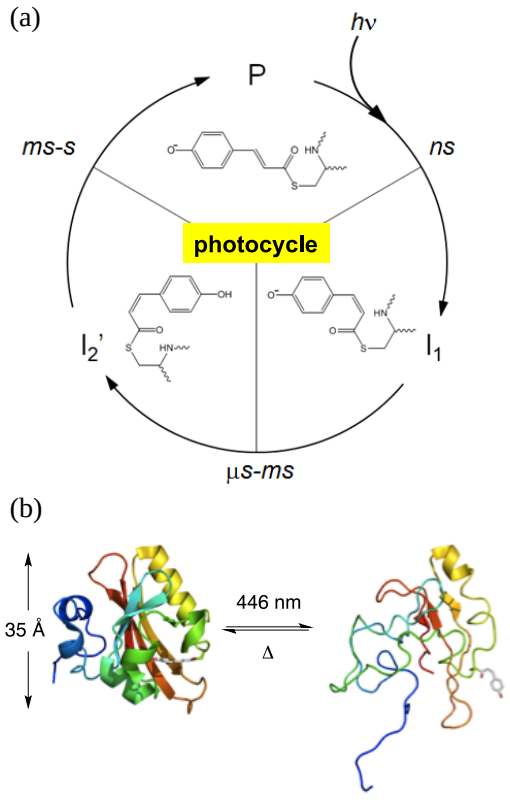

Fig. 1 (a) PYP photocycle. (b) Conformational change of PYP upon light irradiation.

[1] P. L. Ramachandran et al, *J. Am. Chem. Soc.* **2011**, *133*, 9395-9404

Poster 4

Nanoporous Gold for Heterogeneous Catalytic Reduction of Amides

Makoto Nishiguchi,[1] Naoki Asao,[1,2] Yoshinori Yamamoto,[2] and Tienan Jin[1,2]
[1]Graduate School of Science, Tohoku University, Sendai, Japan
[2]WPI Advances Institute for Materials Research, Tohoku University, Sendai, Japan
Email: nisiguti2494@hotmail.co.jp
Key words: Amide, Organosilane, Nanoporous gold, Heterogeneous reduction

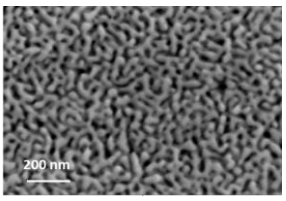

Figure 1. SEM image of AuNPore.

The interesting features of nanoporous gold (AuNPore), such as the three-dimensional (3D) bicontinuous network structure, high surface area, nontoxic nature, high fabrication reproducibility, high recyclability, and rather simple recovery, make it an attractive candidate for a new heterogeneous catalyst. Recent advances in catalytic applications of AuNPore demonstrated its excellent catalytic performance on selective oxidation reactions.[1] However, the catalytic property of AuNPore for the selective reduction has been less investigated.[2] Herein, we report that AuNPore exhibits a remarkable catalytic activity in the reduction of amides to amines.

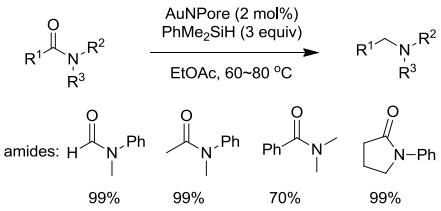

Scheme 1. AuNPore-catalyzed reduction of amides.

AuNPore catalyst was fabricated by the selective dealloying of silver from $Au_{30}Ag_{70}$ alloy foil using 70% HNO_3 for 18 h at room temperature. A scanning electron microscopy (SEM) image reveals that the ligament and nanopore channel are formed uniformly across the entire AuNPore with an average ligament size of ~30 nm (Figure 1). The catalytic reduction activity of AuNPore was examined with various amides in the presence of AuNPore (2 mol%) and dimethylphenylsilane (3 equiv) in ethyl acetate (1 M) at 60 ^{o}C or 80 ^{o}C (Scheme 1). Not only acyclic amides but also cyclic amides produced the corresponding amines in good to high yields. The detailed investigations including the optimization of conditions, substrate scope, reusability, and mechanism will be discussed in this presentation.

Reference

1) (a) N. Asao, N. Hatakeyama, Menggenbateer, T. Minato, E. Ito, M. Hara, Y. Kim, Y. Yamamoto, M. Chen, W. Zhang, A. Inoue, *Chem. Commun*. **2012**, *48*, 4540. (b) N. Asao, Y. Ishikawa, N. Hatakeyama, Menggenbateer, Y. Yamamoto, M. Chen, W. Zhang, A. Inoue, *Angew. Chem. Int. Ed*. **2010**, *49*, 10093.

2) (a) M. Yan, T. Jin, Y. Ishikawa, T. Minato, T. Fujita, L.-Y. Chen, M. Bao, N. Asao, M.-W. Chen, Y. Yamamoto, *J. Am. Chem. Soc*. **2012**, *134*, 17536. (b) M. Yan, T. Jin, Q. Chen, H. E. Ho, T. Fujita, L.-Y. Chen, M. Bao, M.-W. Chen, N. Asao, Y. Yamamoto, *Org. Lett*. **2013**, *15*, 1484.

Poster 5

Synthesis of Rubrene Derivatives and Application for Organic Field-Effect Transistors

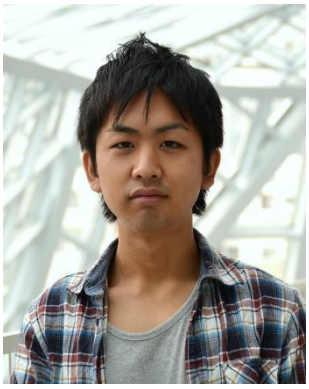

Hirotaka Mutoh,[1] Yoichi Takano,[1] Naoki Asao[1,2]
[1]Graduate School of Science, Tohoku University, Sendai, Japan
[2]WPI Advanced Institute for Materials Research, Tohoku University, Sendai, Japan
E-mail: b2sm5067@s.tohoku.ac.jp
Key word: Halogenated rubrene, Organic semiconductor, OFETs

Organic field-effect transistors (OFETs) amplify and switch electrical signals by using organic semiconductors as an active layer, which have great application as electronic devices such as electronic paper and flexible display.

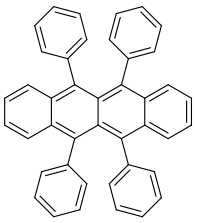
Rubrene

Among the organic semiconductors, rubrene exhibits the highest hole mobility due to its appropriate HOMO energy level for hole injection from electrode and molecular packing structure for the carrier transport[1)]. However, OFETs based on rubrene exhibit a rather lower electron mobility compared to the hole mobility because of its higher LUMO energy level which causes the large electron injection barrier between LUMO and electrode.

One of the efficient strategies for improving electron mobility is the introduction of electron-withdrawing groups such as fluorine or chlorine atom to lower the LUMO energy level of rubrene. Those materials having halogen atoms are able to lower the LUMO level without a great change of the molecular packing structure, which may result in the increased electron mobility. Herein, I synthesized several rubrene derivatives containing fluorine or chlorine atoms for application into the high-performance OFETs.

Scheme 1 shows the synthetic route for the synthesis of rubrene derivatives with fluorine or chlorine atoms on phenyl groups. Photophysical and electronic properties showed that those rubrene derivatives have a lower LUMO energy level than that of rubrene. The new rubrene derivatives are expected to exhibit a higher electron mobility than original rubrene.

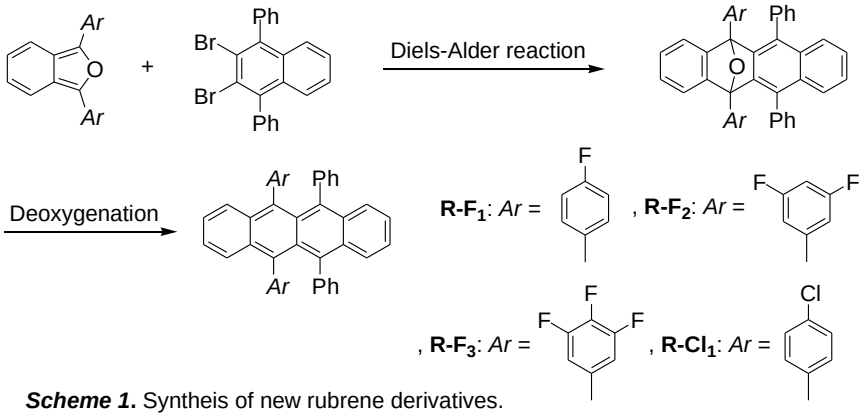

Scheme 1. Syntheis of new rubrene derivatives.

The detailed synthetic method, optoelectronic properties, and transistor properties of the new rubrene derivatives will be discussed in this poster presentation.

1) J. Takaya *et al.*, *Appl. Phys. Lett.*, **2007**, *90*, 102120.

Poster 6

Synthesis of Deuterated Rubrene Derivatives for Organic Field-Effect Transistor

Tsubasa Hoshino,[1] Naoki Asao[1,2]
[1]Graduate School of Science, Tohoku University, Sendai, Japan
[2]WPI Advanced Institute for Materials Research, Tohoku University, Sendai, Japan
E-mail: b2sm5059@s.tohoku.ac.jp
Keyword: rubrene, organic field-effect transistor, deuterium compound, isotope effect

The major application of rubrene is the organic semiconductor with high carrier mobility. Recently, we disclosed that rubrene derivatives having fluorines onto arenes exhibited good hole and electron mobilities as single-crystals semiconductors. However, some derivatives did not give suitable single-crystals for fabrication of OFET devices. On the other hand, Frisbie and his co-workers quite recently reported that deuterated rubrene-d_{28} maintained the remarkable transport properties originally manifested by H-rubrene crystals.[1] In this work, some deuterated rubrene derivatives having fluorines were designed and synthesized. The electrical performance and transport properties would be discussed in the poster presentation.

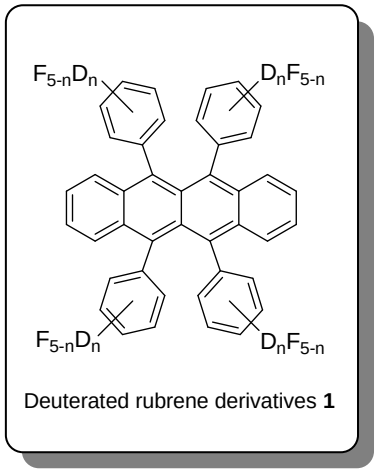

Deuterated rubrene derivatives **1**

Scheme 1

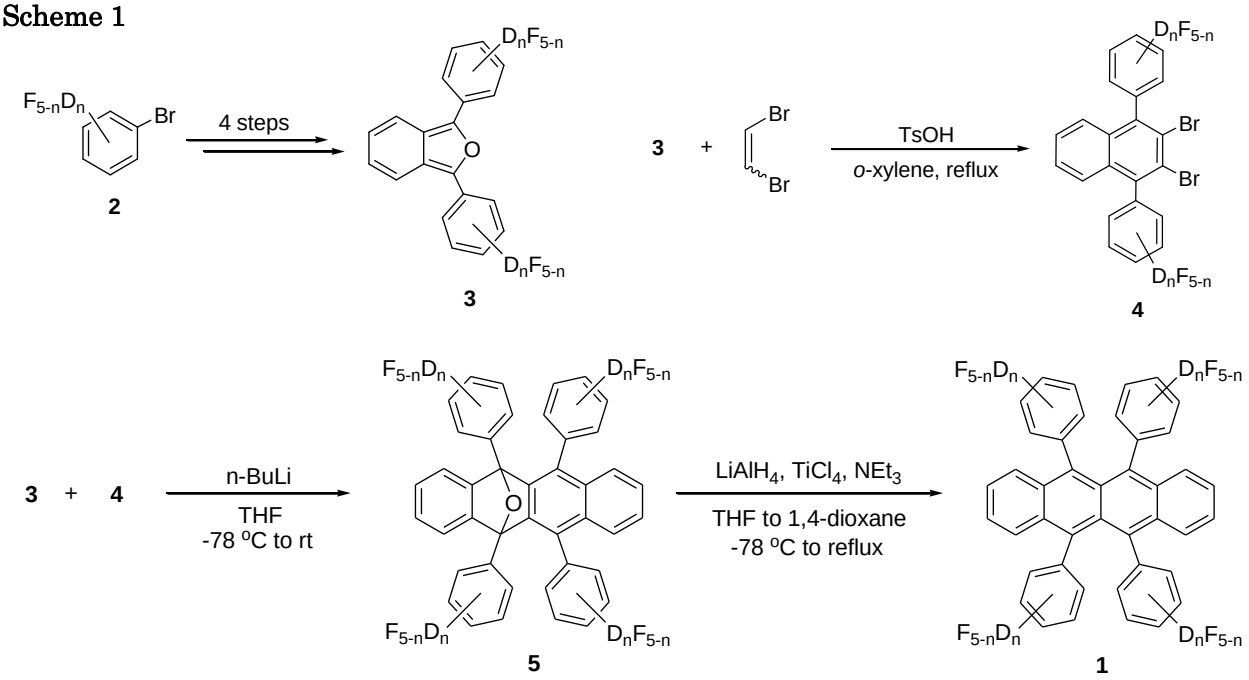

[1] W. Xie, K. A. MacGarry, F. Liu, Y. Wu, P. P.Ruden, C. J. Douglas, C.D. Frisbie, *J. Phys. Chem. C.*, **2013**, *117*, 11522.

Poster 7

Fabrication of Fluorescent Copper Complex Nanoparticles and their Optical Properties

Ryuju Suzuki, Hiromi Noguchi, Tsunenobu Onodera, Hitoshi Kasai, and Hidetoshi Oikawa
Institute of Multidisciplinary Research for Advanced Materials (IMRAM), Tohoku University Katahira 2-1-1, Aoba-ku, Sendai 980-8577, Japan.
Email: b2sm5040@mail.tagen.tohoku.ac.jp
Key words: nanoparticles, fluorescence, copper complexes

Thermally activated delayed fluorescence (TADF) metal complexes show unique optical properties. For example, the quantum yield increases with temperature, and TADF metal complexes provide highly emission at ambient temperature. In addition, the target compounds (Fig. 1) used in the present study hardly show the luminescence in the solution state, called aggregate-induced enhancement of emission (AIEE), which originates from the difference in conformation in both solution and solid states, and may emit comparatively strong TADF in the crystal state. [1]

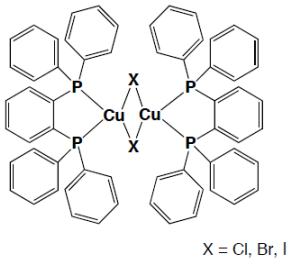

Fig. 1 Chemical structure of [Cu(μ-X)dppb]$_2$

In the present study, we have now paid our attention on "crystal lattice distortion" [2], "the shift of luminescence wavelength" and "temperature coefficient of emission lifetime" [3] under the nanocrystallization of nanocrystallized π conjugated organic compounds, and we try to control the conformation in nano-sized complex, and to clarify the correlation between optical properties, such as luminescence wavelength and quantum yield, and complex structure.

In order to further investigate nanocrystallized TADF complexes, we have employed [Cu(μ-X)dppb]$_2$. Unfortunately, since this complex is much insoluble in common organic solvents, it is very difficult to perform the reprecipitation method to nanocrystallize [Cu(μ-X)dppb]$_2$. So, dppb ligand was first reprecipitated by the conventional reprecipitation method, and then copper(I) bromide solution was subsequently added. Actually, after injecting 200 μL of THF solution of dppb (10 mM) into 10 mL of pure water, 200 μL of acetonitrile solution of copper(I) halide (10 mM) was dropped continuously. As a result, we could obtain reproducibly the fluorescent [Cu(μ-X)dppb]$_2$ nanoparticles as shown in Fig. 2. This method is the combined one of complex formation with nanocrystallization. Further characterization and the evaluation of optical properties are currently under way, and we will report the details on that day.

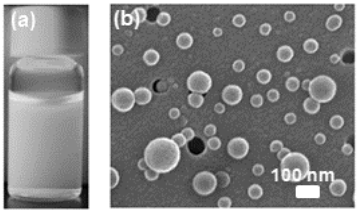

Fig. 2 (a) Photograph of fluorescent nanoparticles dispersion and (b) SEM image of the resulting copper complex

Ref. [1] A. Tsuboyama *et al.*, *Inorg. Chem.*, **46**, 1992 (2007).
[2] S. Takahashi *et al.*, *J. Am. Chem. Soc.*, **124**, 10944 (2002).
[3] H. Oikawa *et al.*, *Single Organic Nanoparticles*, Springer, Berlin, p. 169 (2002).

Poster 8

Fabrication of Dendrimer Nanoparticles and their Complexation Behavior

Akira Miura,[1] Tsunenobu Onodera,[1] Hitoshi Kasai,[1] Takane Imaoka,[2] Kimihisa Yamamoto,[2] and Hidetoshi Oikawa[1]

[1]IMRAM, Tohoku University, Sendai, Japan.

[2]Chemical Resources Laboratory, Tokyo Institute of Technology, Kanagawa, Japan

Email: miuraa@mail.tagen.tohoku.ac.jp

Key words: reprecipitation method, nanoparticle, dendrimer

[Introduction] Dendrimer (DPA-Ph) shows the accumulation property of various metal ions by complexation.[1)] The accumulation number of metal ions in one DPA-Ph would be limited, depending on DPA-Ph structure. However, the physical properties are of much interest in the case of non-limited number of metal ions in DPA-Ph.

In the present study, the formation of DPA-Ph molecular associates (clusters and/or nanoparticles) has been focused as the approach for the purpose of changing the accumulation number of metal ions in a wide range. That is to say, we have fabricated DPA-Ph nanoparticles and investigated their complexation behavior in order to clarify the interaction of DPA-Ph associates with non-limited accumulation number of metal ions.

[Results and Discussion] By applying the reprecipitation method[2)] to DPA-Ph, DPA-Ph nanoparticle dispersion could be successfully fabricated (Figure 1). In $CHCl_3$/cyclohexane (good solvent/poor solvent) system, for example, the spherical nanoparticles became smaller with increasing concentration of the injected solution. These results indicate that the size and shape of DPA-Ph nanoparticles are controllable by changing the reprecipitation conditions.

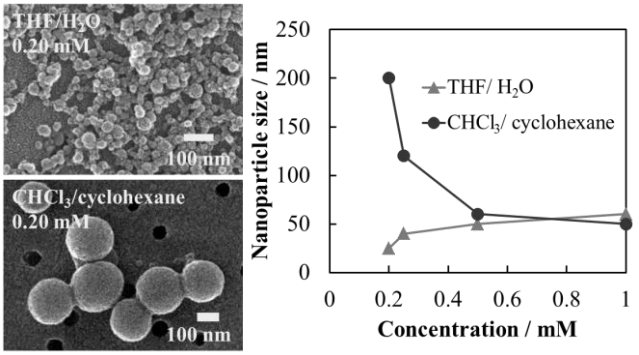

Figure 1 SEM images of DPA-Ph nanoparticles produced by the reprecipitation method, using THF/H_2O or $CHCl_3$/cyclohexane, and the dependence of size for DPA-Ph nanoparticles on concentration of the injected solution.

Next, the complexation of DPA-Ph nanoparticles with $CuCl_2$ has been investigated by the measurement with extinction spectrum. It has become apparent clearly that the complexation behavior is significantly different from that in solution state and that the association state of DPA-Ph nanoparticles is affected by the complexation with $CuCl_2$.

In the near future, we will further clarify the interaction and mechanism of DPA-Ph associates with metal ions in details.

1) K. Yamamoto *et al*., *Nature*, **2002**, *415*, 509-511.

2) H. Kasai *et al*., *Jpn. J. Appl. Phys*., **1992**, *31*, L1132-L1134.

Poster 9

Interaction study between natural products and its targets in yeast

Naoki Kashimoto[1)], Satoru Tamura[1)], Yasuhiro Ishimaru[1)], Shin Hamamoto[2)], Nobuyuki Uozumi[2)], Minoru Ueda[1)].
[1)]Graduate School of Science, Tohoku University, Sendai, Japan
[2)]Graduate School of Engineering, Tohoku University, Sendai, Japan
E-mail: b2sm5020@s.tohoku.ac.jp
Key words: Chemical biology, Identification, Transporter, Yeast, Yeast three-hybrid system.

Many natural products are present in living cells and regulate their function via proteins. Almost all target proteins for the natural products have not been clarified. We aim to confirm the interaction between the natural product and its target in yeast by two methods.

First, we tried to establish the measurement method of the transport activity of the abscisic acid (ABA) efflux transporter using the ABA-poison complex[1)] (Fig. 1). In this strategy, vector control which has not ABA efflux transporter will die. That is because after the ABA-Poison enters into the cell through the plasma membrane, it is decomposed by esterase to release the poison. On the other hand, transformed yeast which has ABA efflux transporter will survive. That is because before the ABA-Poison is discomposed by the esterase to release the poison, it is effused by the ABA exporter. We verified the system by use of ABA-Poison to synthesize **1**, **2** and **3** and now confirm them in the system.

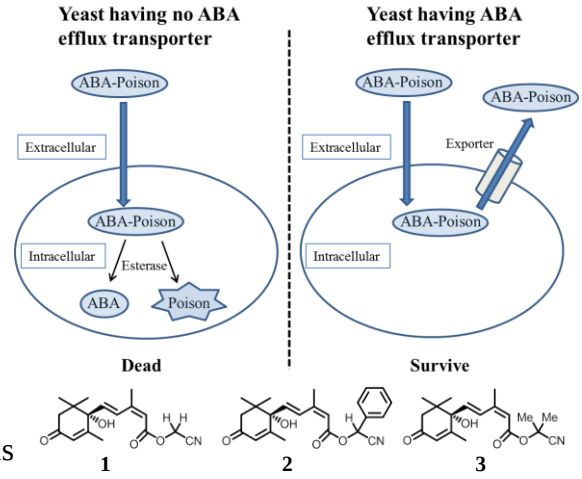

Fig. 1 Measurement method of the transport activity of the ABA efflux transporter.

Second, we confirmed whether coronatine derivatives act as the ligands of COI1 and JAZ9 or not, using yeast three-hybrid (Y3H) system (Fig. 2). Jasmonoyl-L-Ile (JA-Ile) or coronatine as a ligand forms the COI1-JAZ9 complex with COI1 and JAZ9. In this system, we can evaluate the ligandability of derivatives by phenotype of yeast. If the coronatine derivatives act as ligands of COI1-JAZ9 complex, reporter gene will be transcribed and lead to the specific phenotype, growth on a selective medium or change in the color of the yeast. We already created the vector coding COI1 or JAZ9.

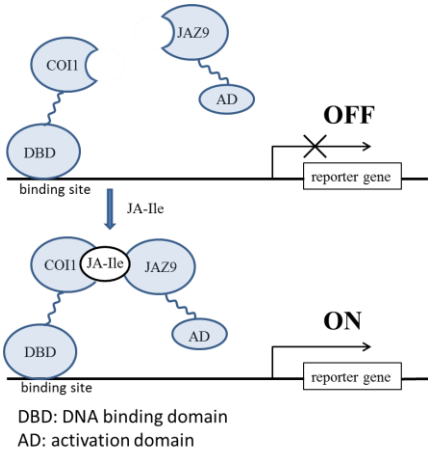

Fig. 2 Y3H system.

Reference 1) T.Kuromori et al. (2010) *Proceedings of the National Academy of Sciences of the USA* **107**:2361–2366

Poster 10

Coronatine derivatives for bioorganic studies on stomatal opening

Ryo Tashita, Syusuke Egoshi, Minoru Ueda.
Graduate School of science, Tohoku University, Sendai, Japan
E-mail: tashita@s.tohoku.ac.jp
Keyword: Chemical biology, Natural products, Coronatine, Jasmonic acid, Compact molecule probe.

Introduction

The natural phytotoxin coronatine (COR) (+)-**1**, isolated from *Pseudomonas syringae* which induces chlorosis in the leaves of Italian rye,[1] has various promising biological activities including root tuberization and potato cell expansion. Jasmonic acid (-)-**2** possesses similar biological activities but coronatine (+)-**1** usually shows greater bioactivities than (-)-**2** in various bioassays.[2] Interestingly, (+)-**1** induces swelling of the guard cells involved in stomatal opening, whereas (-)-**2** is not effective in this bioassay. However, there are no reports on the mode of action of (+)-**1** in the regulation of stomatal movement. In this presentation, we report synthesis of coronatine derivatives and their biological activity in stomatal opening for design of molecule probes which will reveal genuine target protein of coronatine.

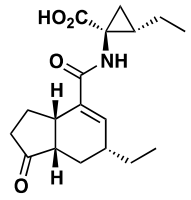

Coronatine (+)-**1**

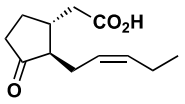

Jasmonic acid (-)-**2**

Result and discussion

In order to investigate structure-activity relationship of coronatine, we synthesized coronatine derivatives with varying carboxyl moiety. They were designed to have an ester bond for compound **3** and **4**, ether bond for **5**, and amide bond for **6**.

Currently, we are examining the bioactivity of these synthetized coronatine derivatives for stomatal opening of the *Arabidopsis thaliana*. Based on this result, molecular probes for the identification of its target protein will be designed and synthesized.

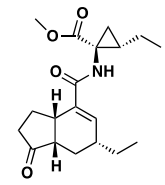

COR-Me ester-**3**

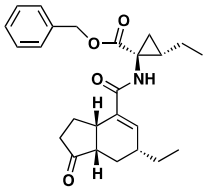

COR-Bn ester-**4**

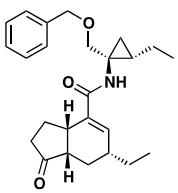

COR-Bn ether-**5**

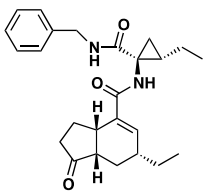

COR-Bn amide-**6**

References

[1] A. Ichihara *et al*., *J. Am. Chem. Soc.* **1977**, *99*, 636-637
[2] Y. Koda *et al*., *Phytochemistry* **1996**, *41*, 93-96

Poster 11

Transformation of Molecular Silicon Clusters

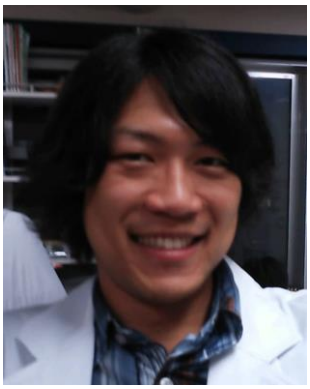

Naohiko Akasaka,[1] Shintaro Ishida,[1] and Takeaki Iwamoto[1]
[1]Graduate School of Science, Tohoku University, Aoba-ku, Sendai 980-8578, Japan.
Email: b2sm5001@s.tohoku.ac.jp
Keywords: Silicon Cluster, Silylene, Elimination, Dimerization

Recently, well-defined molecular organosilicon clusters with 5-20 silicon atoms have attracted much attention because they can be regarded as partial structures of crystalline or amorphous silicon.[1,2] However, reactivity of molecular silicon clusters accompanied by transformation of silicon skeleton are quite limited.[3]

We report herein the structural evolution of Si_5 cluster **1** to Si_8 cluster **2** with elimination of silylene **5** under mild conditions. Thermal decomposition of **1** at 40 °C led to formation of **2** in 61% yield and silene **3** as a byproduct (Scheme 1). Because silene **3** is formed by 1,2-silyl migration of silylene **5**,[4,5] Si_8 cluster **2** would be formed by elimination of silylene **5** from **1** giving disilene **4** and the subsequent dimerization of disilene **4**. Formation of **4** was verified by trapping reactions. Further transformation reactions from **2** will be discussed.

Scheme 1.

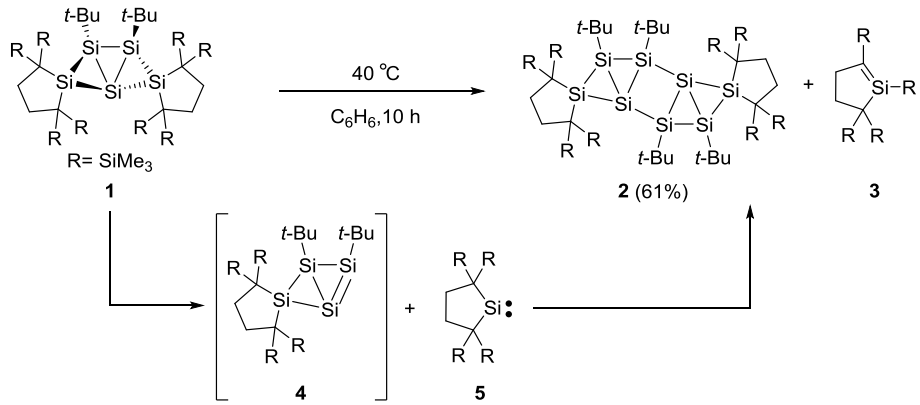

Ref. [1] Hengge, E.; Janoschek, R *Chem. Rev.* **1995**, *95*, 1495. [2] Sekiguchi, A.; Sakurai, H. *Adv. Organomet. Chem.* **1995**, *37*, 1. [3] Abersfelder, K.; Russell, A.; Rzepa, H. S.; White, A. J. P.; Haycock, P. R.;Scheschkewitz, D. *J. Am. Chem. Soc.* **2012**, *134*, 16008. [4] Kira, M.; Ishida, S.; Iwamoto, T.; Kabuto, C. *J. Am. Chem. Soc.* **1999**, *121*, 9722. [5] Ishida, S.; Iwamoto, T.; Kira, M. *Organometallics* **2009**, *28*, 919.

Poster 12

Cycloaddition of an Isolable Dialkylsilylene toward Various Aromatic Ketones

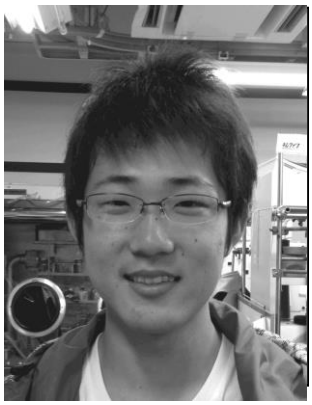

Kenya Uchida, Shintaro Ishida, and Takeaki Iwamoto
Graduate School of Science, Tohoku University Aramakiazaaoba 6-3, Aoba-ku, Sendai 980-8578, Japan.
Email: uchida.k@s.tohoku.ac.jp
Key words: silylene, carbonylsilaylide, dearomatization

Silylenes, silicon analogues of carbene, are the important intermediates in organosilicon chemisry. We have reported synthesis and reactions of isolable dialkylsilylene **1**[1] with various ketones[2,3]. Reaction of **1** with benzophenone afforded dearomatized product, methylenecyclohexadiene **3** probably via carbonyl silaylide **2** as an intermediate (***Scheme 1***) [2]. Although calculated charge distribution suggested that the silicon atom in carbonyl silaylide **2** have somewhat electrophilic character, the electronic character of **2** is elusive. We report herein reactions of **1** with various benzophenone derivatives to elucidate the electronic character of the carbonyl silaylides.

Scheme 1. Reaction of Silylene **1** with Benzophenone

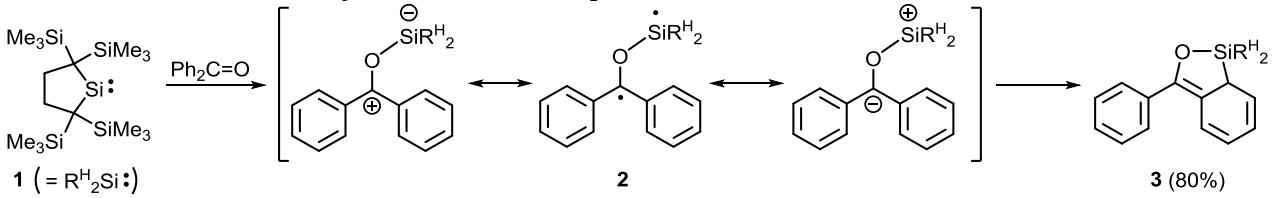

Reactions of **1** with *p*-substituted benzophenone derivatives provided two regioisomers of [1+4] cycloadducts, **5** and **6** (***Table 1***). The cycloaddition occurred predominantly at the electron rich ring. These results suggest that the carbonyl silaylides derived from **1** and benzophenones have electrophilic silicon atom.

Table 1. Reactions of Silylene **1** with Benzophenone Derivatives

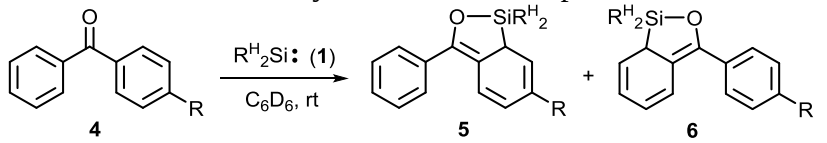

R	Substrate	Yield[a]
NMe_2	**4a**	65% (**5a**), 35% (**6a**)
OMe	**4b**	61% (**5b**), 39% (**6b**)
CF_3	**4c**	44% (**5c**), 56% (**6c**)

(a) Yields were determined by ^{1}H NMR spectra.

(1) Kira, M.; Ishida, S.; Iwamoto, T.; Kabuto, C. *J. Am. Chem. Soc*. **1999**, *121*, 9722. (2) Ishida, S.; Iwamoto, T.; Kira, M. *Organometallics* **2010**, *29*, 5526. (3) Ishida, S.; Uchida, K.; Onodera, T.; Oikawa, H.; Kira, M.; Iwamoto, T. *Organometallics* **2012**, *31*, 5983.

Poster 13

Synthesis, Structure and Dynamic Behavior of Tetraorganosilicates Having 9,10-Disilatriptycene Skeleton

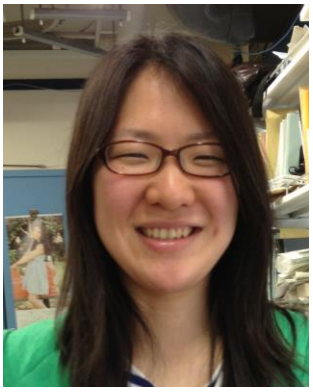

Minori Takiguchi, Shintaro Ishida, and Takeaki Iwamoto
Graduate School of Science, Tohoku University
Email: takiguchi@s.tohoku.ac.jp
Keywords: silicate, pentacoordinate, disilatriptycene

Although anionic pentacoordinate tetraorganosilicates are important class of molecules in various reactions of organosilicon compounds, their structural information is still limited and only two stable tetraorganosilicates with coordination of fluoride and cyanide have been reported (Chart 1).[1,2] We have reported a one-pot synthesis of 9-phenyl-9,10-disilatriptycene (**1**) as shown in Scheme 1.[3] During the course of our synthetic study of 9,10-disilatriptycene derivatives as functional materials based on silyl-substituted rigid π-systems, we obtained stable tetraorganosilicate **4**$^-$ with intramolecular alkoxide coordination. We report herein the detail of the synthesis and structure of **4**$^-$.

Chart 1.

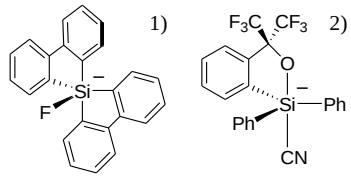

Scheme 1.

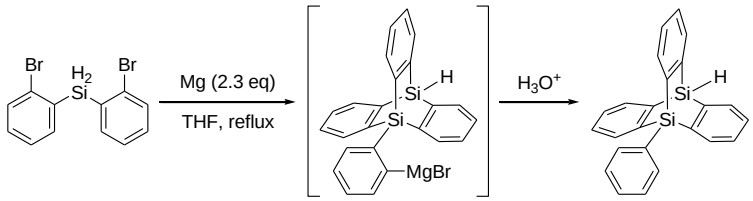

2 **3** **1** (31%)

Silicate **4**$^-$ was synthesized as shown in Scheme 2. Formylation of Grignard reagent **3** generated from **2** with DMF and subsequent reduction with $LiAlH_4$ gave benzylalcohol **6**. Deprotonation and alkylation of **6** with two equivalents of *tert*-BuLi in THF at −78 °C afforded lithium silicate $[Li(thf)]^+ \cdot$**4**$^-$ as a colorless solid in 82% yield. The molecular structure and dynamic behavior in solution of **4**$^-$ will be presented.

Scheme 2.

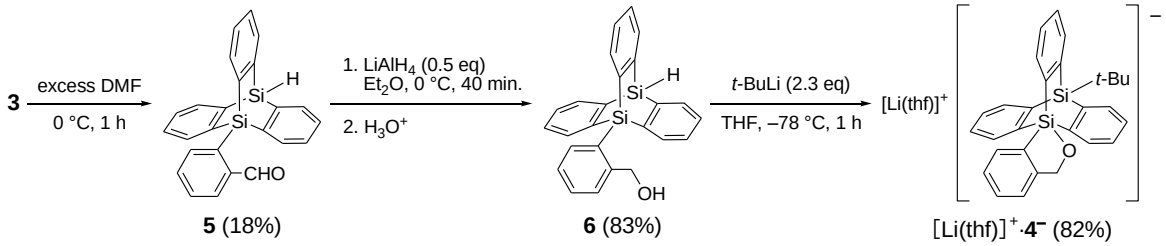

5 (18%) **6** (83%) $[Li(thf)]^+ \cdot$**4**$^-$ (82%)

(1) Couzijn, E. P. A.; van den Engel, D. W. F.; Slootweg, J. C.; de Kanter, F. J. J.; Ehlers, A. W.; Schakel, M.; Lammertsma, K. *J. Am. Chem. Soc.* **2009**, *131*, 3741. (2) Dixon, D. A.; Hertler, W. R.; Chase, D. B.; Farnham, W. B.; Davidson, F. *Inorg. Chem.* **1988**, *27*, 4012. (3) Kuribara, T.; Ishida, S.; Kyushin, S. *Organometallics* **2013**, *32*, 2092.

Poster 14

Asymmetric Mannich reaction of α-Ketoimines Catalyzed by Organocatalyst

Hiroki Shomura, Itaru Sato and Yujiro Hayashi
Graduate School of Science, Tohoku University, Sendai, Japan
E-mail: h-shomura@s.tohoku.ac.jp
Key words: ketoimine, Mannich reaction, oraganocatalyst

[Introduction] The use of organic molecules as catalyst is a powerful tool to construct chiral building blocks. Asymmetric Mannich reaction is one of the most important reactions to form C-C bond, affording β-aminocarbonyl compounds. Our group has revealed the proline derivatives are efficient catalysts in asymmetric Mannich reaction. In this presentation, I report the asymmetric Mannich reaction of α-ketoimines **1** using organocatalyst, which affords γ-oxo-β-aminocarbonyl compound **3** (**Scheme 1**).

Scheme 1

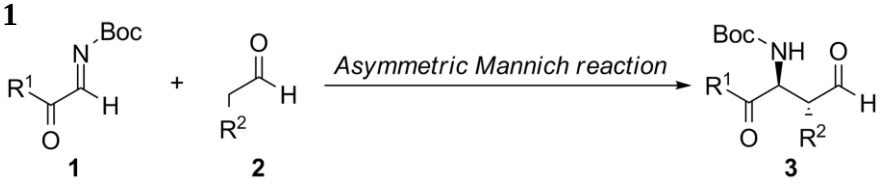

[Results and Discussion] The reaction was carried out with amidosulfone **4**, aldehyde **2**, diarylprolinol silyl ether **5** and KF in $CHCl_3$. Relatively unstable imine was generated in situ from amidosulfone **4** by treatment with base. Unsaturated ester **6** was obtained after the reaction with Wittig reagent with excellent *anti*-selectivity and enantioselectivity (**Scheme 2**). Various aldehydes **2** could be used in this reaction. Since the product possesses several functional groups, further synthetic elaborations are easily available. Thus, the obtained Mannich products are considered to be useful synthetic chiral building blocks.[1]

Scheme 2

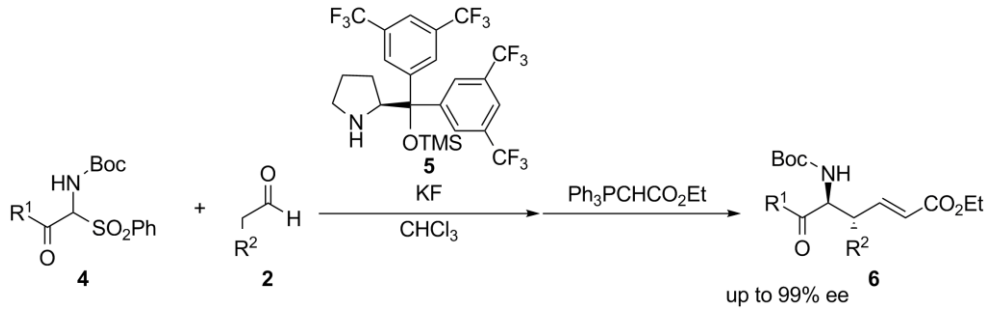

Ref. [1] Y. Hayashi *et al.*, *Chem. Eur. J* . **2013**, *19*, 7678.

Poster 15

p-Benzyne Monochlorination
Synthetic Study of Cyanosporasides A and B

Kei Yamada, Itaru Sato, Yujiro Hayashi and Masahiro Hirama
Graduate School of Science, Tohoku University, Sendai, Japan
E-mail: k-yamada@s.tohoku.ac.jp
Keyword: Cyanosporaside, Enediyne, Monochlorination, *p*-Benzyne Cycloaromatization

【Introduction】

Cyanosporasides isolated from the culture broth of marine actiomyces possess a novel cyclopenta[*a*]indene framework, which is considered as a product of cycloaromatization of bicyclo[7.3.0]trienediyne. Hydrogen and chlorine at C3 and C6 positions should be incorporated during the cycloaromatization.

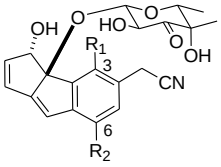

R_1= Cl, R_2= H : Cyanosporaside A (**1**)
R_1= H, R_2= Cl : Cyanosporaside B (**2**)

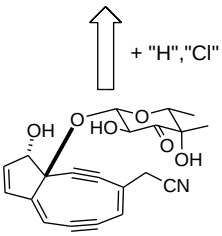

9-membered trienediyne (**3**)

【Result and discussion】

We found that *p*-benzyne biradical generated from a 9-membered enediyne (**9**) undergoes a radical monochlorination in Et_2O/CCl_4 to give **10**, and in striking contrast to an ionic reaction, in the presence of LiCl in DMSO to afford **11**. These regioselective monochlorinations were utilized for selective syntheses of cyanosporasides A (**12**) and B (**13**) protected aglycones.

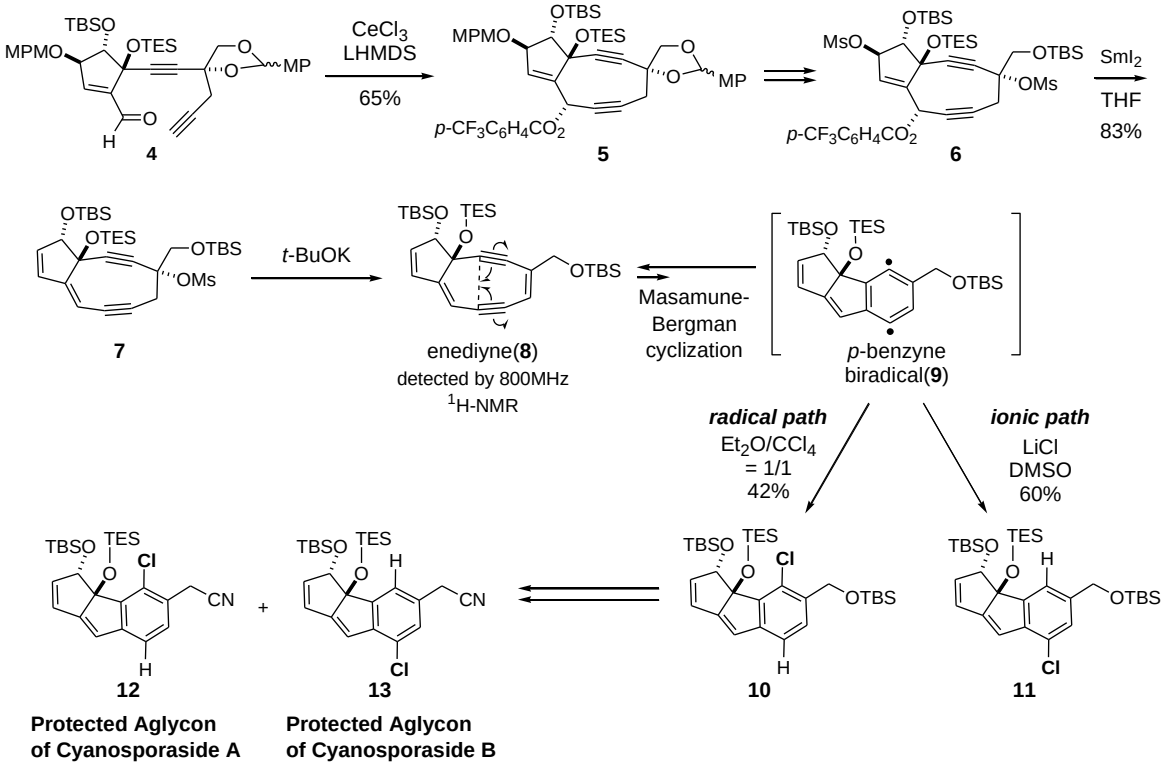

Scheme 1. Total Synthesis of Cyanosporasides A (**12**) and B (**13**) Protected Aglycones.

Poster 16

Total Synthesis of Ustiloxin D

Daisuke Hayashi, Syuji Harada, Itaru Sato, Yujiro Hayashi, and Masahiro Hirama
Graduate School of Science, Tohoku University, Sendai, Japan
E-mail: d-hayashi@s.tohoku.ac.jp
Key words: Ustiloxin D, triarylbismuth, aryl ether, cyclopeptide

【Introduction】 Ustiloxins are antimitotic cyclopeptides containing a 13-membered cyclic core structure with a synthetically challenging chiral tertiary alkyl-aryl ether linkage. The total synthesis of ustiloxin D has been achieved via *O*-arylation of the chiral tertiary alcohol using arylbismuth(III) reagents.

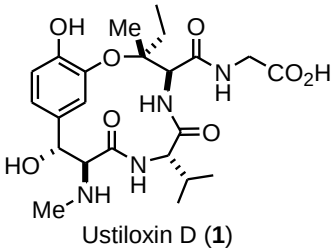

Ustiloxin D (**1**)

【Result and discussion】 Aryl ether formation was conducted via *O*-arylation of tripeptide **3** using Ar_3Bi(III) reagent **2** under our recently developed conditions, in which any epimerized products were not observed. A *para*-selective oxidation of aromatic ring, followed by regioselective protection gave aryl triflate **5**. Heck reaction and Sharpless asymmetric aminohydroxylation afforded **6** possessing a β-hydroxytyrosine moiety. Macrolactamization of **7** smoothly gave rise to macrocycle **8**. Finally, total synthesis of ustiloxin D (**1**) was accomplished through manipulation of the deprotection, *N*-methylation, and deprotection.

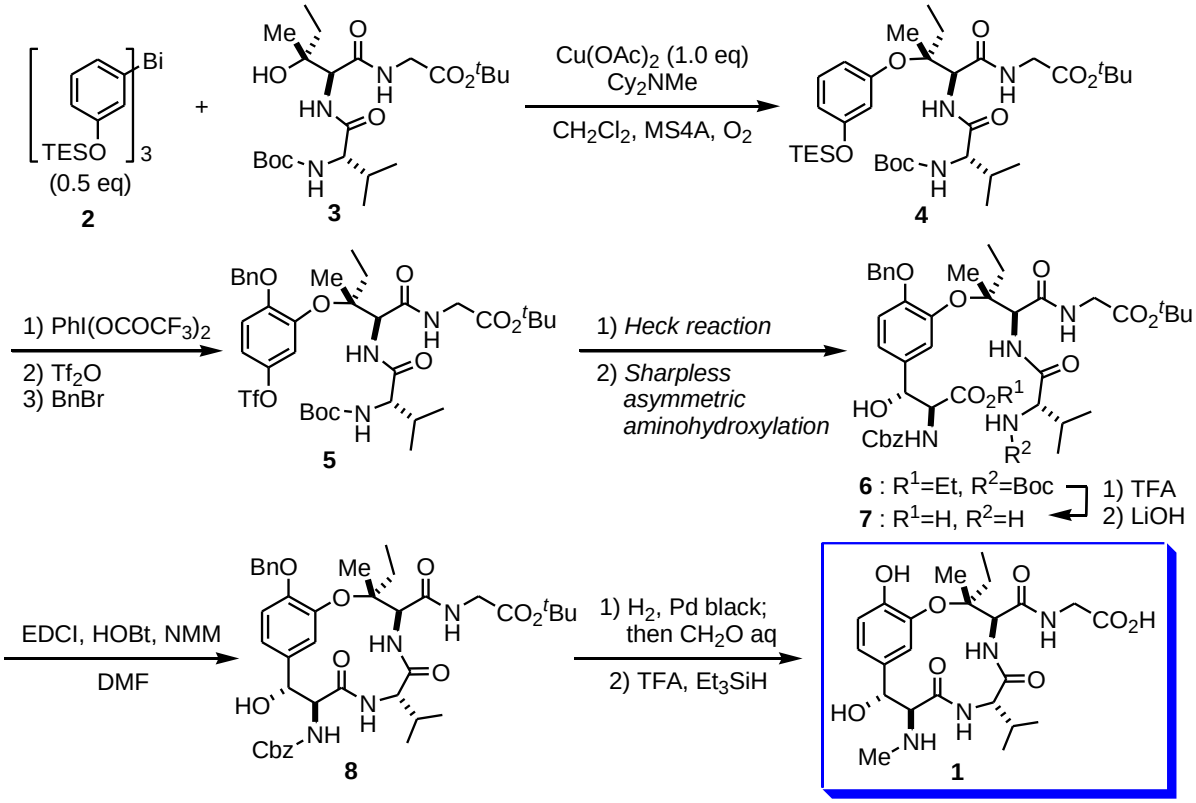

Poster 17

Synthesis of Aziridine Containing Asymmetric Quaternary Carbon Center Catalyzed by Diphenylprolinol Silyl Ether

Taku Hirama, Daichi Okamura, Itaru Sato, and Yujiro Hayashi
Graduate School of Science, Tohoku University, Aoba 6-3, Aoba-ku, Sendai, 980-8578, Japan.
Email: t-hirama@s.tohoku.ac.jp
Key words: organocatalyst, asymmetric reaction, quaternary carbon center

Development of asymmetric organocatalytic reactions is one of the most important area of chemistry. Diphenylprolinol silyl ether developed by our laboratory is highly efficient and general catalyst, and we have reported Michael reaction of nitroalkanes with α,β-unsaturated aldehydes catalyzed by diphenylprolinol silyl ether.[1] On the other hands, asymmetric construction of quaternary carbon center is challenging theme in organic synthesis. In this presentation, diphenylprolinol silyl ether catalyzed addition of hydroxyl amine derivatives to β,β-disubstituted-α,β-unsaturated aldehydes will be described. Asymmetric Michael reaction and subsequent aziridination affords aziridine with chiral quaternary carbon center.

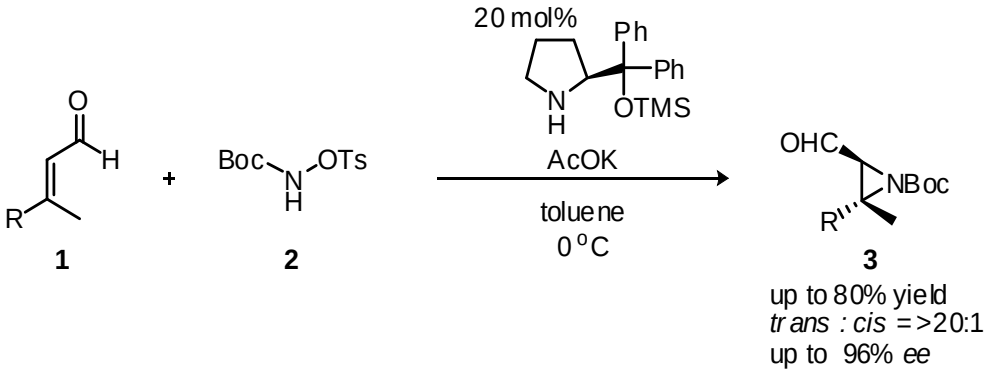

Scheme 1. Asymmetric aziridination of β,β-disubstituted-α,β-unsaturated aldehydes and hydroxyl amine derivative

The aziridination of β,β-disubstituted-α,β-unsaturated aldehydes (1) and hydroxyl amine derivative (2) proceeded in good yield and high diastreo- and enantio- selectivity in the presence of diphenylprolinol silyl ether and potassium acetate (Scheme 1). β,β-Disubstituted-α,β-unsaturated aldehydes with various substitutuents were applicable to this reaction. Relative configuration was determined by NOE experiment of the corresponding alcohol after reduction and major diastereomer had *trans*-configuration (R ≠ H).

[1] Y. Hayashi *et al.*, *Org. Lett.* **2007**, *9*, 5307.

Poster 18

Study on Total Synthesis of Ciguatoxin CTX4B

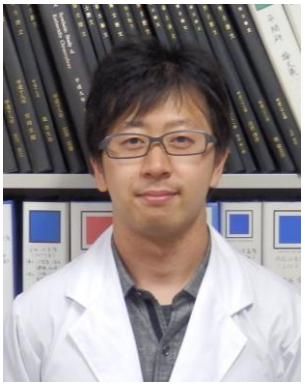

Takuya Koyama, Katsutoshi Takeuchi, Shuji Yamashita,
Yujiro Hayashi, and Masahiro Hirama
Graduate School of Science, Tohoku University, Sendai, Japan
E-mail: koyama@s.tohoku.ac.jp
Keyword: ciguatoxin, cigatera, neurotoxin, polyether, hapten

Ciguatoxins are principal causative toxins of ciguatera seafood poisoning. Recently, we have achieved total syntheses of the three congeners[1] and preparation of their monoclonal antibodies.[2] In this presentation, I will report a synthetic study on CTX4B (**1**) and its left wing hapten (**6**).

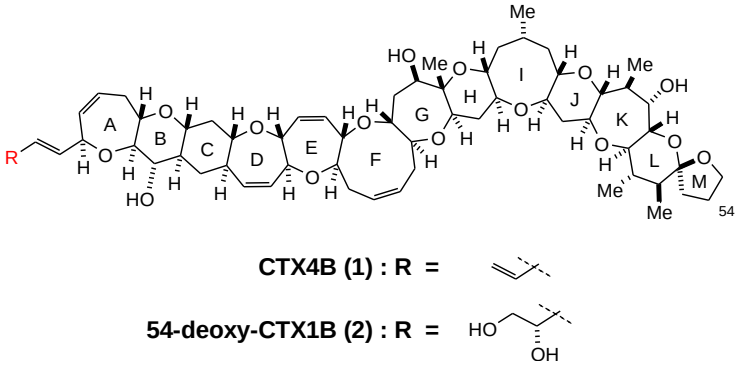

1) Study toward total synthesis of CTX4B (**1**).

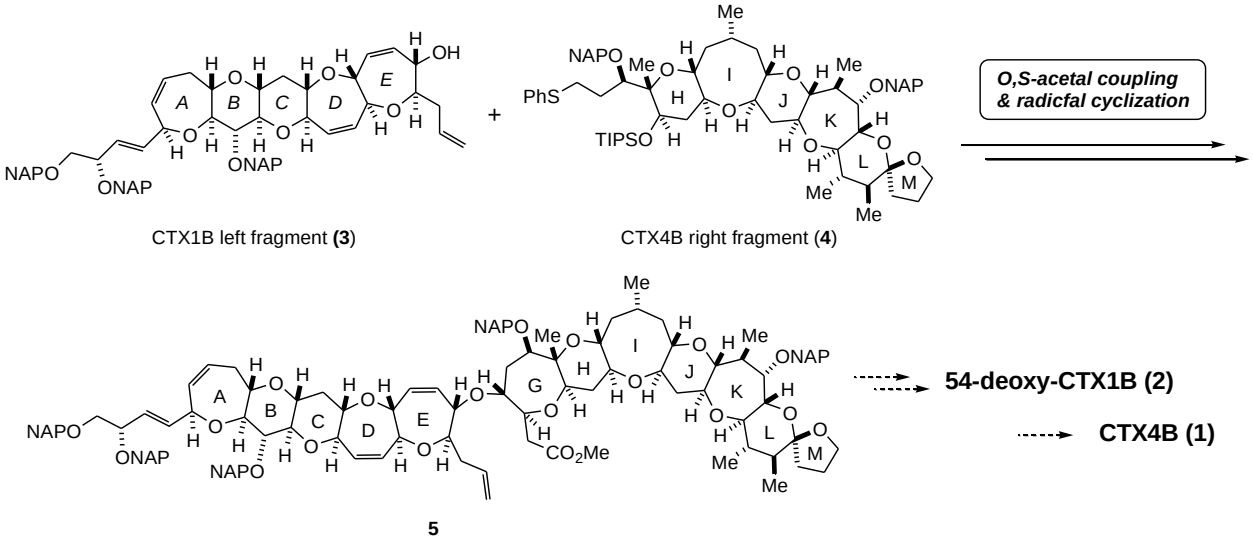

2) CTX4B left wing hapten (**6**) was synthesized from CTX1B-type left fragment (**3**).

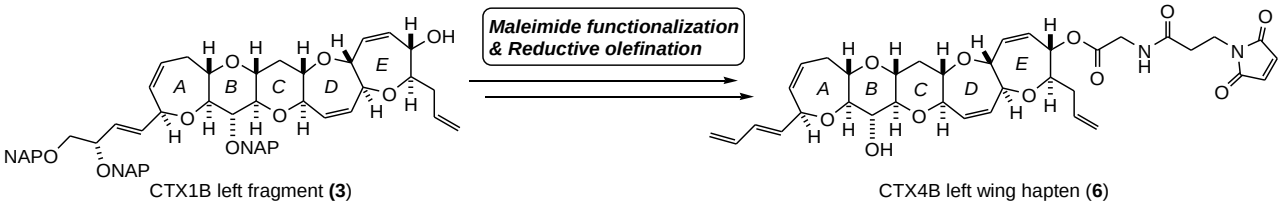

1) Inoue, M.; Miyazaki, K.; Ishihara, Y.; Tatami, A.; Ohnuma, Y.; Kawada, Y.; Komano, K.; Yamashita, S.; Lee, N.; Hirama, M. *J. Am. Chem. Soc*. **2006**, *128*, 9352.
2) T. Tsumuraya, K. Takeuchi, S. Yamashita, M. Hirama, and I. Fujii, *Toxicon*, **2012**, *60*, 348.

Poster 19

Synthetic Study of Presporolide

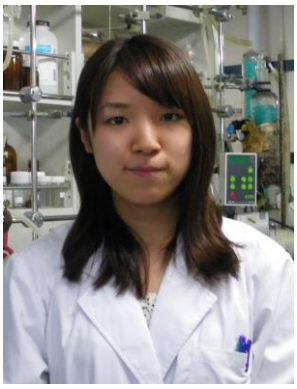

Kanae Terayama, Eri Ozeki, Shuji Yamashita, Yujiro Hayashi, and Masahiro Hirama
Graduate School of Science, Tohoku University, Sendai, Japan
E-mail: terayama@s.tohoku.ac.jp
Keyword: sporolide, 9-membered ring enediyne, 13-membered ring macrolide

Sporolides A and B (**1** and **2**) were isolated from a marine *actinomycete* in 2005. Their chlorinated cyclopenta[*a*]indane motifs suggested a putative precursor presporolide (**3**), which possesses a 9-membered cyclic enediyne structure. In this presentation, our study toward the synthesis of **3** will be reported.

The *O*-arylated compound **6** was synthesized from the optically active 5-membered ring **5** and tris-aryl bismuth(III) reagent. Stereoselective acetylide addition followed by Sonogashira-coupling reaction gave aldehyde **9**. Cerium(III)-mediated 9-membered ring formation and successive Shiina-macrolactonization atropselectively afforded **11**. Finally, reductive olefination using samarium iodide produced an enediyne model compound **12**.

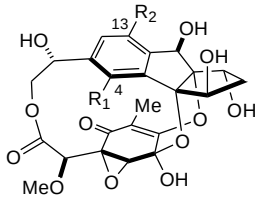

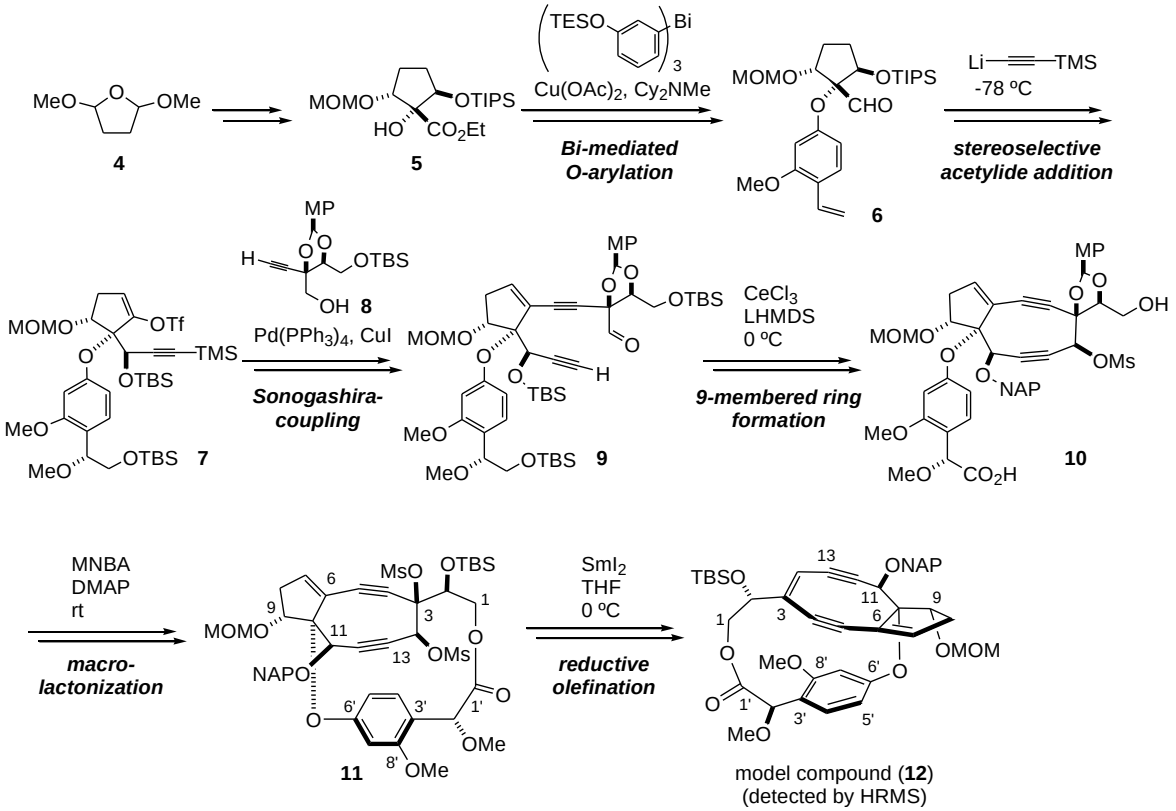

Poster 20

Asymmetric formal [3+2] cycloaddition reaction of succinaldehyde via diarylprolinol-mediated domino aldol/acetalization reaction for the construction of tetrahydrofuran

Kentaro Nishino, Itaru Sato, and Yujiro Hayashi
Graduate School of Science, Tohoku University, Sendai, Japan
E-mail: nishino@s.tohoku.ac.jp
Keywords: formal [3+2] cycloaddition, succinaldehyde, tetrahydrofuran, diarylprolinol

[Introduction] Formal [3+2] cycloaddition reaction is one of the most powerful methods for construction of five-membered ring compounds. Succinaldehyde is a synthetically useful aldehyde, composed of four carbons with two formyl groups, which could be used as a three carbon unit in the formal [3+2] cycloaddition reaction. We reported here asymmetric aldol reaction of succinaldehyde with various aldehyde and successive intramolecular acetalization, which gave chiral tetrahydrofurans.

[Results & Discussions] The reaction of succinaldehyde **1** and ethyl glyoxylate **2** (R = CO_2Et) was initially investigated. Diarylprolinol **3** is found to be a suitable catalyst in the asymmetric aldol reaction.[1] After consecutive aldol reaction and intramolecular acetal cyclization, tetrahydrofuran **4** was obtained with good enantioselectivity. The reaction of electron-deficient aromatic aldehydes also examined (Table 1). The reaction proceeded smoothly and the corresponding tetrahydrofurans were obtained with excellent enantioselectivity. Thus, we have developed an enantioselective synthesis of substituted tetrahydrofurans.

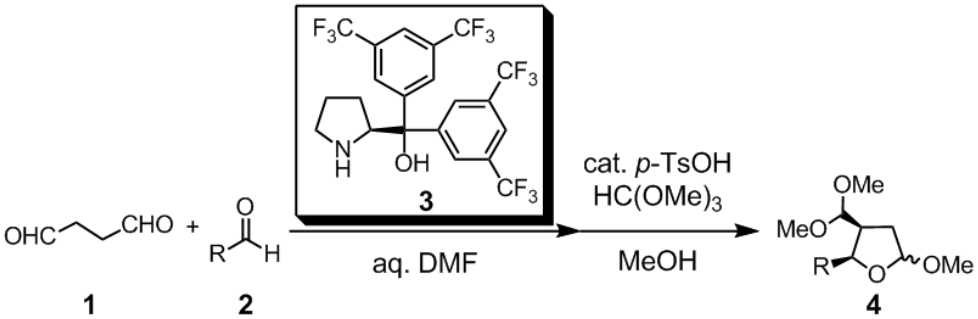

Table 1

entry	R	yield / %	*dr*(*cis* : *trans*)	α : β (*cis*)	*ee* / % (*cis* α)
1	CO_2Et	55	4.3 : 1	4.4 : 1	98
2	4-$NO_2C_6H_4$	54	4.1 : 1	3.5 : 1	99
3	2-ClC_6H_4	41	3.0 : 1	1.4 : 1	96
4	2-$NO_2C_6H_4$	31	4.0 : 1	2.7 : 1	97
5	2,4-$(NO_2)_2C_6H_3$	46	2.7 : 1	2.5 : 1	98
6	3,5-$(CF_3)_2C_6H_3$	53	2.6 : 1	3.6 : 1	> 99.5

1) Y. Hayashi *et al.*, *Angew. Chem., Int. Ed.*, **2008**, 47, 2082-2084.

Poster 21

Organocatalytic asymmetric cyclopropanation of β-disubstituted α,β-unsaturated aldehydes

Yuya Kawamoto, Daichi Okamura, Itaru Sato, Yujiro Hayashi
Graduate School of Science, Tohoku University, Sendai, Japan
E-mail: kawamoto@s.tohoku.ac.jp
Keywords : Organocatalyst, Cyclopropane, Quaternary carbon center

Introduction

Nowadays organosatalyst have gained many organic chemists' interest because of its stabilities against water and air, and many organocatalytic asymmetric reactions have been developed. A cyclopropane motif is a constituent of several natural products and biologically active agents.[1] In addition to serving as drug and agrochemical targets, the rigid cyclopropane scaffolds are important as intermediates in complex molecule synthesis. Quaternary carbon center is also constituent in a great number of natural products. Consequently, asymmetric constructions of quaternary carbon center have been intensively investigated.[2] In this paper, we report a organocatalytic asymmetric cyclopropanation. The reaction between 2-bromonitromethane and α,β-unsaturated aldehydes gave the corresponding cyclopropanes bearing a chiral quaternary center through a domino Michael-alkylation reaction.

Result and Discussion

The reaction between α,β-unsaturated aldehyde **1** with bromonitromethane **2** in the presence of diphenylprolinol silyl ether **3** provided cyclopropanes **4a** and **4b** bearing a chiral quaternary carbon center via domino Michael-alkylation reaction. (Scheme 1). When the reaction was carried out in isopropyl alcohol in the presence of pyridine, we obtained the cyclopropane with high yield and enantioselectivity. The absolute configuration of the product was determined by X-ray analysis.

Scheme 1

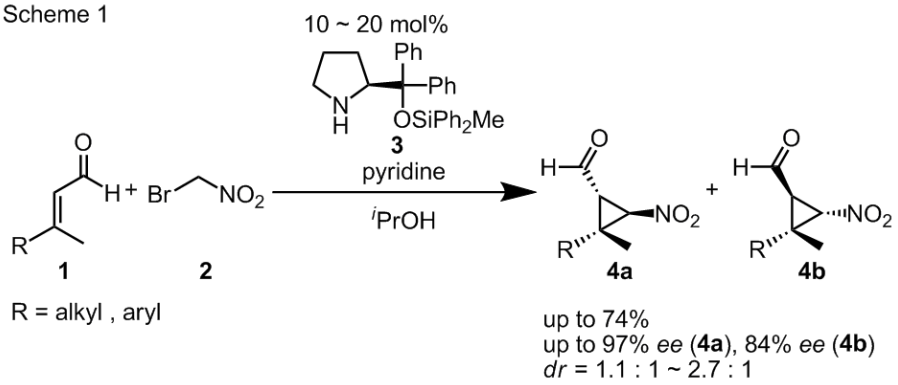

[1] Wessjohann, L. A.; Brandt, W.; Thiemann, T. *Chem. Rev.* **2003**, *103*, 1625.
[2] Fuji, K. *Chem. Rev.* **1993**, *93*, 2037.

Poster 22

Asymmetric Aldol Reaction of Alkynyl Aldehyde Catalyzed by Diarylprolinol

Yuta Kanda,[1] Masahiro Kojima,[2] Yusuke Yasui,[1] Itaru Sato,[1] and Yujiro Hayashi[1]

[1]Graduate School of Science, Tohoku University Aoba 6-6, Aobaku, Sendai 980-8578, Japan

[2]Faculty of Engineering, Tokyo University of Science, Kagurazaka 1-3, Sinjukuku 162-0825

Email: kanda@s.tohoku.ac.jp

Key words: Alkynyl aldehyde, Asymmetric aldol reaction, Diarylprolinol, Organocatalyst

[Introduction]

The aldol reaction is a useful method for constructing β-hydroxy carbonyl compound, and recognized as one of the most important carbon-carbon bond-forming processes in organic synthesis. Since proline-mediated aldol reaction was discovered by List, Lerner, and Barbas in 2000,[1] organocatalysis is rapidly expanding. This time, we found the asymmetric aldehyde-aldehyde cross aldol reaction of alkynyl aldehydes to afford useful chiral building blocks catalyzed by organocatalyst.

[Results and discussions]

The reaction was carried out with alkynyl aldehyde **2**, aldehyde **3**, and diarylprolinol **1** in 1,4-dioxane with water. After Wittig reaction, propargyl alcohol **5** was obtained in good yield with excellent enantioselectivity (Scheme 1).[2] Various aldehydes **2** could be employed in this reaction. Since the obtained product possesses chiral propargyl alcohol groups, further transformation can be easily available.

Scheme 1

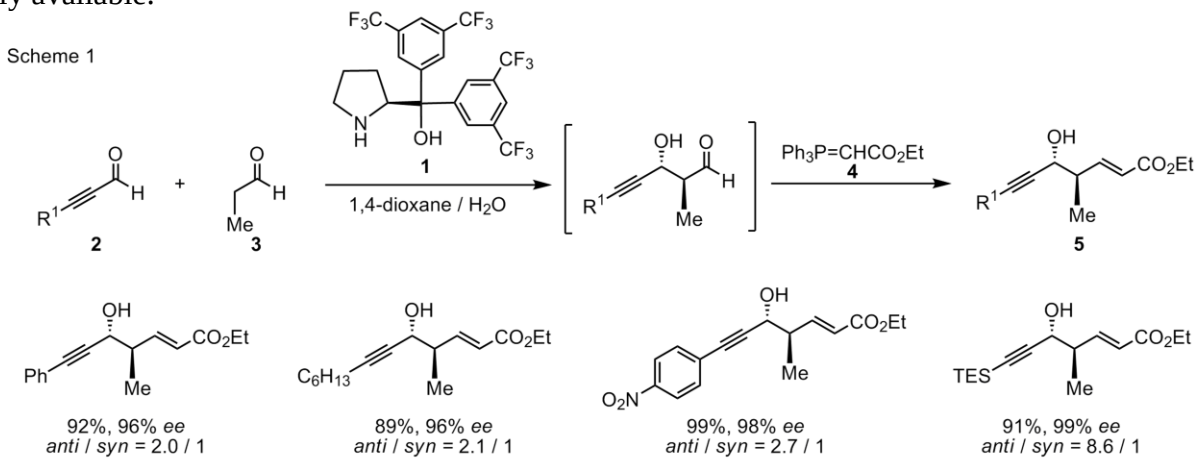

[Reference]

(1) B. List, R. A. Lerner, C. F. Barbas III, *J. Am. Chem. Soc*, **2000**, *122*, 2395–2396.

(2) Y. Hayashi *et al*., *ChemCatChem*, accepted for publication.

Poster 23

Activity of Proline Type Organocatalyst Included Acidic Functional Group

Masataka Ikegami, Takasuke Mukaiyama, Itaru Sato, and Yujiro Hayashi
Graduate School of Science, Tohoku University, Aramaki-Aza Aoba 6-3, Aoba-ku, Sendai, Miyagi 980-8578, Japan
Email: m-ikegami@s.tohoku.ac.jp
Key Words: Organocatalyst, Proline

Introduction

Organocatalyst is used by many reactions in organic chemistry. We aimed to develop a highly active organocatalyst. In 2005, our laboratory found that diphenylprolinol silyl ether is an effective catalyst in Michael reaction.[1] In 2007, we found that the Michel reaction is accelerated in the presence of benzoic acid.[2] From these two results, we thought that if acidic functional group is introduced into diphenylprolinol silyl ether derivative, higher active catalyst would be generated.

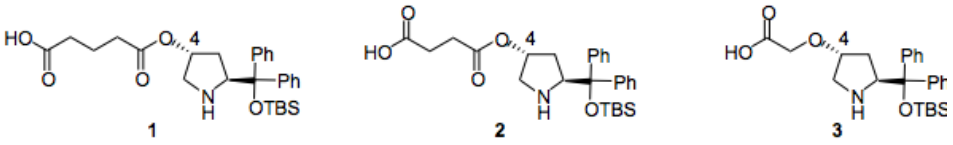

Figure. 3 Types proline derivatives

Results and Discussion

Based on diphenylprolinol silyl ether, we decided to introduce acidic functional group to C-4 part. I made 3 types of proline derivatives **1**, **2**, and **3** (Figure 1) from *trans*-4-hydroxy-L-prolin **4** in 7 to 10 steps. Using these 3 proline derivatives, I investigated catalytic activity in the Michael reaction of aldehyde and nitroalkene. It was found that proline derivative **3** had the highest activity.

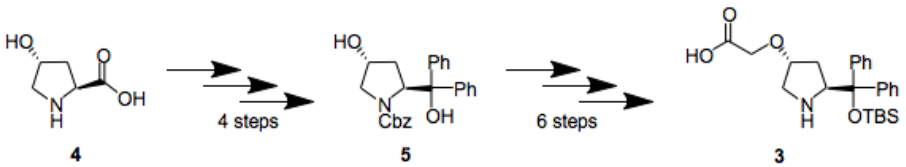

Reference

[1] Y. Hayashi *et al*., *Angew. Chem. Int. Ed.*, **44**, 4212 (2005).
[2] H. Gotoh, Y. Hayashi *et. al.*, *Org. Lett.*, **9**, 5307 (2007).

Poster 24

Asymmetric Carbocyclization of Formyl Alkynes Catalyzed by Diphenylprolinol Silyl Ether and Palladium Dichloride

Yuki Nakanishi, Itaru Sato, and Yujiro Hayashi
Graduate School of Science, Tohoku University, Aoba 6-3, Aoba-ku, Sendai, 980-8578, Japan.
Email: nakanishi@s.tohoku.ac.jp
Key words: organocatalyst, asymmetric reaction, metal catalyst

During recent years, the field of asymmetric organocatalytic reactions has been developing rapidly all over the world. Our laboratory has developed diphenylprolinol silyl ether which is an effective organocatalyst with high selectivity and generality. On the other hand, very large numbers of metal catalytic reactions have also been developed worldwide for a longer time. However, there are few asymmetric reactions using the combination of organocatalyst and metal catalyst. This field of chemistry has a lot of possibilities worth challenging. In this presentation, diphenylprolinol silyl ether and palladium dichloride catalyzed intramolecular carbocyclization of formyl alkynes will be described. Aldehyde is converted into enamine by the organocatalyst with triple bond being activated by the metal catalyst, and cyclopentane having asymmetric quaternary carbon center is formed.

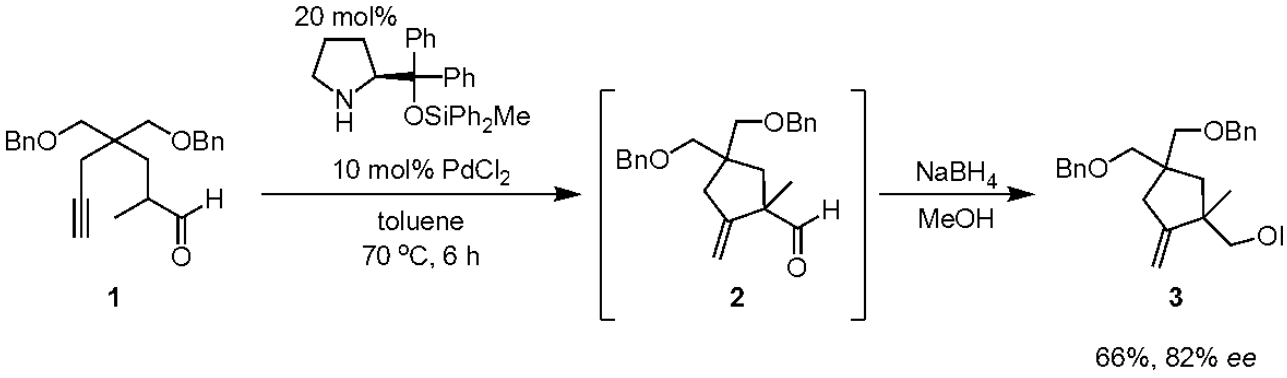

Scheme 1. Asymmetric intramolecular carbocyclization of formyl alkynes

In the presence of diphenylprolinol silyl ether and palladium dichloride, the carbocyclization of formyl alkynes **1** in toluene proceeded at 70 ℃. Aldehyde **2** was converted into alcohol **3** by reduction with $NaBH_4$ in one-pot in 66% yield, 82% *ee* (Scheme 1).

Poster 25

Substituent and Solvent Effects on the Reactions of Acetylide-Silylene Complexes with Acetone

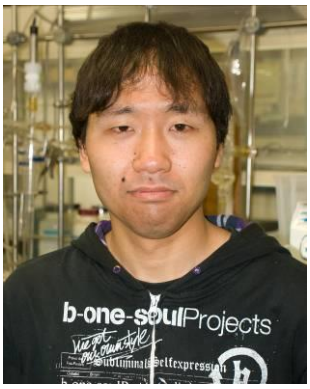

Keita Nakagawa,[1] Kwon Eunsang,[2] Kozo Toyota,[1] and Hiroyuki Sakaba[1]
[1]Graduate School of Science, Tohoku University, Sendai, Japan.
[2]Research and Analytical Center for Giant Molecules, Graduate School of Science, Sendai, Japan.
E-mail: b2sm5048@s.tohoku.ac.jp
Key Words: acetylide−silylene complex, tungsten complex, substituent effect, solvent effect

Previously, we reported the synthesis of novel acetylide−silylene tungsten complexes with bulky substituents (**1**: R = CMe_3, **2**: R = $SiMe_3$) and the selective formation of complexes **3** and **4** in the reactions of **1** and **2** with acetone in toluene, respectively.[1]

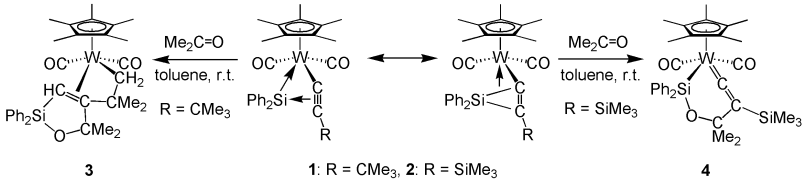

In this study, we investigated the reaction of **2** in acetone at room temperature and found that complex **5** was formed via skeletal rearrangement. To obtain information on the reaction mechanism, we conducted the reaction at -50 °C and succeeded in the isolation of interesting intermediate **6**, which was converted to complex **5** in solution upon warming to room temperature.

We synthesized new derivative **7** with less bulky ethyl substituent, whose solid-state structure was determined by X-ray crystal analysis. Intriguingly, its variable-temperature NMR spectra in toluene-d_8 revealed that complex **7** was in equilibrium with silapropargyl complex **8**. Reactions of **7** with acetone gave π-allyl complexes **9** and **10** depending on the solvent, toluene and acetone, respectively. Details of the X-ray structures of these complexes and the reaction mechanism will be discussed.

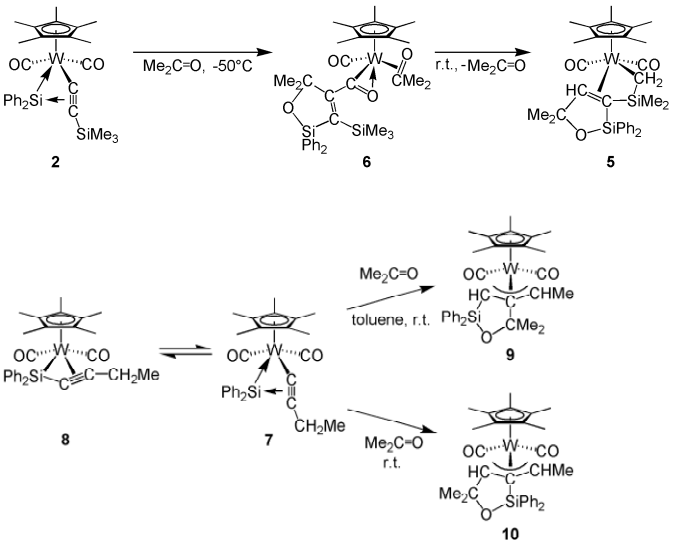

1) H. Sakaba et al., *J. Am. Chem. Soc*. **2005**, *127*, 7276; *Organometallics* **2010**, *29*, 4115.

Poster 26

A Chiral NMR shift Reagent Eu-pdta: Application to Determining Absolute Configurations of β-Amino Acids and β-Hydroxy Acids

Toshinari Honda[1], Kenji Omata[1], Kuninobu Kabuto and Kozo Toyota[1]

[1]Graduate School of Science, Tohoku University, Sendai, Japan

Email : b2sm5061@s.tohoku.ac.jp

Key words : absolute configuration, amino acid, chiral NMR shift reagent

Introduction

We have been developing a chiral lanthanide shift reagent which is promising for assigning the absolute configurations of α-amino acids and α-hydroxy acids. Here, we examined enantiomer discrimination of α-monosubstituted β-amino acids and α,β-disubstituted β-hydroxy acids and α,β-disubstituted β-amino acids.

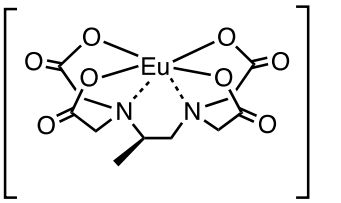

Eu-(*R*)-pdta

NMR measurement

pH of the D_2O substrate solution was once adjusted to the optimal condition for the signal separation. Prepared solution were added to two separate sample tubes then sodium salt of Eu-(*R*)- or (*S*)-pdta was added to each of the solution, respectively. After readjustment of pH, the chemical shift differences ($\Delta\Delta\delta = \Delta\delta(S) - \Delta\delta(R)$) were determined by comparison of two spectra (Figure 1).

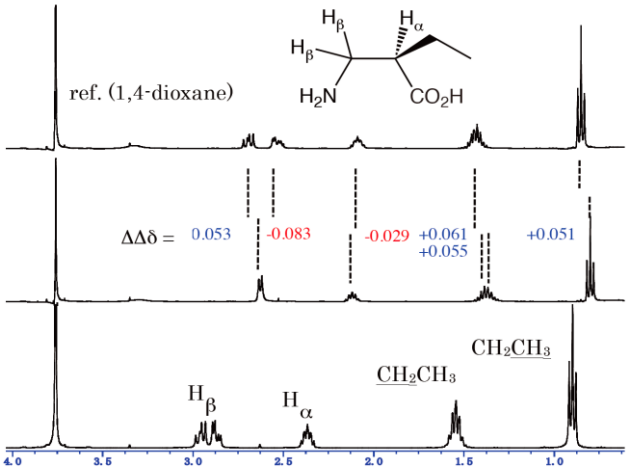

Fig 1. ^{1}H NMR spectra (400 MHz) of (*R*)-2-(aminomethyl)butanoic acid in D_2O: (upper) [Eu-(*R*)-pdta]/[acid]=1.0; (middle) [Eu-(*S*)-pdta]/[acid]=1.0; (bottom) no shift reagent.

Results and discussion

In the case of the α-monosubstituted β-amino acids shown in Figure 2, ΔΔδ values for the α-proton signals were consistently negative and those for the side chain signals were positive. It was noteworthy that a consistent relationship was also found between the signs of ΔΔδ of the β-methylene protons and the absolute configurations of the substrates. The results suggested the further application of the reagent to simultaneous discrimination of two stereogenic carbons. In fact, good correlation was observed between the absolute configurations of α,β-disubstituted β-hydroxy acids and the signs of ΔΔδ. In the session, results of α,β-disubstituted β-amino acids will also be discussed.

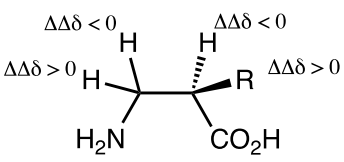

Fig 2. ΔΔδ for α-substituted amino acids

Poster 27

Synthesis of 1,6-Dihydropyrimidines by Copper-Catalyzed Intermolecular Cascade Reaction of *O*-Propargylic Oximes and Isocyanates.

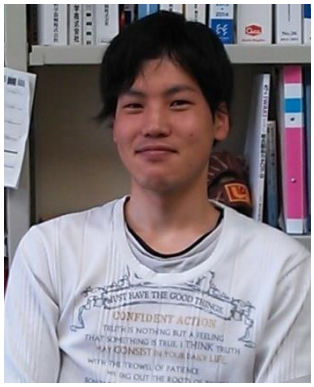

Toshiki Onuma, Dong Zhang, Itaru Nakamura, and Masahiro Terada
Graduate School of Science, Tohoku University Aoba 6-3, Aoba-ku
Sendai 980-8578, Japan.
Email: b2sm5019@s.tohoku.ac.jp
Key words: dihydropyrimidine, copper catalyst, cascade reaction

Intermolecular cascade reaction of a transiently generated reactive intermediate with an external reagent is one of the most efficient approaches to construct highly functionalized organic molecules in a single operation. In particular, it has been demonstrated that reactive intermediates, which possess a wide range of functional group, are readily accessible by π-acidic metal-catalyzed rearrangement that proceeds under mild reaction conditions.

Recently, we found that *N*-allenylnitrone intermediate **A** can be transiently generated by π-acidic metal-catalyzed 2,3-rearrangement of *O*-prapargylic oximes (Scheme1). Furthermore, we utilized the intermediate **A** to intermolecular cascade reaction with olefins, which proceeds via [3+2] cycloaddition with the *N*-allenylnitrone intermediate **A** followed by 1,3-oxygen migration involving cleavage of N-O bond (Scheme 1a)[1]. In this context, we envisioned that the reaction with an isocyanate via [3+2] cycloaddition and N-O bond-cleavage cascade reaction would be succeeded by liberation of CO_2, leading to a different class of heterocyclic skeletons (Scheme 1b). Herein, we report that copper-catalyzed reaction of *O*-propargylic aldoxime **1** and *N*-tosylisocyanate afforded 1,6-dihydropyrimidines **2** in good to acceptable yields (eq 1).

Scheme 1

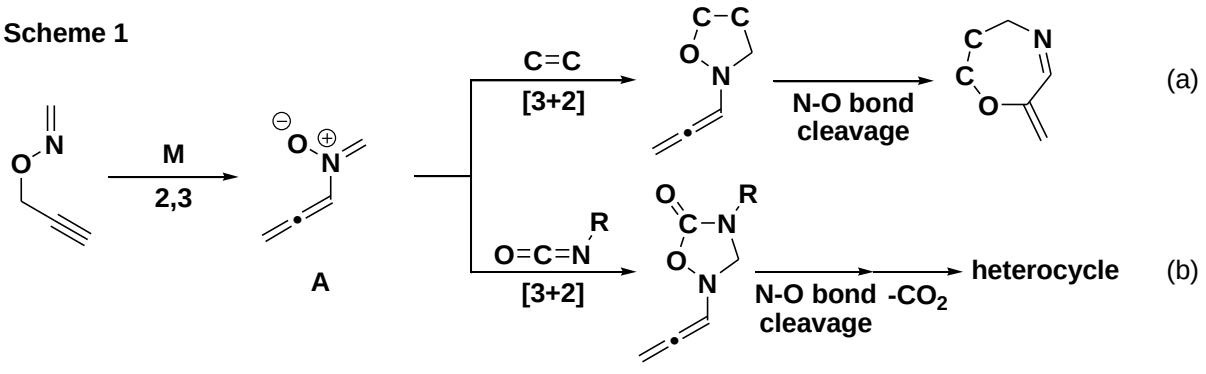

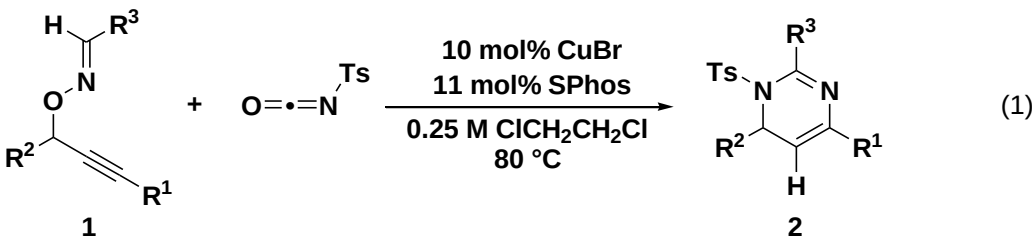

[1] I. Nakamura, Y. Kudo, M. Terada *Angew. Chem., Int. Ed.* doi: 10.1002/anie.201302751

Poster 28

Asymmetric Intramolecular Cyclization of Alkynylesters Catalyzed by Brønsted Base

Kyoko Kimura,[1] Azusa Kondoh,[1] and Masahiro Terada[1]
[1]Graduate School of Science, Tohoku University Aoba 6-3, Aoba-ku, Sendai 980-8578, Japan.
Email: b2sm5024@s.tohoku.ac.jp
Key words: Asymmetric Synthesis, Cyclization, Brønsted Base

Introduction

The intramolecular addition of enols or enolates to alkynes has served as an important method for the construction of cyclic compounds in organic synthesis. Generally activation of a C-C triple bond by π-acidic transition metal complexes or Lewis acids is exploited for this intramolecular cyclization. However, in the most of methods reported to date, the enols or enolates were generated using substrates possessing relatively high acidity at the nucleophilic site such as 1,3-dicarbonyl compounds. In order to overcome this intrinsic limitation, alkynyl silyl enol ethers have also been utilized. In these cases, however, pre-functionalization of substrates is required, and more straightforward methods are desirable. In addition, enantioselective variants of the intramolecular cyclization are very limited.[1] Meanwhile, in an effort to develop the efficient cyclization of the substrates having less acidic nucleophiles, we recently developed the intramolecular cyclization of *o*-alkynylphenyl benzyl ethers and alkynylesters using phosphazene as the Brønsted base catalyst.[2] In our continuous studies on the Brønsted base catalysis, we envisioned to develop an enantioselective method for the intramolecular cyclization of less acidic substrates, that is, activation of a nucleophilic site by a chiral Brønsted base. Herein we report an enantioselective cyclization of alkynylesters catalyzed by a chiral Brønsted base.

Result and Discussion

The reaction was performed in toluene at room temperature for 6 h with alkynylester **2** using a catalytic amount of potassium alkoxide generated in situ from *t*BuOK and chiral Schiff base **1**. **3** was obtained in moderate yield with moderate enantioselectivity.

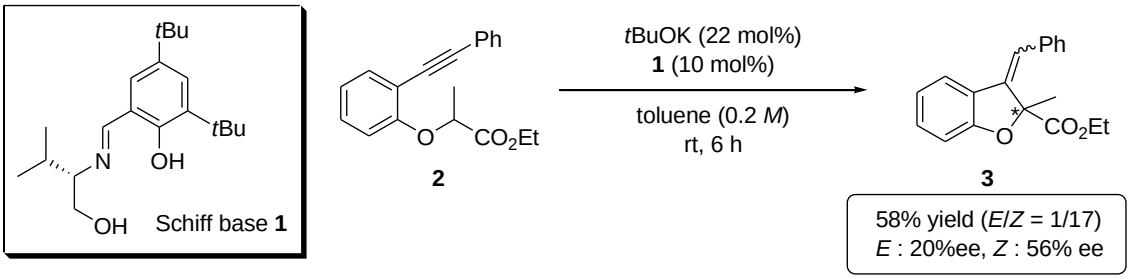

[1] Brazeau, J.-F.; Zhang, S.; Colomer, I.; Corkey, B. K.; Toste, F. D. *J. Am. Chem. Soc.* **2012**, *134*, 2742.
[2] Kanazawa, C.; Goto, K.; Terada, M. *Chem. Commun.* **2009**, 5248.

Poster 29

Chiral Phosphoric Acid Catalyzed Aza-Petasis-Ferrier Rearrangement for Construction of a Quaternary Stereogenic Center

Takazumi Komuro, Yasunori Toda, Azusa Kondoh and Masahiro Terada
Graduate School of Science, Tohoku University Aoba 6-3, Aoba-ku, Sendai 980-8578, Japan.
E-mail: b2sm5029@s.tohoku.ac.jp
Key word: Brønsted acid, Asymmetric catalysis, Organocatalyst, Rearrangement

Optically active *β*-aminocarbonyl compounds are useful as chiral building blocks in organic synthesis. Considerable efforts have been devoted to the development of stereoselective synthesis of *β*-aminocarbonyl compounds so far. However, catalytic asymmetric syntheses of *β*-aminocarbonyl compounds having a quaternary stereogenic center at the *β*-position are still limited, especially using organocatalysts.

Recently, we reported highly stereoselective aza-Petasis-Ferrier rearrangement catalyzed by a chiral phosphoric acid.[1] This 1,3-rearrangement proceeds via C-O bond cleavage to generate an imine intermediate and an enol followed by C-C bond formation to afford *β*-amino aldehydes bearing a teriary stereogenic center at the *β*-position (eq 1, R^1 = H, $R^2 \neq$ H). We envisaged that this reaction can be applicable to the stereoselective synthesis of *β*-amino aldehydes having a quaternary stereogenic center ($R^1 \neq$ H, $R^2 \neq$ H).

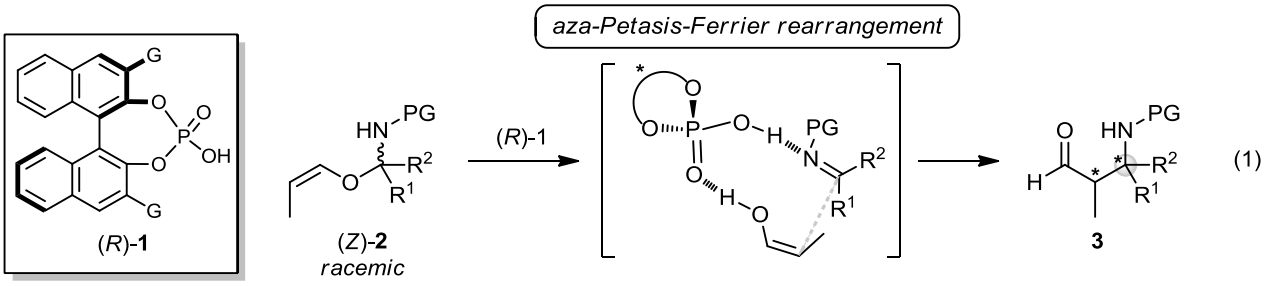

The reactions was performed using hemiaminal vinylether **2**, in which the thio-hydantoin subunit was introduced to facilitate the 1,3-rearrangement, and 5 mol% of chiral phosphoric acid **1** in 1,2-dichloroethane at ambient temperature. As a result, the reaction proceeded with high stereoselectivity albeit in an insufficient chemical yield (eq 2).

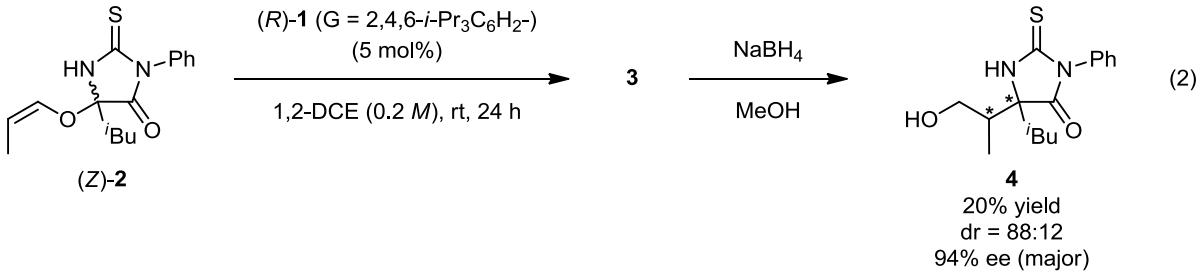

Ref. [1] Terada, M.; Toda, Y. *J. Am. Chem. Soc.* **2009**, *131*, 6354-6355.

Poster 30

Construction of Nitrogen-Containing Medium Rings by Rhodium-Catalyzed 2,3-Rearrangement/Heterocyclization Cascade.

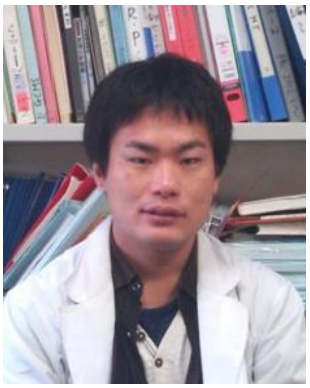

Yoshinori Sato,[1] Itaru Nakamura,[1] and Masahiro Terada[1]
[1]Graduate School of Science, Tohoku University Aoba 6-3, Aoba-ku, Sendai 980-8578, Japan.
Email: b2sm5034@s.tohoku.ac.jp
Key words: rhodium, medium rings, cascade reaction

Catalytic cyclization via formation of metallacyclic intermediate is one of the most powerful tools to synthesize highly elaborate carbocyclic compounds in an efficient manner. In particular, vinylallenes have been extensively utilized as a useful four-carbon unit in this methodology (Scheme 1a). Recently, we demonstrated that the *N*-allenylnitrone, which is regarded as a nitrogen analogue of vinylallene, can be transiently generated by metal-catalyzed 2,3-rearrangement of *O*-propargylic oximes.[1,2] In this context, we expect that cascade reaction via 2,3-rearrangement and aza-metallacyclization realizes construction of multi-substituted heterocyclic skeletons (Scheme 1b) In this poster, we report that the reaction of *O*-propargylic oximes **1** having a cyclopropyl or cyclobutyl group at the oxime moiety in the presence of rhodium catalysts produced the corresponding seven- or eight-membered heterocycles **2** in good to high yields (eq 1).[3]

Scheme 1

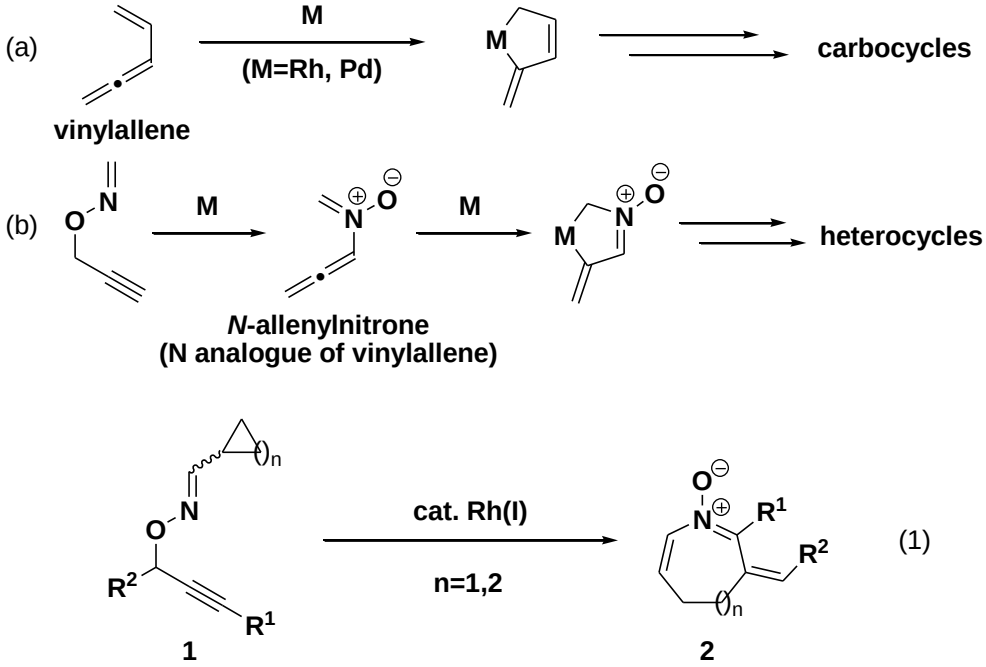

Ref. [1] I. Nakamura, D. Zhang, M. Terada, *J. Am. Chem. Soc.* **2010**, *132*, 7884.
[2] I. Nakamura, T. Araki, D. Zhang, Y. Kudo, E. Kwon, M. Terada, *Org. Lett.* **2011**, *13*, 3616.
[3] I. Nakamura, M. Okamoto, Y. Sato, M. Terada, *Angew. Chem. Int. Ed.* **2012**, *51*, 10816.

Poster 31

Design and Development of C_1 Symmetric Brønsted Acid Catalyst with Dynamic Axial Chirality

Kosuke Funayama, Norie Momiyama, and Masahiro Terada
Graduate School of Science, Tohoku University Aoba 6-3, Aoba-ku, Sendai 980-8578, Japan.
E-mail: k_funayama@s.tohoku.ac.jp
Key words: Brønsted acid, Diels-Alder reaction, Hydrogen Bond

[Introduction]

We have previously developed pseudo C_2 symmetric bis phosphoric acid that has two cyclic phosphoric acid moieties in β-naphthylphenyl skeleton, and succeeded in highly enantioselective Diels-Alder Reaction.[1]

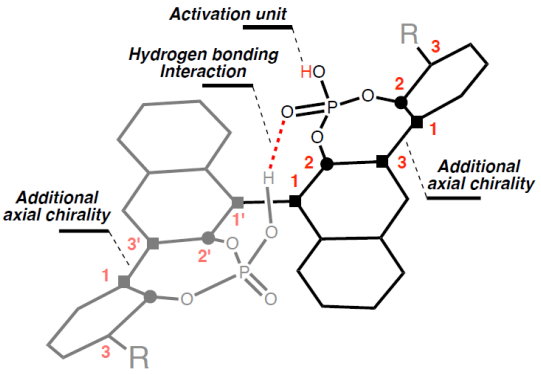

The importance of hydrogen bonding between two phosphoric acid moieties and additional axial chirality has been implied based on some experimental outcomes. However, details of these were not revealed. To get insight into this objective, we designed and synthesized novel C_1 symmetric bis phosphoric acid as novel Brønsted acid catalyst, and examined its potential in detail.

[Result and Discussion]

We synthesized C_1 symmetric bis phosphoric acid with steric group and electron-withdrawing group (EWG) as different aryl substituents. Next, the evaluation of C_1 catalyst was conducted in catalytic asymmetric Diels-Alder reaction of amidodiene and haloacrolein. As a result, the desired cycloadducts were obtained in moderate yield and good enantioselectivity. Bromine, chlorine, and iodine were applicable as halogen of haloacrolein. Pentafluorophenyl group, which is known as strong EWG, afforded the best result. Furthermore, we found that intramolecular hydrogen bonding is essential to highly catalytic activity and controlling dynamic axial chirality based on comparative studies.

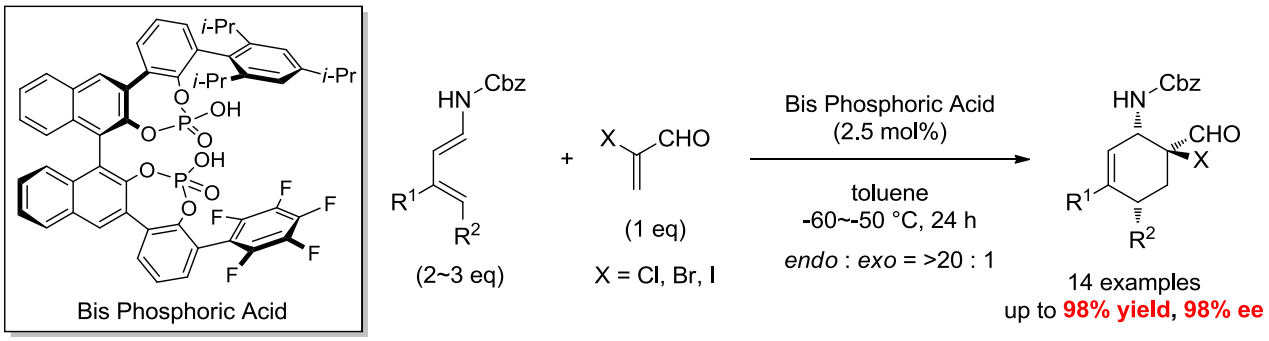

1) Momiyama, N.; Konno, T.; Furiya, Y.; Iwamoto, T.; Terada, M. *J. Am. Chem. Soc.* **2011**, *133*,19294-19297.

Poster 32

Synthesis and Dynamic Behaviors of Cyclophanes: Silacyclophane and Cycloarylene

Sho Kamata, Taisuke Matsuno, Shunpei Hitosugi, Waka Nakanishi, and Hiroyuki Isobe

Department of Chemistry and Advanced Institute for Materials Research (WPI-AIMR), Tohoku University, Sendai 980-8579, Japan.

Email: s.kamata@s.tohoku.ac.jp

Key words: silacyclophane, cycloarylene, atropisomerism

[*Introduction*]

Since their first appearance, cyclophanes continue to attract much interest, because of their unique molecular structures and dynamic behaviors. In this research, we analyzed conformational changes of flexible silacyclopahane (disilanyl double-pillared biscarbazole, ^{Si}DPBC **1**)[1] and belt-persistent [4]cyclo-2,8-anthanthrenylene ([4]$CA_{2,8}$ **2**)[2].

[*Results and discussion*]

<Conformational flexibility of ^{Si}DPBC> ^{Si}DPBC **1** was synthesized from readily accessible 3,6-dibrominated carbazole. The step-like structure of **1** was disclosed by X-ray crystallographic analysis. In the solution phase, **1** fluctuated its structure on an NMR timescale. Theoretical calculation revealed that *anti*- and *syn*-conformers (Figure 1) exist as two major conformations. Therefore, fluctuated behavior of **1** derived from very fast conformational changes between these conformers.

<Atropisomerism in [4]$CA_{2,8}$> [4]$CA_{2,8}$ **2** was synthesized from four anthanthrenylene units by coupling reaction. Because of high ring strain energy of the macrocycle, **2** have persistent belt-structure to exist as six atropisomers. When we subjected one of the six atropisomers to thermal isomerization, the rotation profile indicated that the anthanthrenylene panels rotate in a stepwise, one-by-one manner (Figure 2). The profile was further analyzed using Eyring plots to afford a rotational barrier with $\Delta H^{\ddagger}$ = +21 kcal mol^{-1} and $\Delta S^{\ddagger}$ = –15 cal mol^{-1} K^{-1}.

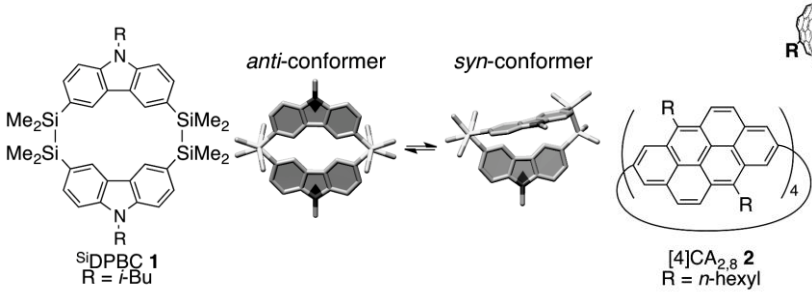

Figure 1. Structure and calculated conformers of ^{Si}DPBC **1**.

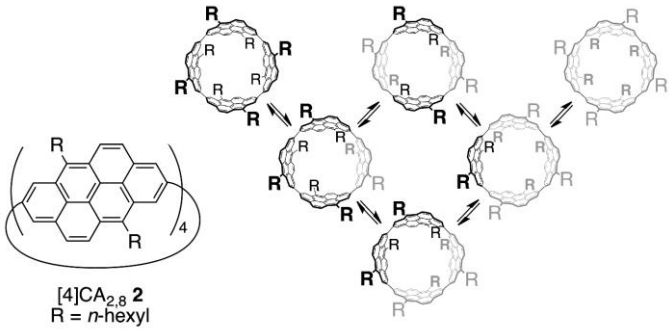

Figure 2. Chemical structure and isomerization path of [4]$CA_{2,8}$ **2**.

1. Nakanishi, W.; Kamata, S.; Hitosugi, S.; Isobe, H. *Chem. Lett.* **2012**, *41*, 1652–1654.
2. Matsuno, T.; Kamata, S.; Hitosugi, S.; Isobe, H. *Chem. Sci.* **2013**, DOI: 10.1039/C3SC50645B.

Poster 33

Synthesis and Properties of Substituted Naphthylene Macrocycle

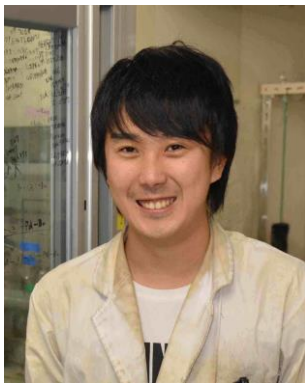

Yuta Nakamura, Jing Yang Xue, Waka Nakanishi, Daiki Tanimoto, Daisuke Hara, Hiroyuki Isobe

Department of Chemistry and Advanced Institute for Materials Research (WPI-AIMR), Tohoku University, Sendai 980-8578, Japan.

Email: y.nakamura@s.tohoku.ac.jp

Key words: Arenes, Macrocycle

[Introduction]

Conjugated macrocycles are an interesting class of compounds because of their potential applications as organic materials and their π-electron rich structures that tolerate chemical modifications. We previously synthesized the first example of cyclonaphthylene, [6]cyclo-2,7-naphthylene ([6]CNAP), which revealed unique properties such as bipolar charge transporting ability and high thermal stability[1]. We envisioned that the introduction of imide moieties should allow us to tune the electronic properties of [6]CNAP with its electron-withdrawing nature. In this presentation, we report the synthesis and properties of fully imide-substituted [6]CNAP (i_6-[6]CNAP **1**).

[Results and Discussion]

As the precursor of **1**, dibrominated ternaphtyl **2** was prepared from commercially available naphthalic anhydride. Ni-mediated homocoupling reaction of **2** proceeded smoothly to give **1** in 62% yield. The solubility of **1** was dramatically improved by introduction of substituents. The electronic property of **1** was investigated with DFT calculation. DFT calculation showed that **1** has lower LUMO level. This result indicated that **1** has the potential as electron transporting material. In this presentation, other physical properties such as UV absorption and fluorescence will be also discussed.

Scheme 1. Synthesis of i_6-[6]CNAP **1**

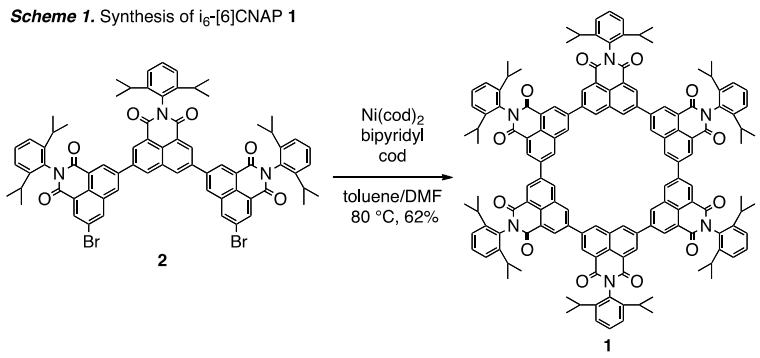

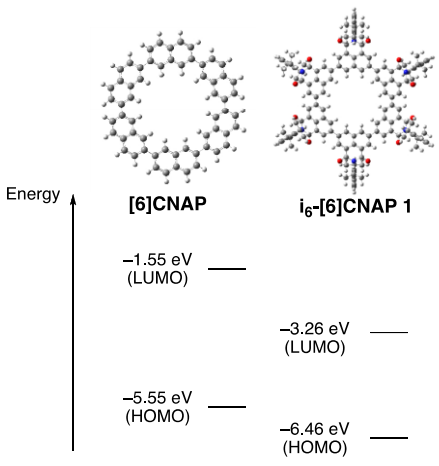

Figure 1. Calculated structure and HOMO-LUMO level

[1] Nakanishi, W.; Yoshioka, T.; Taka, H.; Xue, J. Y.; Kita, H.; Isobe, H. *Angew. Chem. Int. Ed.* **2011**, *50*, 5323-5326.

Poster 34

Development of simplified and large scale synthesis of triazole-linked nucleic acids

Ai Hasome, Tomoko Fujino, and Hiroyuki Isobe
Department of Chemistry and Advanced Institute for Materials Research (WPI-AIMR) Tohoku University, Tohoku University, Sendai 980-8578, Japan
Email: a.hasome@s.tohoku.ac.jp
Key words: DNA, oligonucleotide, solid-phase synthesis

[Introduction] Analogues of DNA and RNA that have nucleobases displayed on artificial neutral backbones are attracting much interest. As a new variant of analogue, we introduced a triazole-linked DNA and RNA (^{TL}DNA, ^{TL}RNA) by copper(I)-catalyzed Huisgen [3 + 2] cycloaddition reaction,[1] and recently demonstrated the unique function of ^{TL}DNA as a lure substrate for an enzyme.[2] Here we showed a revised synthetic protocol for long oligonucleotides with simplified preparation and purification for bioorganic applications.

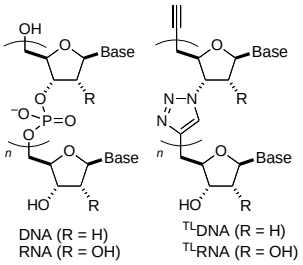

Figure 1. The structures of DNA, RNA, ^{TL}DNA and ^{TL}RNA.

[Results and discussion] First of all, solvent used for cycloaddition reaction was reoptimized. Previously we used DMF/*t*-butanol for the reaction in which sodium ascorbate, a reducing agent, shows poor solubility. We found that DMF/water is the best solvent for dissolving all reagents and, therefore, proceeding cycloaddition reaction rapidly and efficiently to give hexathymine. The high solubility also enabled us to prepare the stock solution for each reagent. Next, autowashig protocol was introduced after each operation step. We used diethyl dithiocarbamate aqueous solution, acetonitrile and dichloromethane in a programmed manner, which efficiently removed reagents and the copper. The protocol eliminated waste of time for the complicated purification operations for the synthesis of long oligonucleotides. In the presentation, we also present on the large-scale synthesis for oligonucleotides under optimized conditions.

Scheme 1. Simplified and large-scale synthesis of ^{TL}DNA.

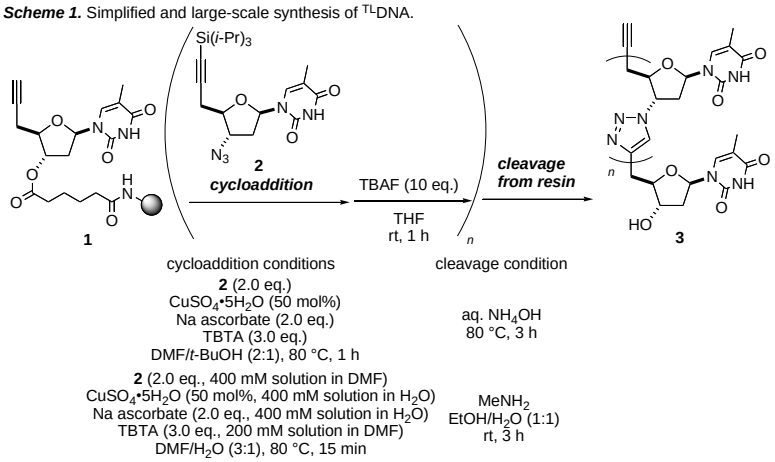

[1] (a)Isobe, H.; Fujino, T.; Yamazaki, N.; Guillot-Nieckowski, M.; Nakamura, E. *Org. Lett*. **2008**, *10*, 3729-3732; (b) Fujino, T.; Yamazaki, N.; Hasome, A.; Endo, K.; Isobe, H. *Tetrahedron Lett*. **2012**, *53*, 868-870.

[2] Fujino, T.; Yasumoto, K.; Yamazaki, N.; Hasome, A.; Sogawa, K.; Isobe, H. *Chem Asian J*. **2011**, *6*, 2956-2960.

Poster 35

Molecular Bearing of Finite Carbon Nanotube and Fullerene in Ensemble Rolling Motion

Takashi Yamasaki, Shunpei Hitosugi, Ryosuke Iizuka, and Hiroyuki Isobe
Department of Chemistry and Advanced Institute for Materials Research (WPI-AIMR), Tohoku University, Sendai 980-8578, Japan.
Email: t.yamasaki@s.tohoku.ac.jp
Key words: Carbon nanotube; Fullerene; Peapod; Bearing; Association

In the 1950s, the nanoscale molecular bearing that can realize ultralow friction appeared in the Feynman's prediction. In 2000, ultralow friction of multi-wall carbon nanotubes was demonstrated by electron microscopy in a form of linear bearing. However, this observation was limited to single molecule observation, because inhomogeneous molecular structures of available carbon nanotubes allow for handling only as a mixture of various structures. Recently, we synthesized [4]cyclochrysenylene ([4]CC) as a finite single-wall carbon nanotube (SWNT) molecule[1,2]. In this study, we constructed a molecular bearing with a finite SWNT "bearing" and a fullerene "journal" and demonstrated its anisotropic rolling motion under the ensemble dynamics[3].

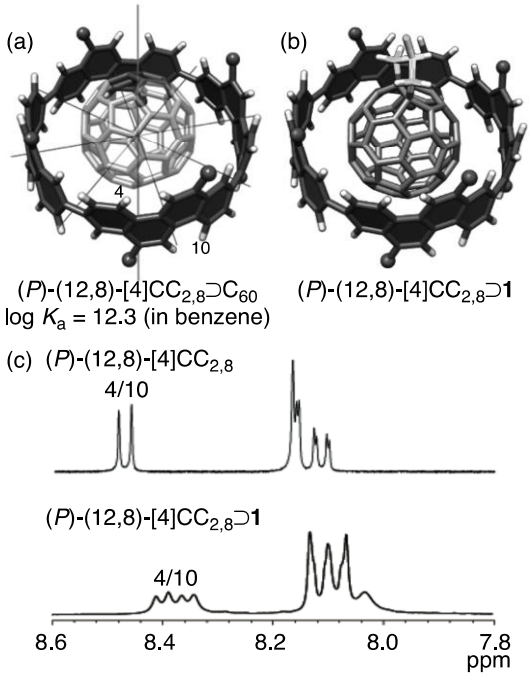

***Figure* 1**. (a) A molecular model of (*P*)-(12,8)-[4]CC⊃C$_{60}$. (b) A molecular model of (*P*)-(12,8)-[4]CC⊃**1** and (c) the aromatic resonances in ^{1}H NMR spectra in CD_2Cl_2.

The strong association between [4]CC and fullerene was confirmed. The maximum values of association constant of (*P*)-(12,8)-[4]CC⊃C$_{60}$ was recorded in benzene as log K_a = 12.3 (Figure 1a). This association value was the highest value recorded for supramolecular systems in apolar solvents. A "shaft" moiety was then introduced onto the C$_{60}$ journal (Figure 1b). From NMR analysis of (*P*)-(12,8)-[4]CC ⊃ **1**, proton resonances of north and south positions of chrysenylene were observed as a set of two independent signals, while these from four chrysenylene units appeared as equivalent resonances (Figure 1c). The results demonstrated that the journal in the bore rolls rapidly on the NMR timescale around the C_4 symmetry axis. Furthermore, variable temperature NMR analysis suggested that the dynamic behavior of fullerene journal depended on the temperature.

1. Hitosugi, S.; Nakanishi, W.; Yamasaki, T.; Isobe, H. *Nat. Commun.* **2011**, *2*, doi: 10.1038/ncomms1505.

2. Hitosugi, S.; Yamasaki, T.; Isobe, H. *J. Am. Chem. Soc.* **2012**, *134*, 12442-12445.

3. Isobe, H.; Hitosugi, S.; Yamasaki, T.; Iizuka, R. *Chem. Sci.* **2013**, *4*, 1293-1297.

Poster 36

Structural Changes and Physical Properties of Copper(II) Complexes through Chemisorptions.

Kiyonori Takahashi,[1] Norihisa Hoshino,[1, 2] Shin-ichiro Noro,[3] Takayoshi Nakamura,[3] and Tomoyuki Akutagawa[1, 2]

[1]Graduate School of Engineering, Tohoku University 6-6, Aoba, Aramaki, Aoba-ku, Sendai 980-8579, Japan.

[2]Institute of Multidisciplinary Research for Advanced Materials (IMRAM), Tohoku University 2-1-1, Katahira, Aoba-ku, Sendai 980-8577, Japan.

[3]Research Institute for Electronic Science, Hokkaido University, N20W10, Kita-ku, Sapporo, 001-0020, Japan.

Email: jintokut@mail.tagen.tohoku.ac.jp

Key words: Cu binuclear complex, Chemisorptions, Structural Change, Magnetic Property

Structural changes induced by the outer stimuli coupled with physical responses have been much attracted attentions to achieve new functional dynamic molecular materials.

Herein, we report the structural changes and magnetic properties of copper (II) complexes through H_2O and/or pyridine chemisorptions. The chemisorption effects for the initial crystal of Cu(II)-binuclear coordination polymer of $[Cu_2(2,3\text{-}F_2BA)_4(pz)]_\infty$ (**1a**), here 2,3-F_2BA and pz were 2,3-difluorobenzoate and pyrazine, respectively, were examined.

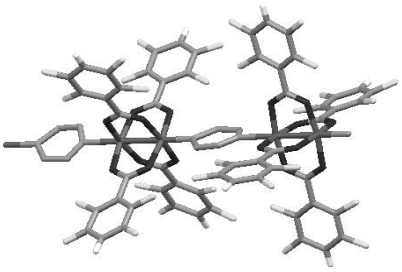

Fig. 1 Crystal structure of **1a**. F_2BA ligands have orientational disorder.

The crystal structure of green-colored **1a** was formed by the one-dimensional $[Cu(II)_2(2,3\text{-}F_2BA)_4(pz)]_\infty$ polymer chain, where the binuclear paddle-wheel type $Cu_2(2,3\text{-}F_2BA)_4$-units were bridged by the axial pz ligand (Fig. 1). The void spaces among the one-dimensional chains were observed in crystal **1a**, which were occupied by CH_3CN molecules in the as-grown crystals. When the green-colored single crystals of **1a** were immersed with H_2O and/or pyridine vapor, the crystal colors were changed to white-blue (**1b**) and/or dark-blue (**1c**), respectively. The PXRD measurement of crystals **1b** and **1c** showed the structural changes from that of **1a** through the chemisorptions. The $\chi_m T$ - T plots of crystal **1a** revealed the strong antiferromagnetic coupling, whereas those of crystals **1b** and **1c** showed the ferromagnetic and paramagnetic behavior, respectively. The significant structural changes were associated with the magnetic ones, which will be discussed in detail.

Poster 37

Preparations, crystal structures, and electronic states of thiadiazole- and triazole-fused *p*-benzoquinones

Masahiro Sato,[1] Takashi Takeda,[1, 2] Norihisa Hoshino,[1, 2] and Tomoyuki Akutagawa[1, 2]

[1]Graduate School of Engineering, Tohoku University, 6-6 Aramaki-aza-aoba, Aoba-ku, Sendai, 980-8579, Japan.

[2]Institute of Multidisciplinary Research for Advanced Materials (IMRAM), Tohoku University, 2-1-1 Katahira, Aoba-ku, Sendai, 980-8577, Japan.

Email: masa_104@mail.tagen.tohoku.ac.jp

Key words: *p*-benzoquinone, thiadiazole, triazole

Organic electronic devices have an advantage of flexibility, low-cost device fabrication, light-weight etc., in contrast with the inorganic devices. From these points of views, new p-type organic semiconductors have been developed for the application of organic field effect transistor (OFET) with high mobility. On the contrary, the molecular structures of n-type organic semiconductors with high mobility are quite significantly limited in number. Herein, we noticed the electronic active molecular structure of *p*-benzoquinone (BQ) derivatives. The crystal structure and redox properties of thiadiazole-fused BQ (**1**) and newly prepared triazole-fused BQ (**2**) are discussed.

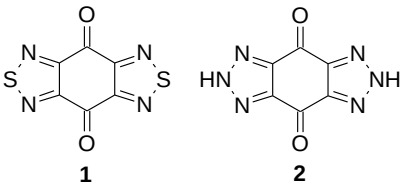

1 **2**

Figure Molecular structures of compound **1** and **2**

Although the preparation of **1** has been already reported, the crystal structures and physical properties of electron-acceptor **1** have not been examined enough.[1] Both of the X-ray crystal structural analysis and calculation of intermolecular transfer integrals revealed the three-dimensional intermolecular interactions of LUMO and HOMO through the π-stacking and intermolecular S~N contacts. In addition, we could newly obtain the Na^+ salt of anionic triazole-fused BQ (**3**) (Scheme). The crystal structure of compound Na^+(**3**)•2(H_2O) showed the π-stacking and hydrogen-bonding network structures. Details of crystal structures and redox properties will be discussed.

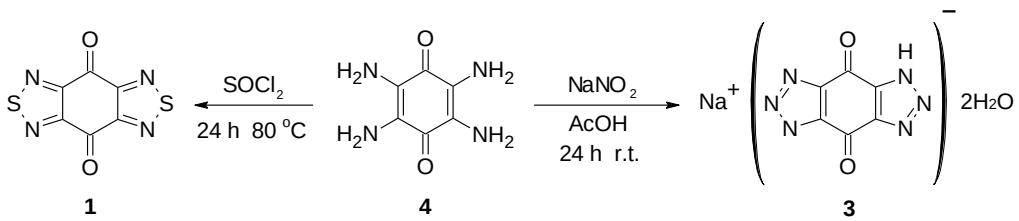

1 **4** **3**

Scheme Preparations of compound **1** and Na^+ **3** 2H_2O

[1] R. Neidlein et al. *Chem. Ber*. **1982**, *115*, 2898-290.

Poster 38

Evaluation of pH at Alumina-Water by SFA Fluorescence Spectroscopy

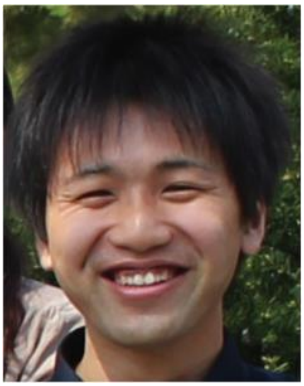

Kawashima Masataka,[1] Saito Yuko,[1] Inomata Kyeong A,[2] Kasuya Motohiro, [1] and Kurihara, Kazue[1,2]

[1]Institute of Multidisciplinary Research for Advanced Materials (IMRAM), Tohoku University, Katahira 2-1-1, Aoba-ku, Sendai, 980-8577, Japan.

[2]WPI Advanced Institute for Materials Research (WPI-AIMR), Tohoku University, Katahira 2-1-1, Aoba-ku, Sendai, 980-8577, Japan.

Email: kawasima@mail.tagen.tohoku.ac.jp

Key words: Surface Forces Measurement, Fluorescence Probe Method, Electric Double Layer, Alumina-Water Interface, pH

Study of pH at the solid-liquid interfaces is important in many research fields such as biochemistry and electrochemistry. We evaluated the pH of water between mica and silica surfaces by varying the surface separation (D) using surface forces apparatus (SFA) fluorescence spectroscopy which we have developed[1), 2)]. In this study, we evaluated pH at an alumina–water interface in the same way because the surface chemistry of aluminas plays a key role in their performance as catalysts and as dielectrics in microelectronics

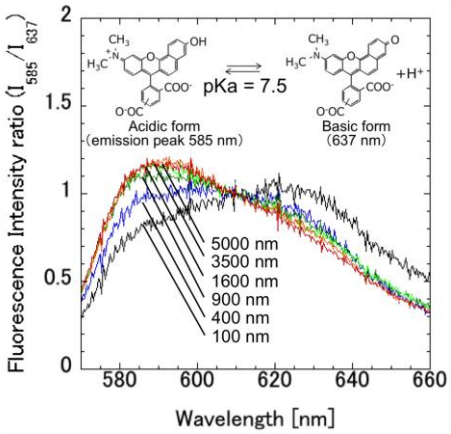

Fig. 1. Fluorescence spectra of C.SNARF-1 in water between alumina surfaces at various D's (Inset : Acid-base equilibrium of C.SNARF-1).

5-(and-6)-carboxy SNARF-1 (C.SNARF-1 shown in Fig. 1 inset) was used as a pH sensitive fluorescence probe. Fig. 1 shows the fluorescence spectra of C.SNARF-1 in water (2×10^{-5} M, pH 6.5) between alumina surfaces at various D values. When D decreased, the fluorescence intensity of the peak at 585 nm (I_{585}) ascribed to the acidic form of C.SNARF-1 decreased and the intensity of the peak at 637 nm (I_{637}) ascribed to the basic form increased. From these spectrum changes due to the acid-base equilibrium of C.SNARF-1, we evaluated pH of water between alumina surfaces, which increased with decreasing D as shown in Fig. 2. In addition, we measured surface forces between alumina surfaces in water for evaluating the surface potential. pH of the interfacial water estimated from this potential corresponded to that evaluated from the fluorescence measurement, indicating that pH increase could be attributed to concentrated hydroxide ions in the electric double layer of the positively charged alumina surface.

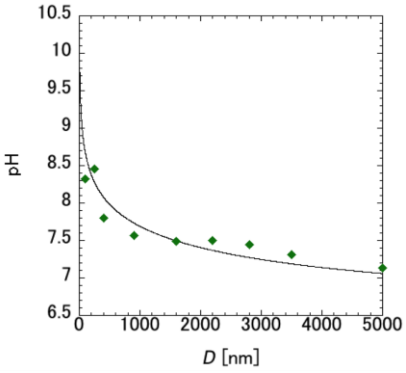

Fig. 2. pH values of water between alumina surfaces evaluated from I_{585}/I_{637} at various D's. Solid line was estimated from the result of the surface forces measuremanent.

Ref. [1] D. Fukushi, M. Kasuya, H. Sakuma, and K. Kurihara, *Chem. Lett.* **40**, 776 (2011).
[2] Y. Saito, M. Kasuya, K. Kurihara, *Chem. Lett.* **41**, 1282 (2012).

Poster 39

Microsecond dynamics of ubiquitin folding detected by single molecule fluorescence spectroscopy.

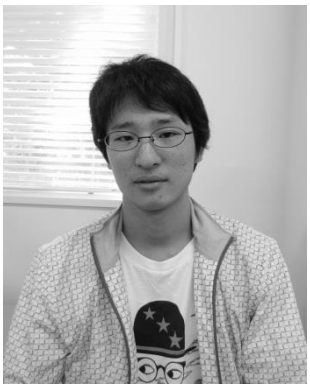

Masataka Saito[1], Hsin-Liang Chen[3], Rita P.-Y. Chen[3], Kiyoto Kamagata[1, 2], Hiroyuki Oikawa[2], Satoshi Takahashi[1,2]
[1]Graduate School of Science, Tohoku University Aoba 6-6, Aoba-ku, Sendai 980-8579, Japan.
[2]Institute of Multidisciplinary Research for Advanced Materials (IMRAM), Tohoku University Katahira 2-1-1, Aoba-ku, Sendai 980-8577, Japan.
[3]Institute of Biological Chemistry (IBC), Academia Sinica, 128, Academia Road Sec. 2, Nankang, Taipei 115, Taiwan.
Email: saitom2@mail.tagen.tohoku.ac.jp
Key words: protein folding, single molecule, FRET, microfluidics, intermediate state

Elucidation on how proteins fold on the potential energy surface with several minima corresponding to intermediate states is important to understand the design principles of protein structures. Piana *et al*. recently examined the folding of ubiquitin by an atomistic molecular dynamics simulation, and suggested various conformations involved in the process [1]. The folding of ubiquitin has also been the subjects of intensive experimental investigations. Ubiquitin is considered to fold via a two-state mechanism that involves the native and denatured states. In contrast, the complex pathways involving the on and off pathway intermediates have also been proposed. Most of the past experiments are based on the ensemble measurements, which may hide the information of each molecule by ensemble averaging. By contrast, the time series investigation at the single molecule level might reveal the intermediates directly. In this investigation, we observed the folding dynamics of ubiquitin by using single molecule fluorescence spectroscopy.

We recently developed single molecule fluorescence detection system that can monitor the rapid dynamics of single proteins at the time resolution of 120 μs [2].Our system consists of a microfluidic tip, a line confocal microscope and a CCD image sensor. We flow the dye labeled molecules in the microfluidics without immobilization and track time series at the single molecule level.

We observed the labeled ubiquitin at several denaturant concentrations. We use a mutant of ubiquitin, in which Cys is inserted between Met1 and Gln2 and Ser65 is substituted with Cys. We obtained time series of single molecule fluorescence and calculated the FRET efficiency. Histograms of the FRET efficiency at several conditions are shown in Fig.1. At 0 M Gdn concentration, ubiquitin possesses a native conformation, and it denatures at 5 M Gdn concentration. Thus, we assigned the distribution at around 0.7 at 0 M to the native state and at 0.4 at 5 M to the denatured state. On the other hand, a new peak at 0.6 was observed at 2 M and 4 M. These data suggest that ubiquitin populates another intermediate which is neither native nor denatured state at moderate Gdn concentrations. The FRET efficiency of intermediate state is close to the native state than denatured state. Accordingly, we suggest that the intermediate possess a rather compact conformation.

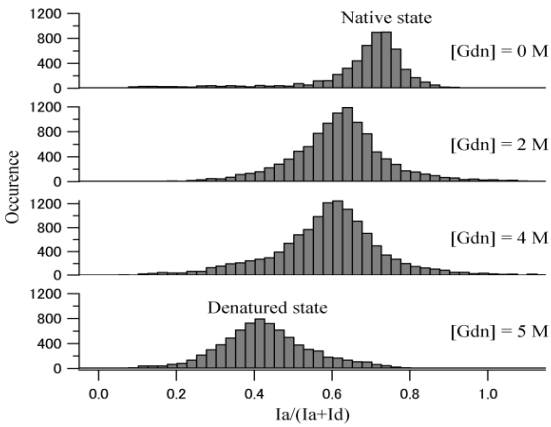

Fig. 1. Histograms of FRET efficiency at each denaturant concentration.

[1] Piana, S., Lindorff-Larsen, K., Shaw, D. *Proc*. *Natl*. *Acad*. *Sci*. USA **110**, 5915-5920 (2013).
[2] Oikawa, H. *et al*., *Scientific. Reports*. submitted.

Poster 40

Direct observation of the multiple sliding modes of a tumor suppressor p53

Agato Murata,[1] Risa Kashima,[2] Yuji Itoh,[1] Takashi Tokino,[3] Satoshi Takahashi,[4] and Kiyoto Kamagata[4]

[1]Graduate School of Science, Tohoku University Katahira 2-1-1, Aoba-ku, Sendai 980-8577, Japan.

[2]Cardiovascular Research Institute, UCSF School of Medicine, 555 Mission Bay Blvd South, San Francisco CA 94158

[3]Department of Medical Genome Sciences, Research Institute for Frontier Medicine, Sapporo Medical University, Chuo-ku, Sapporo060-8556, Japan

[4]Institute of Multidisciplinary Research for Advanced Materials (IMRAM), Tohoku University Tohoku University Katahira 2-1-1, Aoba-ku, Sendai 980-8577, Japan.

Email: b2sm5068@s.tohoku.ac.jp

Key words: protein, DNA, single-molecule measurements, diffusion

Tumor suppressor p53 is a transcription factor that controls cell cycle arrest, apoptosis and DNA repair. p53 binds to the target sequence on DNA genome within physiological time scales. The efficient search for the binding sites of p53 is partially attributed to the 1D sliding. The 1D sliding of p53 has been directly investigated by single molecule techniques, and analyzed by assuming a diffusive movement described by a single diffusion constant. However, it is conceivable that p53 has multiple sliding modes depending on the quaternary structures of the p53-DNA complex. In this study, the sliding of p53 along DNA was measured by a single-molecule fluorescence microscopy by introducing a new method of preparing the extended DNA on the surface of coverslip.

We observed the diffusive movement of p53 along DNA (Fig. 1). The observed trajectories of p53 were analyzed by the change point analysis of diffusion constants, which can detect boundaries of trajectories with different diffusion constants. We found that local segments of the trajectories between the change points can be classified into at least two groups with different diffusion constants. The results clearly demonstrate that p53 has multiple sliding modes. The population of two groups depends on the concentration of $MgCl_2$, suggesting that $MgCl_2$ acts as a suppressor of the sliding. Further analysis suggests that the multiple sliding modes might be caused by inhomogeneous interactions between the DNA binding domain of p53 and DNA.

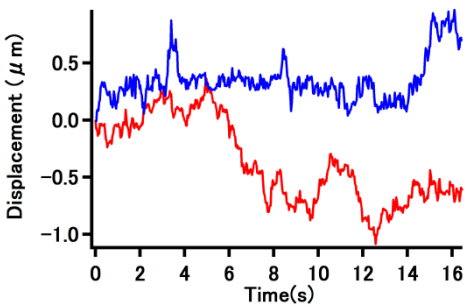

Fig. 1. Trajectories of p53 on DNA

Poster 41

A high visible light induced NO_x gas destruction activity of carbon doped TiO_2

Xiaoyong Wu, Qiang Dong, Shu Yin, and Tsugio Sato
Institute of Multidisciplinary Research for Advanced Materials, Tohoku University, 2-1-1, Katahira, Aoba-ku, Sendai 980-8577, Japan
Email: wxy521@mail.tagen.tohoku.ac.jp
Key words: carbon doped TiO_2, solvothermal reaction, visible light, photocatalytic activity

TiO_2, one of the most promising photocatalysts, has attracted lots of attention in recent years due to its high oxidative power, abundance, chemical stability, environmentally friendly and low cost [1]. Unfortunately, there is a key drawback for the widespread application of TiO_2 that can only absorb UV light (about 5% of solar light) owing to its wide band gap (3.2 eV for anatase). In this work, an effective C doped TiO_2 with the whole range of visible light absorption has been prepared by a facile solvothermal method with the assistant of post-solvothermal reaction calcination. In the following description, the samples calcined at 165 ^oC, 265 ^oC and 400 ^oC after solvothermal reaction were denoted as CT-BE-165, CT-BE-265 and CT-BE-400, respectively, and the sample without heating was denoted as CT-BE.

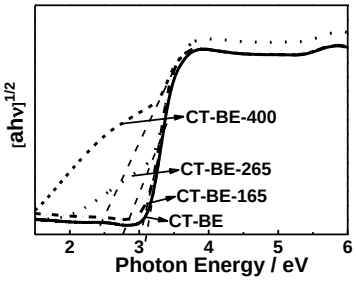

Fig.1 the Kubelka–Munk plots for the corresponding reflectance spectra of samples.

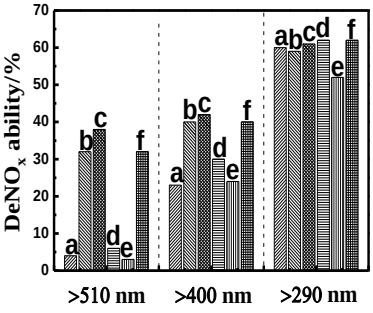

Fig.2 $DeNO_x$ ability of CT-BE (a), CT-BE-165 (b), CT-BE-265 (c), CT-BE-400 (d), P25 (e) and N-TiO_2 (f).

The XRD patterns of C doped TiO_2 samples prepared by the solvothermal reaction followed by calcinations at different temperatures showed that all the diffraction peaks of samples could be well indexed to the anatase phase of TiO_2 (JCPDS file No. 21-1272), and no other impurity peaks were appeared. After calcining specimens at 165 ^oC and 265 ^oC, the products presented outstanding visible light absorption, and the corresponding band gaps have been dramatically decreased (shown in Fig. 1), which should be due to the induction of doped carbon in TiO_2 during the calcination process. Fig. 2 exhibits the NO_x gas destruction ability of samples under the irradiation of different wavelengths of light. It is apparent that the C doped sample calcined at 265 ^oC represented the best visible light induced photocatalytic performance among all samples and also much superior to those of P25 and N doped TiO_2.

Ref. [1] M. Gratzel, Nature, 2001, 414, 338.

Poster 42

Extraction of electron-ion differential scattering cross sections from angle-resolved rescattering photoelectron spectra of C_2H_4 and C_2H_6 measured using IR laser pulses

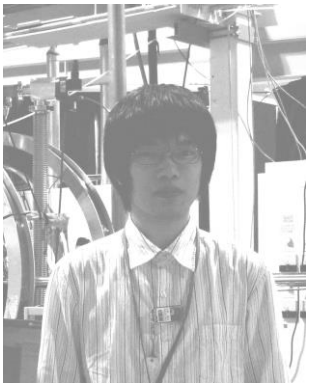

Yuta Ito,[1] Misaki Okunishi,[1] Kozo Shimada,[1] Robert R. Lucchese,[2] Toru Morishita,[3] and Kiyoshi Ueda[1]

[1]Institute of Multidisciplinary Research for Advanced Materials (IMRAM), Tohoku University, Katahira 2-1-1, Aoba-ku, Sendai 980-8577, Japan.

[2]Department of Chemistry, Texas A&M University, College Station, TX 77843-3255, USA.

[3]Department of Applied Physics and Chemistry, University of Electro-Communications, 1-5-1 Chofu-ga-oka, Chofu-shi, Tokyo 980-8579, Japan.

Email: y-ito@mail.tagen.tohoku.ac.jp

Key words: rescattering photoelectron, tunnel ionization, femtosecond laser

When atoms or molecules are exposed to strong laser fields, a part of the electrons released by tunnel ionization will be driven back by the oscillating electric field into recollisions with their parent ions. Elastic scattering electrons have structural information of the parent ions. Therefore it is expected that ultrafast dynamics of atoms and molecules can be observed with a femtosecond time resolution. In our laboratory, we have measured rescattering photoelectron spectra of atoms and molecules using laser pulses at 800 nm [1]. In this study, we measured rescattering photoelectron spectra of C_2H_4 and C_2H_6 using IR laser pulses at a longer wavelength to increase the momentum of the recolliding electron.

An optical parametric amplifier pumped by Ti:Sapphire laser pulses at 800 nm (1 kHz, 100 fs durations) is used to obtain IR laser pulses at 1.3 μm. The IR pulses are focused onto a sample gas effusively introduced in a vacuum chamber. Angular distributions of photoelectrons are obtained by continuously rotating the polarization direction of the optical fields using a half wave plate.

Fig. 1 shows an angle-resolved rescattering photoelectron spectrum of C_2H_4 measured using the 1.3 μm laser light. Rescattering electrons having recollision momentum around 1.5 a.u. are observed, while only up to 1.0 a.u. in the case of 800 nm. Differential scattering cross sections (DCSs) extracted from this experiment and theoretical calculations are shown in Fig. 2. We have obtained fairy good agreement between experimental and theoretical DCSs for the rescattering at higher collision momenta.

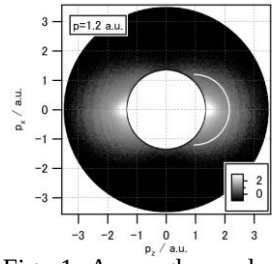

Fig. 1 An angle-resolved rescattering photoelectron spectrum of C_2H_4.

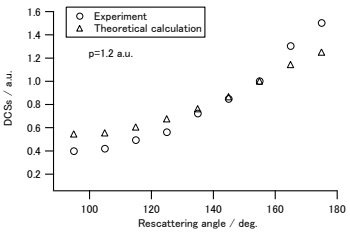

Fig. 2 Comparison of DCSs extracted from the experiment and theoretical calculations.

References [1] M. Okunishi *et al*., Phys. Rev. Lett. **100**, 143001 (2008); M. Okunishi *et al*., Phys. Rev. Lett. **106**, 063001 (2011); C. Wang *et al*., J. Phys. B: At. Mol. Opt. Phys. **45**, 131001 (2012).

Poster 43

Multiphoton multiple ionization of Argon clusters by X-ray free electron laser

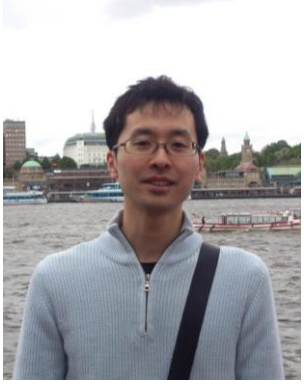

Tetsuya Tachibana,[1] Zoltan Jurek,[2] Per.Johnsson,[3] Hironobu Fukuzawa,[1,4] Koji Motomura,[1] Kiyonobu Nagaya,[4,5] Marco Siano,[6] Shin-ichi Wada,[4,7] Subhendu Mondal,[1] Miku Kimura,[1] Yuta Ito,[1] Tsukasa Sakai,[5] Kenji Matsunami,[5] Hironori Hayashita,[7] Jumpei Kajikawa,[7] XiaoJing Liu,[8] Emmanuel Robert,[8] Catalin Miron,[8] Raimund Feifel,[9] Jon Marangos,[6] Kensuke Tono,[10] Yuichi Inubushi,[4] Takaki Hatsui,[4] Makina Yabashi,[4] Beata Ziaja,[2] Sang-kil Son,[2] Robin Santra,[2,11] Makoto Yao,[5] and Kiyoshi Ueda[1,4]

[1] IMRAM, Tohoku Univ., [2] CFEL, DESY, [3] Lund Univ., [4] RIKEN SPring-8 Center, [5] Kyoto Univ., [6] Imperial College London, [7] Hiroshima Univ., [8] Synchrotron SOLEIL, [9] Uppsala Univ., [10] JASRI, [11] Univ. of Hamburg

Email: t-tachi@mail.tagen.tohoku.ac.jp

Key words: Multiphoton multiple ionization, X-ray free electron laser, SACLA, Argon clusters.

We have studied multiphoton multiple ionization dynamics of Argon clusters irradiated by intense X-ray pulses obtained from a new X-ray free electron laser (XFEL) facility, the SPring-8 Angstrom Compact free electron LAser (SACLA) [1]. Electron energy spectra have been measured using a Velocity Map Imaging (VMI) spectrometer as a function of cluster size. The measured electron spectra exhibit dependence on the cluster size. The experimental results are compared with theoretical calculations.

The experiment has been carried out at the experimental hutch 3 (EH3) of the beamline 3 (BL3) of SACLA. The XFEL beam is focused by the Kirkpatrick-Baez (KB) mirror system to a focal size of ~1 μm (FWHM) in diameter [2]. The cluster beam was introduced as a pulsed supersonic jet to the focus point of the XFEL radiation [3]. The targets were Argon clusters with a mean cluster size of 100–1000. Electrons produced by photoionization of the clusters by the XFEL were accelerated toward a position-sensitive detector consisting of a set of microchannel plates (MCPs) followed by a phosphor screen, and recorded using a CCD camera synchronized to the arrival of the XFEL pulse in the interaction chamber. The measured two-dimensional (2D) projection allows the three-dimensional (3D) momentum distribution of the ejected electrons to be obtained using a mathematical inversion procedure. Our VMI spectrometer could collect all electrons emitted into 4π sr for kinetic energies up to ~900 eV.

This study was supported by the X-ray Free Electron Laser Utilization Research Project and the X-ray Free Electron Laser Priority Strategy Program of the MEXT, by JSPS, by the Proposal Program of SACLA Experimental Instruments of RIKEN and by the IMRAM project.

References: [1] T. Ishikawa *et al.*, Nat. Photon., **6**, 540 (2012). [2] H. Yumoto *et al.*, Nat. Photon., **7** 43 (2013). [3] K. Nagaya *et al.*, J. Electron. Spectrosc. Relat. Phenom. **181**, 540 (2010).

Poster 44

Synthetic studies of clionamines, autophagy-modulating amino steroids isolated from *Cliona celata*

Akiyuki Yoshida, Yuuki Sato, Konosuke Hiramatsu, Teiko Yamada, Shigefumi Kuwahara, Hiromasa Kiyota
Graduate School of Agricultural Science, Tohoku University,
1-1, Tsutsumidori-Amamiya, Aoba-ku, Sendai 981-8555, Japan
Email: skuwahar@iochem.tohoku.ac.jp
Key words; amino steroid, spiro dilactone, autophagy

Clionamines A-D (**1**-**4**) were isolated by Keyzers and co-workers from a marine sponge *Cliona celata* in 2010.[1] Clionamine D (**4**) has an unprecedented spiro dilactone structure and modelate auto-phagy modulating activity. We aim to establish synthetic routes to A-D *via* a common intermediate.

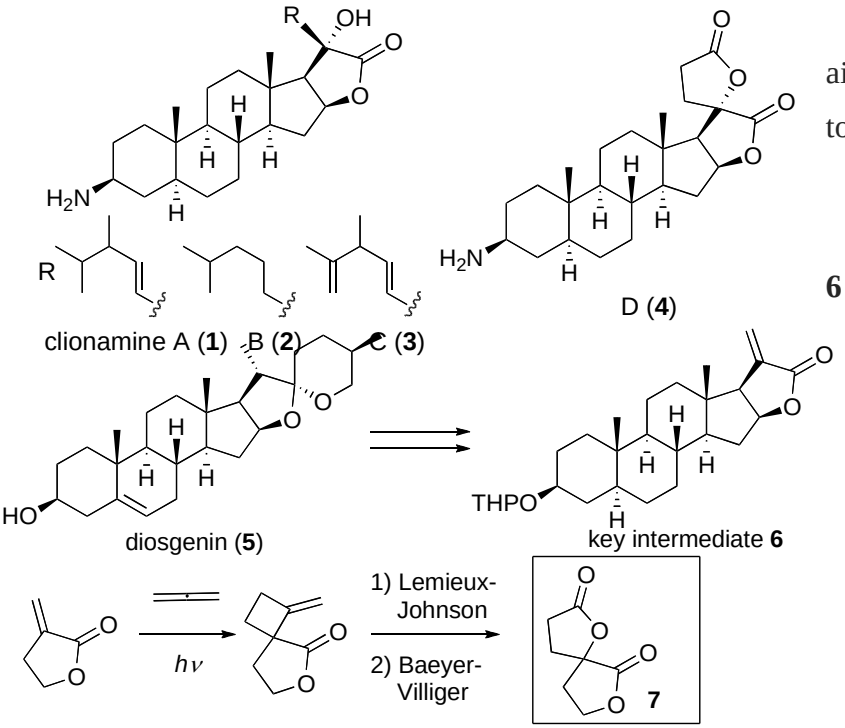

A key intermediate **6** was prepared from diosgenin (**5**) in 4 steps including Baeyer-Villiger-like reaction.[2] We have suceeded in constructing the model dilactone **7** using [2+2]photocyclization reaction.

[1] R. E. Keyzers *et al.*, *Org. Lett.* **2010**, *10*, 2959.

[2] B. Jung *et al.*, *Tetrahedron* **2008**, *64*, 469.

Poster 45

Synthesis of putative biosynthetic intermediates in early stage for paralytic shellfish toxins, and their identification in toxin producing microorganisms

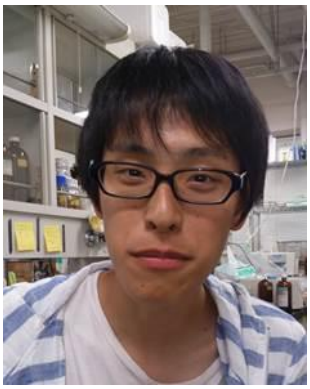

Shigeki Tsuchiya[1], Yuko Cho[1], Keiichi Konoki[1], Kazuo Nagasawa[2], Yasukatsu Oshima[3] and Mari Yotsu-Yamashita[1]

[1]Graduate School of Agricultural Science, Tohoku University Amamiya 1-1, Aoba-ku, Sendai 981-8555, Japan.

[2]Faculty of Technology, Tokyo University of Agriculture and Technology 2-24-16 Naka-cho, Koganei-shi, Tokyo 185-0031, Japan

[3]Graduate School of Life Sciences, Tohoku University Amamiya 1-1, Aoba-ku, Sendai 981-8555, Japan.

Email: b2am1334@s.tohoku.ac.jp

Key words: saxitoxin, paralytic shellfish toxins, biosynthetic intermediates

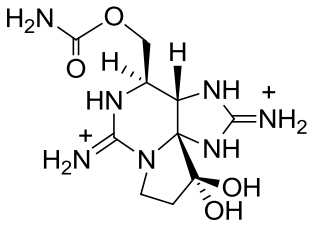

Fig.1 Chemical structure of Saxitoxin

The putative biosynthetic pathways for paralytic shellfish toxins (PSTs) in cyanobacteria and dinoflagellates have been recently reported based on the corresponding gene clusters and genes required for saxitoxin synthesis found by Neilan and Jakobsen *et al*. We chemically synthesized some intermediates predicted in early stage in biosynthesis of PSTs, and attempted to identify them in the PSTs producing cyanobacteria, *Anabaena circinalis,* and dinoflagellates, *Alexandrium tamarense,* and also in a non-toxic strains of them using LC/MS. The arginine derivatives bearing an ethyl ketone moiety and imidazole moiety, which were predicted as the first and second intermediates of PSTs biosynthesis, were detected in both of toxic strains of *A. circinalis* and *A. tamarense*. Furthermore, the presence of another compound derived from the second intermediate was also suggested in both of these toxic strains by LC-MS/MS.

Ref. [1] Llewellyn. L, et al., *Nat. Prod. Rep.* **2006**, 23, 200-222.

[2] Kellmann R. et al., *Appl. Environ. Microbiol.* **2008**, 74, 4044-4053.

[3] Mihali T. K. et al., *PLoS One* **2011**, 6, e14657.

[4] Stüken A. et al., *PLoS One* **2011**, 6, e20096.

[5] Omura T. et al., *La mer* **2003**, 41, 86-93.

[6] Turrell E. et al., *J. AOAC Int.* **2008**, 91, 1372-1386.

Poster 46

Investigation on Amount of Interstitial Mg in Mg_2Si

M. Kubouchi[1], K. Hayashi[1], and Y. Miyazaki[1]
[1]Department of Applied Physics, Graduate School of Engineering, Tohoku University, Japan.
Email: hayashik@crystal.tohoku.apph.ac.jp
Key words: Interstitial Mg, Single Crystal X-ray Diffraction

【Introduction】Mg_2Si is well known as a promising thermoelectric material due to lightweight, less-toxic and natural abundance. Although theoretical calculation of electronic state indicates that Mg_2Si is p-type, experimentally prepared Mg_2Si is commonly n-type. It is believed that Mg ion exists at an interstitial site, i.e., (1/2 1/2 1/2) of anti-fluorite-type structure, leading to the increase of electron carrier density [1]. However, there is no report that verifies interstitial Mg amount experimentally. In this study, we try to adjust the amount of interstitial Mg by preparing Mg_2Si_x (x = 1.0, 1.05, 1.1, 1.15, 1.2) samples. The amount of interstitial Mg is evaluated using single crystal X-ray diffraction (XRD).

【Experimental】Polycrystalline Mg_2Si_x samples were synthesized by means of a spark plasma sintering technique. We performed powder and single crystal XRD measurements. The crystal structure was refined using the crystallographic computing system, JANA2006 [2]. The Seebeck coefficient was measured by using an automated Seebeck tester to check the carrier type of Mg_2Si_x.

【Results】All samples exhibited negative Seebeck coefficient, indicating that Mg_2Si_x was n-type.

In the powder XRD patterns of Mg_2Si_x, the XRD peaks of Mg_2Si ($Fm\bar{3}m$) were confirmed; however the Si impurity peak was found for the samples with $x \geq 1.1$. We analyzed diffraction patterns of Mg_2Si single crystals picked up from Mg_2Si_x. The patterns were in good agreement with the calculated ones assuming the interstitial Mg. The occupancies at Mg (1/4 1/4 1/4), Si (0 0 0) and interstitial Mg (1/2 1/2 1/2) sites were 98, 100 and ~1 %, respectively. The existence of interstitial Mg in all samples well explained the n-type characteristic of Mg_2Si_x. From the above results, we could verify that Mg_2Si contained interstitial Mg regardless of the ratio of Si to Mg.

[1] A. Kato *et al.*, *J. Phys.: Condens. Matter* **21** (2009) 205801.
[2] V. Petricek *et al.*, *JANA2006 The crystallographic computing system*, Institute of Physics, Praha (2006).

Poster 47

Oxidative Stability of Copper Nanoparticles Produced by Supercritical Hydrothermal Synthesis

Takuya Morioka[1], M. Takesue[1], H. Hayashi[2], R. L. Smith Jr.[1]
[1]Graduate school of Environmental Studies, Tohoku University, Sendai, 980-8579, Japan, [2]National Institute of Advanced Industrial Science and Technology, 983-8551, Japan
E-mail: takuya-m@scf.che.tohoku.ac.jp
Key word: Copper nanoparticles, supercritical hydrothermal synthesis

Abstract

Copper nanoparticles (CuNPs) suitable for conductive inks were produced by continuous supercritical hydrothermal synthesis (SHS). However, CuNPs is easily oxidized at ambient conditions in water. In this work, oxidative stability of CuNPs produced by SHS method in the various solvents was studied with the aim of determining CuNPs long-term stability.

The apparatus used is shown in Figure 1. Precursor solution, containing 0.01 M $Cu(HCOO)_2$ and polyvinylpyrrolidone (PVP), and 0.1 M HCOOH solution were mixed (400 °C, 30 MPa). Product particles were redispersed in various solvents (water, methanol, ethanol and 2-propanol) and analyzed by UV-vis spectroscopy.

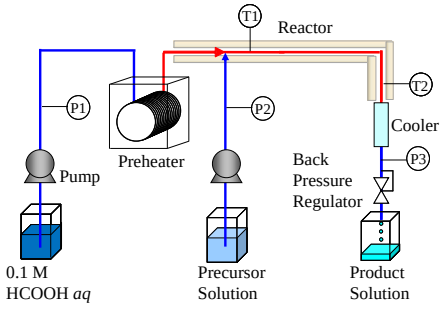

Fig.1 Flow apparatus for synthesizing CuNPs.

Fig. 2 shows the UV-vis spectra of the CuNPs dispersion solutions. After being re-dispersed, all solutions exhibited an absorption band at 573 nm, which is due to the surface plasmon resonance (SPR) band of CuNPs[1)]. However, the SPR band in distilled water after 1 day became very small and shifted to longer wavelengths. After 2 days no SPR band could be observed, showing that oxidation of CuNPs occurred[2)]. For the case of methanol, SPR gradually decreased. On the other hand, SPR band in ethanol and 2-propanol were maintained even after 30 days. Considering the solvent properties, the dielectric constant of each is in the order of water > methanol > ethanol > 2-propanol. It is probable that modifier PVP covers tightly around the CuNPs with decreasing dielectric constant of dispersion solvent, thereby CuNPs were protected from any dissolved O_2 oxidation agents. Thus, PVP exists in different conformations on the CuNPs: extended (water) or compacted (alcohols).

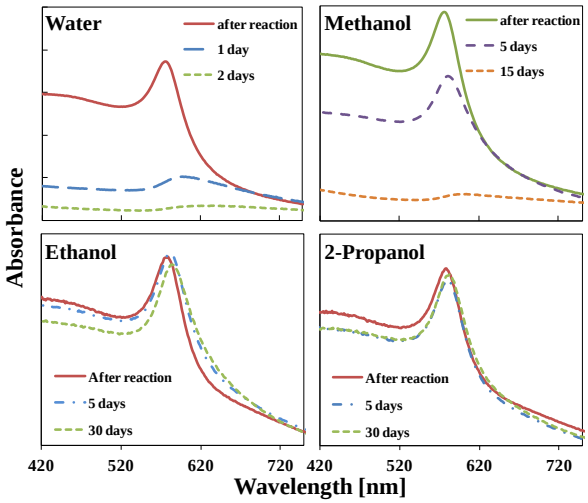

Fig.2 Time dependence of UV-vis spectra for each solution.

Reference: 1) I. Lisiecki *et al.*, *J. Phys. Chem.*, **100**, 4160 (1996), 2) P. Kanninen *et al.*, *J. Colloid Interface Sci.*, **318**, 88(2008).

Poster 48

Effect of hydrothermal treatment on charcoal from waste wood in the absence and presence of additives

Yoshimasa Higashino,[1] Masayuki Iguchi,[1] Taku M. Aida,[1] Masaru Watanabe[2] and Richard Lee Smith Jr.[1]
[1]Grad. School of Environ. Studies, Tohoku University, [2]Grad. School of Eng., Tohoku University. Aoba 6-6-11-414, Aoba-ku, Sendai 980-5864, Japan
Email: yoshimasa-h@scf.che.tohoku.ac.jp
Key words: hydrothermal, waste wood

Activated carbon is important for wastewater management. Typically, commercial activated carbons are made from coal or coconut shell and imported from foreign countries. For sustainable management of water, activated carbon produced at a local area, waste wood is a candidate as a starting material for making activated carbon. Conventionally, carbon from wood, namely charcoal, is activated at high temperatures (600~800 ˚C) after alkaline solution treatment. To reduce input energy and develop an effective method for the activation, hydrothermal treatment could be an alternative method because energy required for drying can be reduced and hydrolysis of condensation bonds in charcoal can occur along with functional group attachment. In this study, a charcoal pyrolyzed from waste wood at 400˚C was treated under hydrothermal condition, at 200˚C for 5 h in the absence and in the presence of additives (sulfuric acid, potassium hydroxide and citric acid). The yield of the treated charcoal was evaluated on a weight basis and analyzed. Table 1 shows the results. The specific surface area became higher after treatment in pure water (Table 1) and in the presence of citric acid. From the yield and ultimate analyses, H_2SO_4 and KOH became attached on the surface of the treated charcoal. However, functionalization may have prevented hydrothermal (or thermal) reactions from occurring on the charcoal surface. To activate the charcoal more effectively, a two-step process is probably needed along with consideration of other additives.

Table 1 Results of charcoals treated at hydrothermal condition at 200 ℃ for 5h.

Treatment	Yield [%]	Surface area [m^2/g]	O [%]	S [%]
Raw charcoal	-	3	23.5	0.41
Water	98.8	121	13.7	0.42
0.5 mol/kg H_2SO_4	104.2	24	15.8	1.54
4.0 mol/kg H_2SO_4	112.4	4	27.2	5.97
0.5 mol/kg KOH	107.0	17	19.3	0.42
1.0 wt% Citric acid	97.3	112	16.3	0.54

Poster 49

Molecular Shape Recognition of Hetero-Double-Helix Ethynylhelicene Oligomers by Helicene-Grafted Chiral Silica Nanoparticles

Masamichi Miyagawa[1], and Masahiko Yamaguchi[1]
[1]Graduate School of Pharmaceutical Sciecnce, Tohoku University Aoba 6-3, Aoba-ku, Sendai 980-8578, Japan.
Email: b1yd1010@s.tohoku.ac.jp
Key words: nanoparticles, helicenes, recognition, hetero-double-helix, gel

Nanoparticles with large surface areas can be grafted with organic molecules, and such surface modification can be used to change their properties. We synthesized (*P*)-helicene-grafted chiral silica nanoparticles, (*P*)-**1**, by the reaction of propylamine-grafted silica nanoparticles with diameters 70 nm and helicene acid chloride in *i*Pr$_2$O.[1] Helicene loading was 0.15 mmol/g calculated from CD, UV-Vis and elemental analysis. During grafting, (*P*)-**1** did not form irreversible aggregation, which was confirmed by DLS and AFM.

We reported that (*P*)-**1** recognized molecular shape of molecules. Ethynylhelicene oligomers are under equilibrium between double-helix and random-coil. When (*P*)-**1** was added to double-helix and random-coil solutions, precipitates formed with double-helix faster than with random-coil.

Since a mixture of (*P*)- and (*M*)-ethynylhelicene oligomers formed hetero-double-helix, which aggregated to fiber gel in a solvent.[2] Random-coil, hetero-double-helix, and the gel are under equilibrium. Examined in this study was molecular shape recognition in the hetero-double-helix system by (*P*)-**1**.

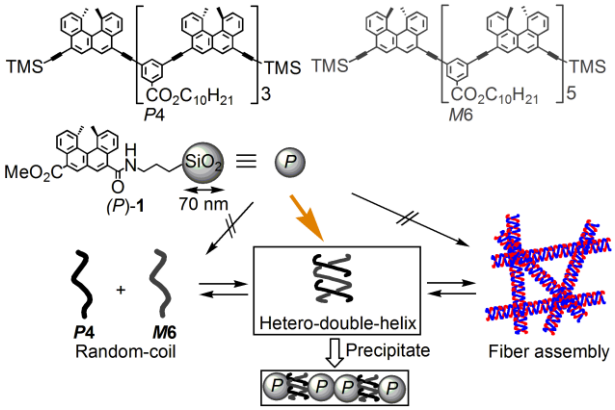

A mixture of (*P*)-**1**, (*M*)-ethynylhelicene hexamer *M*6, and (*P*)-ethynylhelicene tetramer *P*4 in toluene was settled at room temperature, heated at 100 °C, and then settled for 5 h. (*P*)-**1** formed precipitates during a gel formation. The precipitates were separated by centrifugation, and 31% yield hetero-double-helix was obtained from the precipitate. A mixture of (*P*)-**1** and random-coil *M*6 or *P*4 did not form precipitates. Leaving a mixture of (*P*)-**1** and *M*6/*P*4 gel for 5 h and 48 h gave same yield of hetero-double-helix. These results indicated that (*P*)-**1** recognized hetero-double-helix, and not random-coil and fiber assembly.

Ref. [1] W. Ichinose, M. Miyagawa, Z. An, M. Yamaguchi, *Org. Lett.*, **2012**, *14*, 3123-3125. [2] a) R. Amemiya, M. Mizutani, M. Yamaguchi, *Angew. Chem. Int. Ed.*, **2010**, *49*, 1995-1999. b) K. Yamamoto, N. Oyamada, M. Mizutani, Z. An, N. Saito, M. Yamaguchi, M. Kasuya, K. Kurihara, *Langmuir*, **2012**, *28*, 11939−11947. c) N. Saito, M. Shigeno, M. Yamaguchi *Chem. Eur. J.*, **2012**, *18*, 8994-9004. d) K. Yamamoto, Z. An, N. Saito and M. Yamaguchi, *Chem. Eur. J.*, **2013**, DOI: 10.1002/chem.201300659.

Poster 50

Chiral recognition of hexadehydrotribenzo[12]annulene containing helicene

Nozomi Saito[1, 2], Ryo Terakawa[1], and Masahiko Yamaguchi[1]
[1]Graduate School of Pharmaceutical Sciences, Tohoku University. Aoba 6-3, Aoba-ku, Sendai 980-8578, Japan.
[2]Tohoku University International Advanced Research and Education Organization. Aoba 6-3, Aoba-ku, Sendai 980-8578, Japan.
Email: b1yd1008@s.tohoku.ac.jp
Key words: chiral recognition, annulene, helicene, dimeric aggregate

Chiral recognition or discrimination in a mixture of racemic compounds is an interesting subject. Although there are many examples of dimer formation in solution by strong interaction such as metal-ligand coordination and hydrogen bonds, that by only π-π interaction is rarely known, and more extensive studies are needed for better understanding. Herein we describe dimer formation of a new class of compounds with twisted faces by π-π interaction.

Previously, we synthesized chiral hexadehydrotribenzo[12]annulene containing helicene (*P*)-**1** and examined its properties in solution. (*P*)-**1** showed concentration-dependent change of ^{1}H NMR spectra, which indicated aggregation in solution. The dimerization constant 5.8×10^2 M^{-1} was obtained by ^{1}H NMR (35 °C, $CDCl_3$) curve fitting method, which agreed with vapor pressure osmometry (VPO) experiment (35 °C, $CHCl_3$). Single-crystal X-ray analysis showed that (*P*)-**1** had two different chiral faces and formed dimeric aggregate by overlap of the twisted π-faces. It may be likely that same interaction occur in solution.

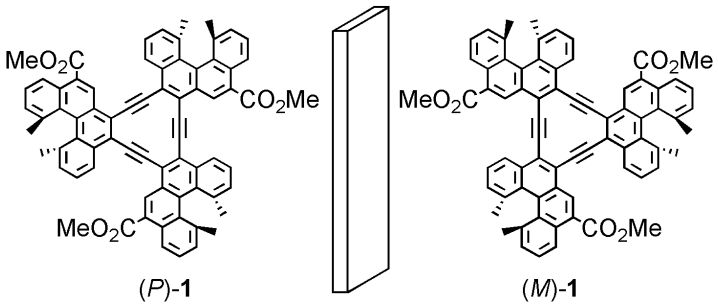

In this work, the antipode (*M*)-**1** was synthesized, and the aggregation of (*Rac*)-**1** was examined. Chloroform solution of (*P*)-**1** and (*M*)-**1** were mixed in 1:1 ratio, and the solution of (*Rac*)-**1** was obtained. The dimerization constant of (*Rac*)-**1**, 5.5×10^2 M^{-1}, was obtained by ^{1}H NMR (25 °C, $CDCl_3$) curve fitting method, which was lower than that of (*P*)-**1**, 1.1×10^3 M^{-1}. Considering that this value is the average of the dimerization constants of (*P*)-**1**/(*P*)-**1**, (*M*)-**1**/(*M*)-**1**, and (*P*)-**1**/(*M*)-**1**, the dimerization constant of (*P*)-**1**/(*M*)-**1** was estimated 2.0×10^2 M^{-1}. In this system, homodimer formation was stronger than heterodimer formation.

Poster 51

Molecular Thermal Hysteresis in the Helix-dimer/random-coil Structural Change of Sulfonamidohelicene Oligomers in Solution

Masanori Shigeno,[1] Yo Kushida,[1] and Masahiko Yamaguchi[1*]
[1]Graduate School of Pharmaceutical Sciences, Tohoku University.
Aoba 6-6, Aoba-ku, Sendai 980-8578, Japan.
Email: b3yd1002@s.tohoku.ac.jp
Key words: Molecular Thermal Hysteresis, Helix Dimer, Helicene, Induction Period

Thermal hysteresis is a phenomenon, in which different responses occur during heating and cooling. Molecular assemblies of solid, liquids, and bulk polymers can exhibit thermal hysteresis, which are explained by strong and multiple cooperative interactions between molecules. In contrast, thermal hysteresis of molecules in solution of nonpolar solvents, in which solvent/solvent and solvent/solute interactions are weak, is essentially not known with an exception of our bis(ethynylhelicene) oligomers.[1)]

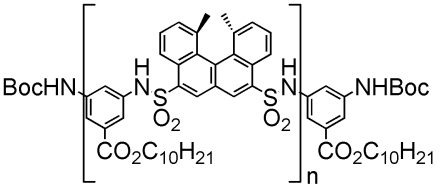

(*M*)-**n** (n = 1-7, 9)

Our group has been studying the helix dimer formation of helicene oligomers.[2)] Ethynylhelicene oligomers and amidohelicene oligomers showed structural changes between helix dimer and random coil in solution. In this study, we synthesized sulfonamidohelicene oligomers up to the nonamer level by repeated coupling reactions with a building block and deprotection reactions of terminal *t*-butoxycarbonyl groups. Among them, tetramer formed a helix dimer in 1, 3-difluorobenzene, which was determined by strong Cotton effects in CD and vapor pressure osmometry (VPO) studies. The structural change between the helix dimer and random coil exhibited molecular thermal hysteresis: cooling from 70 °C to 50 °C showed CD spectra of a random coil; warming from 45 °C to 50 °C showed CD spectra of a helix dimer. The thermal hysteresis was examined under different heating/cooling modes, and mechanism on the basis of the population change will be discussed.

CD spectra (0.5 mM, 1, 3-difluorobenzene) of (*M*)-**4**

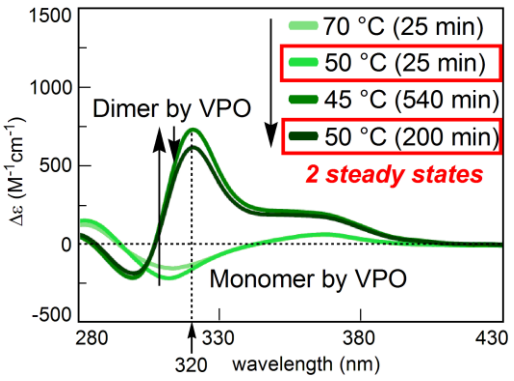

Δε (320 nm)/temperature profiles of (*M*)-**4**
(0.5 mM, 1, 3-difluorobenzene) at a rate of 0.25 K/min

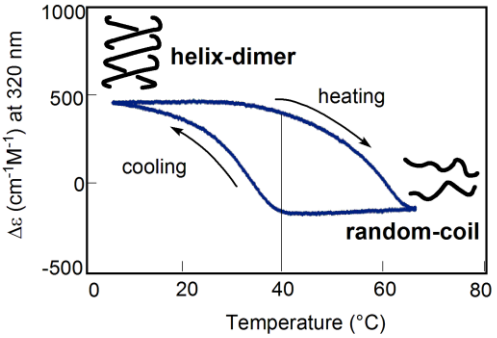

(1) Sugiura, H.; Amemiya, R.; Yamaguchi, M. *Chem. Asian. J.* **2008**, *3*, 244. (2) Yamaguchi, M. *J. Synth. Org. Chem.* **2011**, *69*, 17. (3) Shigeno, M.; Kushida, Y.; Yamaguchi, M. *Chem. Eur. J.* DOI: 10.1002/chem.201204556.

Poster 52

DMN-AZADO : Development of a Highly Active Catalyst for Selective Oxidation of Primary Alcohols

Ryusuke Doi [1], Masatoshi Shibuya [2], Yusuke Sasano [1], Yoshiharu Iwabuchi [1]
[1]Graduate School of Pharmaceutical Sciences, Tohoku University, 6-3 Aoba, Aramaki, Aoba-ku, Sendai 980-8578 (Japan)
[2]Graduate School of Pharmaceutical Sciences, Nagoya University, Furo-cho, Chikusa-ku, Nagoya 464-8601 (Japan)
E-mail: r-doi@s.tohoku.ac.jp
Key word: AZADO catalyst, selective oxidation, primary alcohol

Selective conversion of "one" functional group in the presence of "some" same functional groups by a catalyst-controlled manner is an attractive method in terms of improving atom economy and synthetic efficiency. Alcohol oxidation is a pivotal reaction in organic synthesis, and development of the method has been studied actively. Alcohol oxidation using catalytic amount of TEMPO (2,2,6,6-tetramethylpiperidine *N*-oxyl, **1**), (TEMPO oxidation) is known as one of few versatile methods to conduct selective oxidation of primary alcohols in the presence of secondary alcohols. However, this oxidation has room for improvement because excess amount of the catalyst was often needed to oxidize primary alcohols adjacent to sterically bulky substituents. We have disclosed that 2-azaadamantane *N*-oxyls (AZADOs, **2-4**) exhibit superior catalytic activity to TEMPO in primary and secondary alcohol oxidation.[1,2] We undertook to develop more efficient catalyst oxidizing primary alcohols selectively than TEMPO.

Figure 1. Nitroxyl radicals

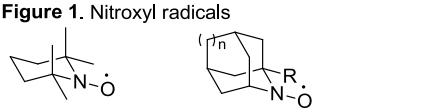

We designed 1,5-dimethyl-nor-AZADO (DMN-AZADO, **5**) in which the two methyl groups of TEMPO are merged into azanoradamantane skeleton. **5** was prepared on a gram scale from glutaryl chloride in 8 steps.

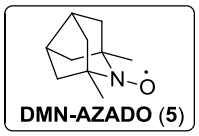

To clarify the selectivity and the catalytic efficiency, we compared reactivity of DMN-AZADO with those of TEMPO and 1-Me-AZADO about oxidation of diol **6** (**Scheme 1**). In the case of TEMPO, decomposition proceeded before the oxidation of primary alcohol completed. When 1-Me-AZADO was used, 48% of ketoaldehyde **8** was generated. We confirmed that DMN-AZADO oxidized primary alcohol selectively to afford hydroxy aldehyde **7** in high yield.

Scheme 1. Comparion of catalytic efficiencies in alcohol oxidation

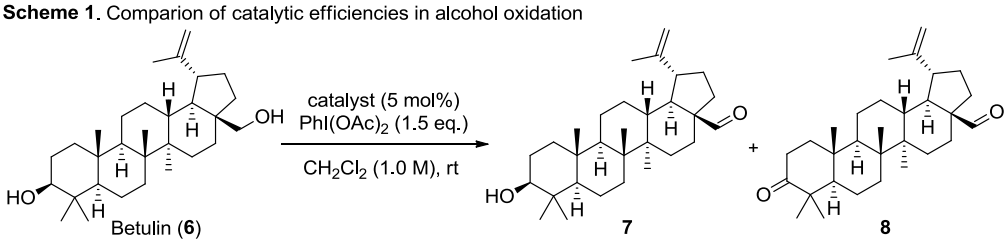

	7	8
TEMPO (4 h)	32%	0%
1-Me-AZADO (25 min)	48%	48%
DMN-AZADO (45 min)	**92%**	**0%**

References

1) Iwabuchi, Y. *et al. J. Am. Chem. Soc.* **2006**, *128*, 8412. 2) Iwabuchi, Y. *et al. Chem. Pharm. Bull.* **2011**, *59*, 1570.

Poster 53

Synthesis and cytotoxic activity of C_5-curcuminoid-thiol adducts

Aki Kohyama[1], Shunsuke Sugiyama[2], Hiroyuki Yamakoshi[1], Naoki Kanoh[1], Yoshiharu Iwabuchi[1], Hiroyuki Shibata[3]

[1]Graduate School of Pharmaceutical Science Tohoku University, Sendai, Japan, [2]Institute of Development, Aging and Cancer, Tohoku University, Sendai, Japan, [3]Akita University Graduate School of Medicine and Faculty of Medicine, Akita, Japan.

Email: a-kohyama@s.tohoku.ac.jp

Key words: curcumin, antitumor, reversible Michael reaction, prodrug,

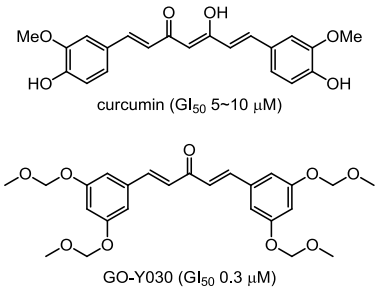

Figure 1 : curcumin and GO-Y030

[Introduction] Curcumin, the major active constituent of Turmeric, is an attractive target of medicinal chemistry because it has been found to exhibit various activities such as anti-inflammatory, antioxidant, and antitumor. In our laboratory, we discovered cytotoxic curcumin analogues named C_5-curcuminoids featuring the reactive dienone structure. In the investigation of the structure activity relationship, we found a highly active C_5-curcuminoid, namely, GO-Y030 which showed GI_{50} values against several cancer cell lines in submicromolar range. GO-Y030 showed chemopreventive ability in familial adenomatous polyposis (FAP) mouse without apparent toxicities *in vivo*. And we found that GO-Y086 covalently binds target protein Far Upstream Binding Protein 2 (FUBP2). In the present study, we report that reversible Michael reaction is important for antitumor activity. In addition, we developed C_5-curcuminoid-thiol adducts prodrug to improve water solubility.

[Result and Discussion] To prove reversibility of C_5-curcuminoids Michael reaction *in vitro*, we monitored reaction mixture, consisting GO-Y030 and cysteamine in d_6-DMSO, by ^{1}H-NMR spectroscopy. As a result, Michael reaction and following retro Michael reaction was observed. Next, we synthesized thiol adducts of GO-Y030, which were evaluated their cell growth suppressive effects against human colon cancer HCT116 by MTT assay. Almost every compound exhibited as high activity as GO-Y030. In particular, glutathione adduct GO-Y140 had high water solubility.

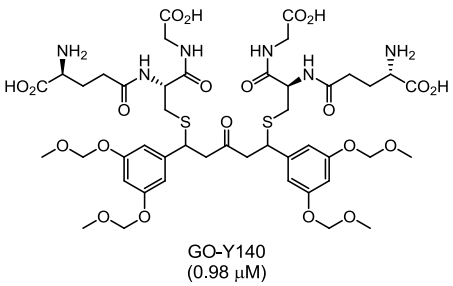

Figure 2 : water soluble C_5-curcuminoid

[Conclusion] We propose that reversible Michael reaction is crucial properties for tumor-specific cytotoxicity and for targeting FUBP2. In addition, we successfully synthesized a water-soluble C_5-curcuminoid GO-Y140.

Poster 54

Synthetic Study of FD-891

Ayano Kawamata, Yuta Miyazaki, Kenzo Yahata, Naoki Kanoh, Yoshiharu Iwabuchi
Graduate School of Pharmaceutical Sciences, Tohoku University, Sendai, Japan
E-mail: a.kawamata@s.tohoku.ac.jp
Key word: antitumor natural product, total synthesis

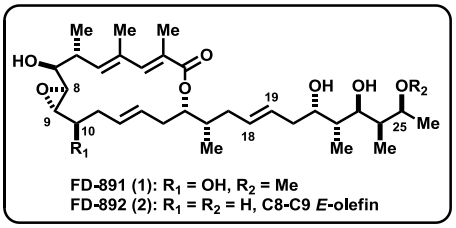

FD-891 (**1**) and FD-892 (**2**) are 16-membered macrolides isolated from *Streptomyces graminofaciens* A-8890 by Mizoue and coworkers[1]. FD-891 (**1**) is shown to exhibit cytotoxicity against several tumor cell lines *in vitro*, and >100 times more potent than FD-892 (**2**). Intrigued by their structures and the difference in their biological activity, several years ago we commenced the synthetic efforts toward these macrolides and their analogues. Herein, we report the synthesis of macrolactone moiety **3** and side chain moiety **4** of **1**.

Synthesis of macrolactone moiety **3** is summerized in Scheme 1. Aldehyde **5** was successfully converted to the aldol adduct **7** in high yield via a vinylogous Mukaiyama aldol reaction (VMAR)[2] using chiral vinylketene silyl *N*,*O*-acetal **6**. Wittig homologation followed by esterification gave ester **10**. Ring closing metathesis (RCM) of **10** gave macrolactone **3** in a highly stereoselective manner.

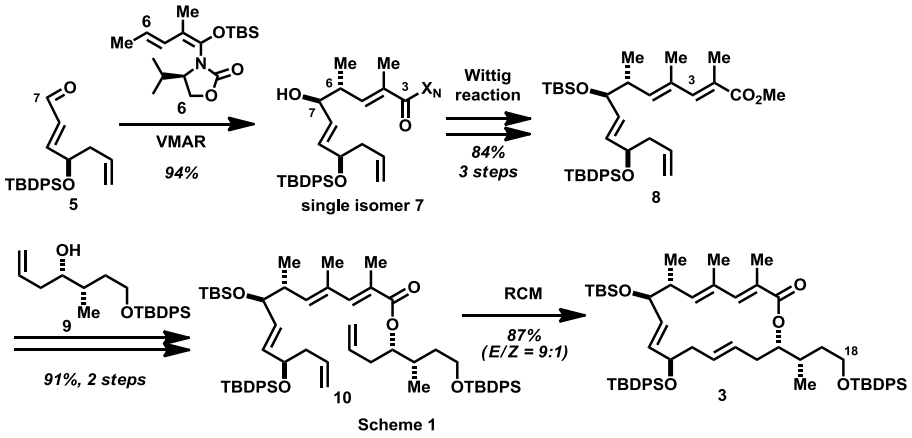

Scheme 1

Synthesis of side chain **4** is shown in Scheme 2. Brown asymmetric crotylboration of aldehyde **11** gave the desired C21–C22 *syn* adduct **12**. Evans aldol reaction of aldehyde derived from **12** afforded the corresponding C23–C24 syn aldol adduct **13** with high diastereoselectivity. Side chain moiety **4** was then obtained via Corey-Bakshi-Shibata (CBS) reduction of ketone derived from **13**.

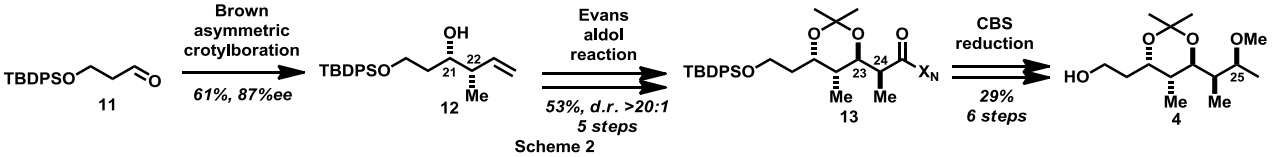

Scheme 2

Ref. 1) K. Mizoue *et al. J. Antibiot.* **1994**, *47*, 1226. 2) S. Kobayashi, S. Hosokawa *et al. J. Am. Chem. Soc.* **2004**, *126*, 13604.

Poster 55

Synthetic Study of Oligo-piperazic Acid-containing Natural Product Piperidamycin F

Naoki Sekioka[1], Masahito Yoshida[1], Motoki Takagi[2], Miho Izumikawa[3], Kazuo Shin-ya[3], Takayuki Doi[1]

[1] Graduate School of Pharmaceutical Sciences, Tohoku University, Sendai
[2] Fukushima Medical University, Fukushima
[3]Advanced Industrial Science and Technology, Tokyo
E-mail: n-sekioka@s.tohoku.ac.jp

Key word: cyclodepsipeptide, natural product, total synthesis.

Piperidamycin F (**1**), isolated from mutant strains of a soil-isolated *Streptomyces species* that don't produce antibacterials, is a 18-membered cyclodepsipeptide, consisting of five unnatural amino acids and 2-hydroxy-3-methylpentanoic acid.[1)] **1** exhibits a strong antibacterial activity against gram negative bacteria and an anaerobic gram-negative bacillus. We have recently accomplished the total synthesis and structure determination of linear peptide JBIR-39 (**2**)[2)], thus our next aim is the total synthesis of **1**.

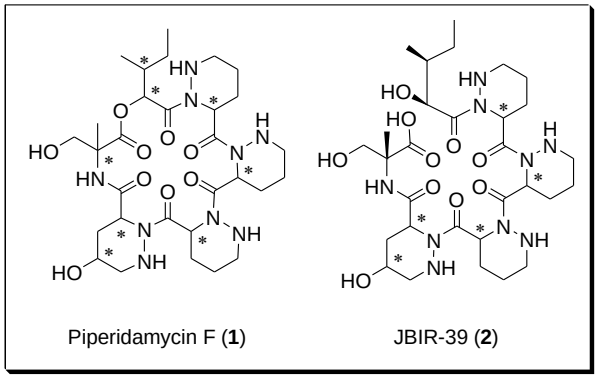

After extensive study for the acylation of **3**, we found that $Sc(OTf)_3$ effectively promoted the coupling of **3** and **4**, and the synthesis of the desired hexapeptide **8** was achieved. The further modification leading to **9** is now under investigation. The details of our synthesis will be discussed.

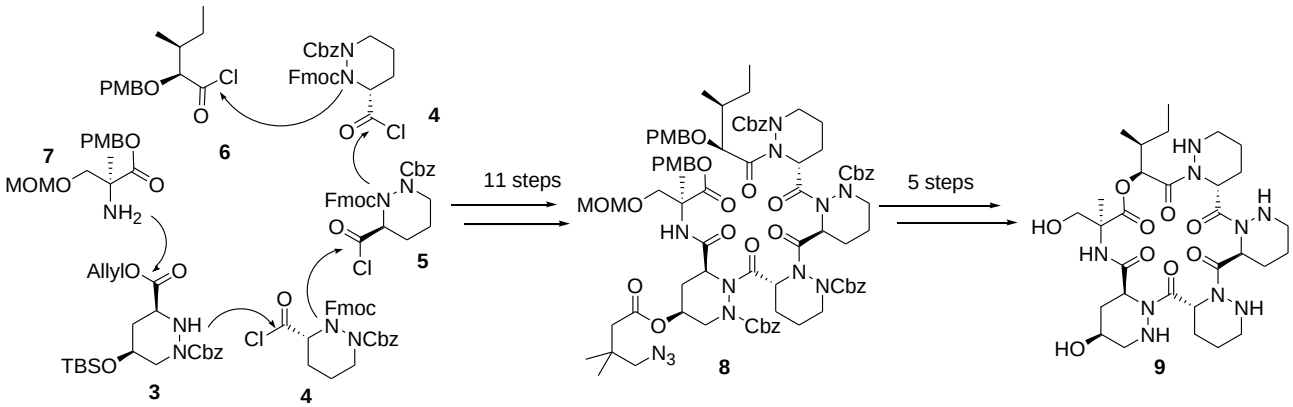

Ref) 1) Hosaka, T.; Kameyama, M.; Muramatsu, H.; Murakami, K.; Tsurumi, Y.; Kodani, S.; Yoshida, M.; Fujie, A.; Ochi, H. *Nat. Biotechnol.* **2009**, *27*, 462-464. 2) Kozone, I.; Izumikawa, M.; Motohashi, K.; Nagai, A.; Yoshida, M.; Doi, T.; Takagi, M.; Shin-ya, K. *J. Marine Sci. Res. Development*, **2011**, doi:10.4172/2155-9910.1000101

Poster 56

Synthetic study of JBIR-108

Koichi Fujiwara[1], Hirokazu Tsukamoto[1], and Takayuki Doi[1]
[1]Graduate School of Pharmaceutical Sciences, Tohoku University, Sendai, Japan
E-mail: k.fujiwara@s.tohoku.ac.jp
Key word: 2-hydroxy-3(2*H*)-furanone, NADH-fumarate reductase

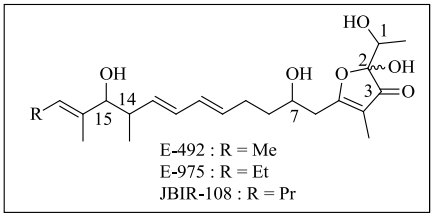

JBIR-108 was isolated by Shin-ya and co-workers from *Streptomyces* sp. RJ76. E-492 and E-975, analogues of JBIR-108, were isolated by McAlpine and co-workers from *Streptomyces* sp. Eco86 and they were found to inhibit NADH-fumarate reductase moderately, which can be a good target for antiparasitic drugs. Although their structures including JBIR-108 were elucidated by a combination of mass spectrometry and NMR spectroscopy, their relative and absolute configurations are still unclear. Particularly, it is difficult to determine the C1 stereochemistry by Mosher's method due to lack of protons in the furanone moiety. To determine their absolute configurations, we planned the synthesis of JBIR-108 featuring a 2-hydroxy-3(2*H*)-furanone.

Vinylogous Mukaiyama aldol reaction of aldehyde **1** with vinylketene silyl *N*,*O*-acetal **2** provided desired alcohol **3** in high diastereoselectivity. After transformation of alcohol **3** to enone **4**, CBS reduction of **4** afforded alcohol **5** in high diastereoselectivity. Alcohol **5** was converted into alkenyl iodide **6**, which was subjected to Migita-Stille coupling reaction with alkenylstannane **9**, prepared from aldehyde **7** via asymmetric crotylation. Removal of all acetyl groups in diene **10**, simultaneous oxidation of triol **11**, followed by spontaneous cyclization of triketone **12** afforded 2-hyroxy-3(2*H*)-furanone **13**. Proposed structure of JBIR-108 (**14**) was synthesized by removal of all TES groups. Structure determination of JBIR-108 is currently under investigation.

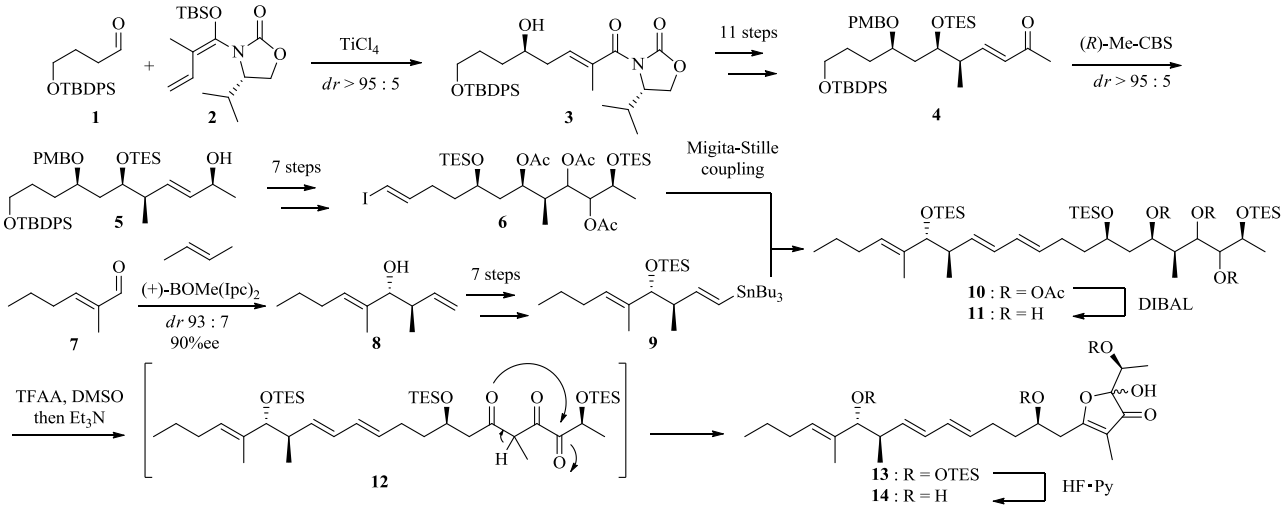

Poster 57

Synthetic Studies on Leuconoxine.

Atsushi Umehara,[1] Hirofumi Ueda,[1] and Hidetoshi Tokuyama[1]
[1]Graduate School of Pharmaceutical Sciences, Tohoku University, Sendai, Japan. Email: b2yd1019@s.tohoku.ac.jp
Key words: alkaloid, Mizoroki-Heck reaction, natural product synthesis

Leuconoxine (**1**), isolated from leaves and stem of *Leuconotis eugenifolius* by Yamauchi and co-workers in 1994, is a pentacyclic indole alkaloid, having diazafenestrane system and contagious tetrasubstituted and quaternary carbon centers. These unique structural features inspired us to initiate synthetic studies toward leuconoxine (**1**). In this paper, we report our strategy for construction of the pentacyclic rings of leuconoxine (**1**) utilizing intramolecular Mizoroki-Heck reaction.

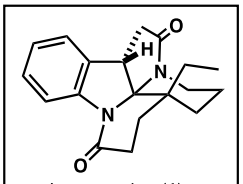

Preparation of a substrate for Mizoroki-Heck reaction commenced with synthesis of 2-iodoindole **5** via Fukuyama indole synthesis. Indole **5** was synthesized from 2-iodoaniline (**1**) by a five-step sequence in high yield. On the other hand, carboxylic acid **9** was synthesized from 1,4-cyclohexanedione (**6**) in 5 steps. Since condensation of two fragments **5** and **9** under the conventional conditions resulted in poor yields (Table 1, entries 1-3), we carried out extensive optimization. To this end, we found that the treatment **9** with Boc_2O followed by addition of **5** in the presence of DMAP and Et_3N was effective to furnish the desired amide **10** in good yield. The intramolecular Mizoroki-Heck reaction with **10** proceeded smoothly to provide expected δ-lactamindole **11** in high yield. Construction of the pentacyclic skeleton of leuconoxine (**1**) and further transformation are currently under investigation.

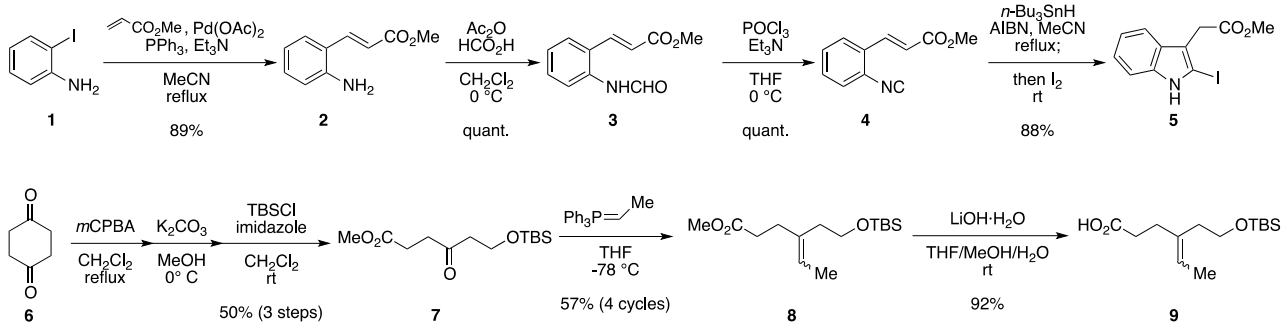

Table 1

entry	conditions	yield (%)
1	WSCD·HCl, DMAP, **5**	0
2	$(COCl)_2$, DMF; then **5**, NaH	0
3	EtOCOCl, Et_3N; then **5**, DMAP, Et_3N	9
4	Boc_2O, Py; then **5**, DMAP, Et_3N	58

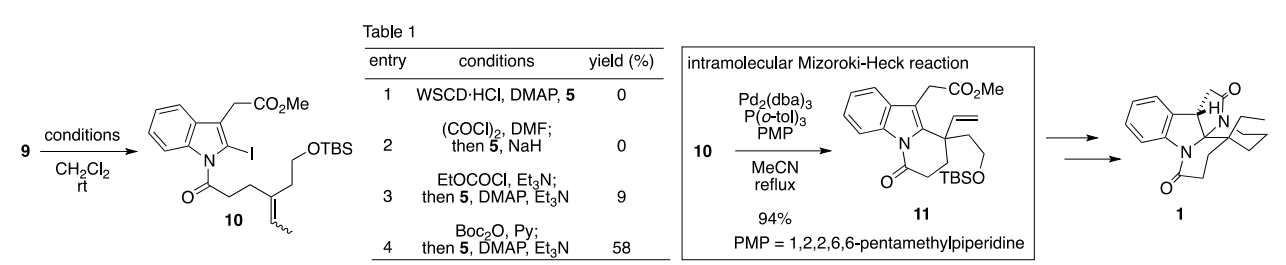

Poster 58

Total Synthesis of (–)-Acetylaranotin

Taichi Kurogi, Hideto Fujiwara, Shun Okaya, Kentaro Okano, Hidetoshi Tokuyama*
Graduate School of Pharmaceutical Sciences, Tohoku University
Aoba 6-3, Aoba-ku, Sendai 980-8578, Japan.
Email: b3yd1003@s.tohoku.ac.jp
Key words: dihydrooxepine, diketopiperazine, oxidation, rearrangement, total synthesis

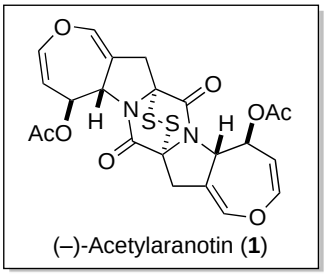

(–)-Acetylaranotin (**1**)

(–)-Acetylaranotin (**1**), isolated from the metabolite of the fungus *Arachiniotus aureus* by Neuss and co-workers in 1968, displays inhibitory activity against viral RNA polymerase and antiproliferative activity against HCT116 colon cancer cell line. In spite of its significant biological activities, only one total synthesis has been reported by Reisman and co-workers,[1] possibly due to the difficulty in constructing the characteristic fused dihydrooxepine skeleton. Herein we report a recently accomplished total synthesis of **1** based on the efficient formation of the dihydrooxepine.

The enone **2** was converted to **3** via a regioselective formation of dienol silyl ether and vinylogous Rubottom oxidation.[2] Subsequent protection of the hydroxyl group and Baeyer-Villiger oxidation using a combination of TFAA and UHP proceeded to give enol lactone **4**. After conversion to enol triflate, dihydrooxepine **5** was obtained by a palladium-catalyzed reduction.

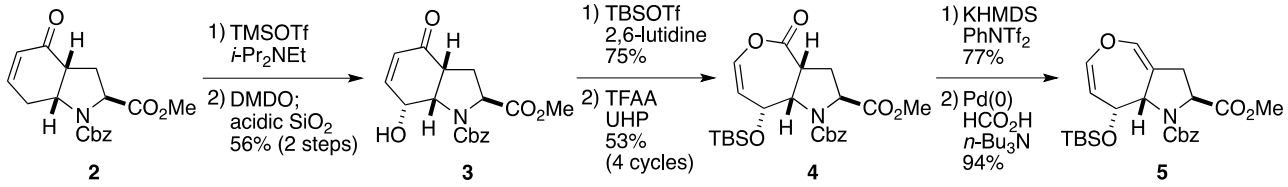

Condensation of the monomer units **6** and **7** was carried out using BOPCl to afford amide **8** in high yield. Known diol **9** was then synthesized by a four-step sequence, including the formation of diketopiperazine and the stereochemical inversion of the two hydroxyl groups. Finally, following the Reisman's protocol, we have accomplished the total synthesis of (–)-**1**.[3]

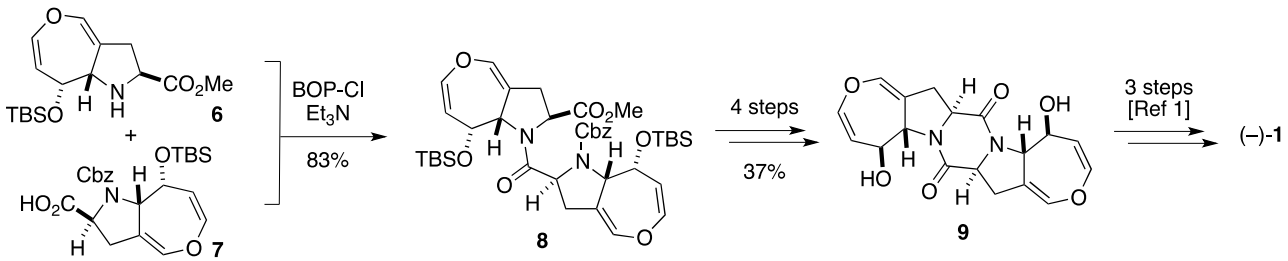

Ref. [1] S. E. Reisman *et al.*, *J. Am. Chem. Soc.* **2012**, *134*, 1930. [2] I. Kuwajima *et al.*, *Synlett* **1994**, 993. [3] H. Tokuyama *et al.*, *Angew. Chem. Int. Ed.* **2012**, *51*, 13062.

Poster 59

Total syntheses of Penostatin B and E

Kosuke Fujioka,[1] Hiromasa Yokoe,[2] Masahiro Yoshida[3] and Kozo Shishido[3]

[1]Graduate School of Pharmatical Sciences, Tohoku University, Aoba 6-3, Aoba-ku, Sendai 980-8578, Japan.

[2]Hoshi University, Ehara 2-4-41, Shinagawa-ku, Tokyo 142-0063, Japan.

[3]Graduate School of Pharmaceutical Sciences, The University of Tokushima, 1-78-1 Sho-machi, Tokushima 770-8505, Japan.

Email: b3yd1008@s.tohoku.ac.jp

Key words: Total synthesis, Relay-RCM, Pauson-Khand reaction

Penostatins B (**1**) and E (**2**) are representatives of nine molecules in this family that have been isolated from the mycelia of a strain of *Penicillium sp.* OUPS-79 originally separated from the marine alga *Enteromorpha intestinalis* by Numata and co-workers in 1996. Most of these natural products have tricyclic core including diene, enone, and dihydropyran moieties. Except for penostatin D, all the penostatins exhibited significant cytotoxicity against cultured P388 cells. We herein report total syntheses of (±)-penostatin B (**1**) and (+)-penostatin E (**2**).

The synthesis of (±)-penostatin B (**1**) commenced with an indium-mediated pentadienylation of aldehyde **3** using pentadienyl tin **4** and subsequent Pauson-Khand reaction to provide tetrahydroindanone **5**. After tetrahydroindenone **5** was converted to triene **6**, tricyclic lactone **7** was obtained in high yield *via* Relay-RCM in the presence of Grubbs 2nd catalyst, which led to the first total synthesis of (±)-penostatin B (**1**).[1]

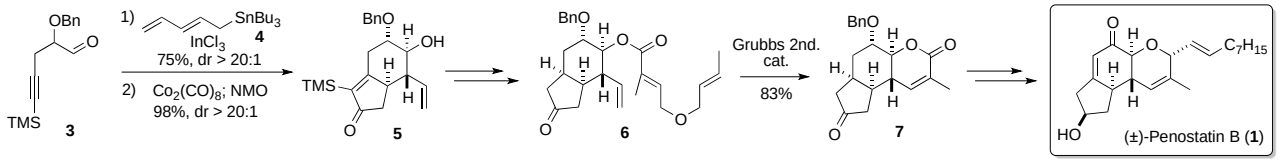

On the otherhand, (+)-penostatin E (**2**) was synthesized starting from Hosomi-Sakurai allylation of the known optically active aldehyde (*R*)-**3** with allyl silane **8**. Pauson-Khand reaction was then performed to give tetrahydroindanone **9** as a single diastereomer in 94% yield over two steps. Compound **9** was converted to tricyclic lactone **11** *via* aldehyde **10** by Ando-HWE olefination, and concomitant lactonization. Finally, the first enantiocontrolled total synthesis of (+)-penostatin E (**2**) was accomplished *via* conversion to lactol and elongation of the side chain by Wittig reaction.

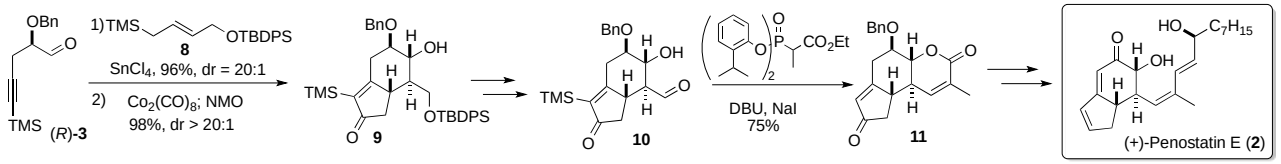

Ref. [1] Fujioka, K.; Yokoe, H.; Yoshida, M.; Shishido, K. *Org. Lett.* **2012**, *14*, 244–247.

Poster 60

Radioactivity of wild mushrooms in Miyagi prefecture

Ayumi Irisawa,[1] Yasushi Kino,[1,] and Tsutomu Sekine[2]
[1]Department of Chemistry, Tohoku University, Sendai 980-8579, Japan
[2]Center for the Advancement of Higher Education, Tohoku University, Sendai 980-8579, Japan
Email: irisawa@s.tohoku.ac.jp
Key words: Radioactive caesium, accumulation of elements in mushroom, Fukushima Daiichi nuclear plant

Introduction

On March 11, 2011, Fukushima Daiichi nuclear plant accident occurred in Japan, and huge amount of radioactive caesium had been released into the environment. Not only external exposure from environmental radioactive substances but also internal exposure from food strongly attracts people's interest. Higher uptake of radioactive caesium in mushrooms than in other agricultural products was found in 1960' when hundreds of nuclear weapons testing in the atmosphere were carried out. After the Chernobyl accident, a lot of investigations were made about contamination of mushrooms, but little was made inside the Unions of Soviet Socialist Republics just after the accident because of political reasons. Just after the Fukushima accident, we have collected mushrooms in Miyagi prefecture, in cooperation with the Sendai Mushroom Society.

Method

Mushrooms were dried under the mild condition, and were put into U8-type polypropylene containers. Gamma-ray measurements were carried out with a high-pure Ge semiconductor detector. Radioactivities of Cs-134 and Cs-137 were determined at the gamma-ray energies of 796 keV and 662 keV and decay correction was made to March 11, 2011. Some samples were destructed with nitric acid / hydrogen peroxide, and analyzed with ICP-MS in order to determine concentration of stable Cs-133.

Result and discussion

The number of samples in which we measured radioactivity was over 200 of mushrooms and 50 of substrates. We found positive correlation between air dose rate and concentration of radioactive Cs in mushroom. The sum of radioactive Cs concentration varied in the range from 0.03 ± 0.02 Bq kg^{-1} in *Amanita hemibapha* to $3{,}110 \pm 20$ Bq kg^{-1} in *Lactarius leaticolorus* wet in 2011 and 7 ± 2 Bq kg^{-1} in *Amanita ibotengutake* to $24{,}600 \pm 100$ Bq kg^{-1} in *Hygrocybe cuspidata* in 2012. Concentrations of radioactive Cs in most of mushrooms increased in these two years, indicating radioactive Cs would not have been in stationary states. Because of the mobility of Cs are as changing. That to necessary to consecutive research about Cs radioactivity in mushroom, eventually Cs transfer in environment.

Poster 61

A Study of Ore Model Positronium Formation in Ar Gas.

Yosuke Sano,[1] Yasushi Kino, [1] Tsutomu Sekine, [2] and Toshitaka Oka, [1,2]
[1]Department of Chemistry, Tohoku University Sendai 980-8578, Japan.
[2]Center for the Advancement of Higher Education, Tohoku University, Sendai 980-8576, Japan.
Email: y.sano@s.tohoku.ac.jp
Key words: positron deceleration, Ore model positronium formation

【Introduction】 A high energetic positron emitted from ß$^+$-decay rapidly slows down to thermal energy in materials. During the slowing down process, some of positrons form a positronium (Ps). This positronium formation process was called the Ore process. However, the positron slowing down process was too fast to observe the Ore process as a function of time. In order to observe the Ore process, we developed a new analysis method.

A positron injected into Ar gas annihilates with one of surrounding electrons and emits, in the most case, two γ-rays. On the other hand, Ps annihilates by itself and emits two or three γ-rays. The annihilation γ-rays are Doppler shifted in the laboratory frame due to the center of mass velocity of the electron-positron pair. To observe the positron energy and the Ps formation process, we measured the Doppler broadening and positron lifetime simultaneously from the two annihilation γ-rays. The Ar gas pressure was controlled to be 7.5, 3.5 and 2.0 MPa at room temperature.

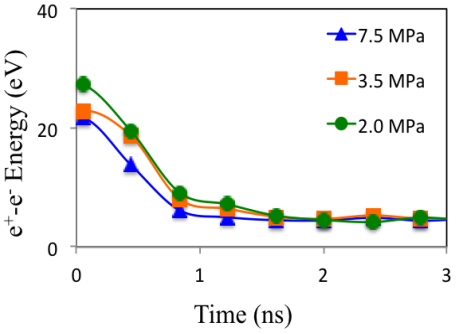

Fig.1 Annihilation time dependence of positron kinetic energy obtained from the Doppler broadening.

【Results & Discussion】Figure 1 shows the annihilation time dependence of positron and the orbital electron in Ar kinetic energy obtained from the Doppler broadening. The Ar and positron inelastic scattering threshold is 11.7 eV. Above the kinetic energy of 11.7 eV, the positron lost its energy immediately by inelastic scattering. Below the kinetic energy, positron lost its energy by only elastic scattering. One can see a negative correlation between the pressure and decrease of the kinetic energy until 2 ns. Figure 2 shows the p-Ps (One of the Ps state which has the singlet spin state) distribution of annihilation time (f_{ps}). The pressure dependence of the Ar gas was observed. We calculated the f_{ps} from the p-Ps lifetime (125 ps) and the instrumental function, by assuming Ps only formed at t = 0 ns (dashed line). The peak of the dashed line was narrower than that of experimental values. This suggests that Ps formed within a finite time interval.

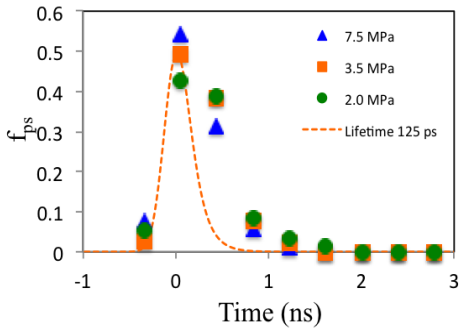

Fig.2 f_{ps} vs time

Poster 62

Radioactive caesium contamination of soil in Fukushima and miyagi.

Takashi Sugimoto,[1] Ayumi Irisawa,[1] Kazuma Koarai,[1] Gohei Hayashi,[2] Manabu Fukumoto,[2] Yasushi Kino,[1] and Tutomu Sekine[1,3]

[1]Graduate School of Science, Tohoku University Aoba 6-3, Aoba-ku Sendai, 980-8578, Japan.

[2]Institute of Development, Aging and Cancer, Tohoku University Seiryo-machi 4-1, Aoba-ku Sendai, 980-8575, Japan.

[3]Center for the Advancement of Higher Education, Tohoku University Kawauchi 41, Aoba-ku Sendai, 980-8576, Japan.

Email: b2sm5037@s.tohoku.ac.jp

Key words: Fukushima Dai-ichi Nuclear Power Plant accident, ^{137}Cs , Depth distribution.

Various artificial radioactive nuclides were released into the air because the nuclear accident at the Fukushima Daiichi Nuclear Power Plant (FDNPP) occurred as a consequence of the magnitude 9.0 earthquake and the resulting Tsunami on March 11, 2011. Out of the radionuclides found in atmospheric fallout from the FDNPP accident, ^{137}Cs with a physical half-life of 30 years is the largest source of concern for people who live in the polluted area. We measured radio activities of 100 soil samples collected in Miyagi Prefecture and in the evacuation zone of the FDNPP. Most of the measured radiocaesium deposition densities were consistent with the distribution map of radiation dose by MEXT. Some of the samples, however, gave quite different values from the distribution map. In order to understand variety of the deposition densities, we should therefore take chemical property of the soil and environmental effects into account.

For this purpose, we investigated the vertical distribution in soil profile and particle size dependence of radiocaesium concentration. We collected soil core samples with a depth of 30 cm, and measured the vertical distribution of the radionuclides. More than 90% of radiocaesium was found in the upper 5.0 cm in the soil profile and radiocaesium concentrations decreased with depth. Comparing the vertical distributions collected in the time interval of five months, found a decrease in radiocaesium density at the surface of the ground because of the weathering effect. On the other hand, naturally-occurring radionuclides, ie ^{40}K, ^{226}Ra and ^{228}Ra, distributed independent of the depth from the surface of the ground. We divided the soil samples into some fractions depending on the particle size. The radiocaesium concentration decreased with the size of the particle.

Poster 63

Binding Energy Analysis of Trapped Electrons in Organic Solids by Positron Annihilation Lifetime Spectroscopy

Shogo Nakamura[1], Yasushi Kino[1], Tsutomu Sekine[2], Toshitaka Oka[1,2]

[1] Department of Chemistry, Tohoku University, Sendai, Japan

[2] Center for the Advancement of Higher Education, Tohoku University, Sendai, Japan

E-mail: b2sm5050@s.tohoku.ac.jp

Keyword: positronium, organic solid, trapped electrons

【Introduction】When a positron from β^+ decay is injected into materials, it collides with surrounding molecules and loses its energy by generating secondary electrons. Some of thermalized positrons catch an electron and form a bound state called “positronium”. Generally, positronium formation in organic solid occurs by catching the unbound or weakly bound electrons. The latter electrons are called “trapped electrons”. The trapped electrons are in metastable states and observed in the organic solid irradiated by β^+ ray. In the organic solid, some of secondary electrons are bound into the trapping site among molecules and stabilized. This is the process of generating trapped electrons. Thus, an increase of trapped electrons in the organic solid enhances positronium formation. As a remarkable character of trapped electrons, it is known that trapped electrons can be released from trapping site by light irradiation.

【Experimental】A glass tube degassed by a freeze-thaw method having a ^{22}Na source and organic liquid in its inside was handled as a sample. The sample was put in a cryostat and cooled down to 45 K. While keeping the constant temperature, we changed light condition by optical filters. Positron Annihilation Lifetime Spectroscopy (PALS) was carried out and we measured the wavelength dependence of the inhibition of positronium formation in solid *n*-heptane and 1-hexanol under light irradiation.

【Results and discussion】In solid *n*-heptane, o-Ps intensity under the light restricted to 520 nm and longer wavelength agreed with the result under the light passed through no optical filters. This result indicates that there would be hardly any trapped electrons having binding energy higher than 2.4 eV. On the other hand, it was detected that maximum value of the binding energy of trapped electrons in solid 1-hexanol was 1.6 eV. Therefore, maximum depth of the trapping site in solid *n*-heptane was deeper than the depth of the trapping site in solid 1-hexanol by 0.8 eV.

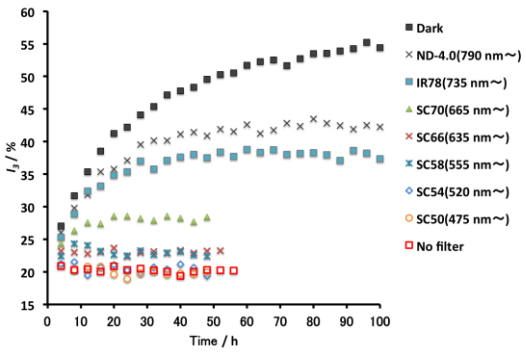

Fig 1. O-Ps intensity in solid *n*-heptane (45 K)

Poster 64

Development of abasic site-containing DNA duplex-based aptamer for theophylline detection

Yusuke Sato, Yushuang Zhang, Seiichi Nishziawa, and Norio Teramae
Graduate School of Science, Tohoku University Aoba 6-3, Aoba-ku, Sendai 980-8578, Japan.
Email: treezys@hotmail.com
Key words: aptamer, theophylline, label free

【Introduction】

In 2009, our group has reported a simple DNA duplex aptamer for theophylline, where an abasic site (AP site) was utilized as an active cavity for binding events. [1] In this aptamer, 2-aminopurine was used adjacently to the AP site, and the nucleotide opposite the AP site served as a kind of receptor for theophylline, which enables highly selective detection of theophylline over caffeine and theobromine. However, the need of the modification with 2-aminopurine makes the assay expensive and the photosensitive property of 2- aminopurine was also problematic.

In this work, a modification-free AP site-containing DNA duplex aptamer (AP-aptamer) is developed based on the competitive binding with a fluorescent ligand, riboflavin. [2] In the absence of theophylline, riboflavin binds to the receptor nucleotide opposite the AP site, accompanied by fluorescence quenching of riboflavin. Upon addition of theophylline, the competitive binding of theophylline with riboflavin occurs, which results in an effective fluorescence restoration due to the release of riboflavin from the AP site.

【Results and Discussion】

From the examination of the optimization of AP-aptamers, the complex of riboflavin with a 23-mer AP-aptamer (**23C**; 5'-TCT GCG TCC AGX GCA ACG CAC AC-3'/5'-GTG TGC GTT GCC CTG GAC GCA GA-3', X = AP site, Spacer C3) possessing cytosine as a receptor nucleotide was found to show the selective and effective fluorescence response to theophylline. The limit of detection for theophylline was estimated as 1.1 μM and this value is almost comparable to those of theophylline-binding RNA aptamer-based methods as previously reported (0.1-1.2 μM). Furthermore, fluorescence detection of theophylline was successfully demonstrated with high selectivity in serum samples using the riboflavin-**23C** complex. In addition, a good linear correlation was obtained between the fluorescence response and the concentration of the serum theophylline in the range from 5.0 μM to 160 μM. Therefore, the riboflavin-**23C** complex is applicable to the monitoring of serum theophylline in the therapeutic range (60-100 μM).

[1] M. Li, Y. Sato, S. Nishizawa, T. Seino, K. Nakamura, N. Teramae, *J. Am. Chem. Soc.*, **2009**, 131, 2448-2449.
[2] Y. Sato, Y. Zhang, S. Nishizawa, T. Seino, K. Nakamura, M. Li, and N. Teramae, *Chem. Eur. J.*, **2012**, 18, 12719-12724.

Poster 65

Synthesis and Photophysical Properties of Tetraphenylethylene-Substituted Porphyrazines

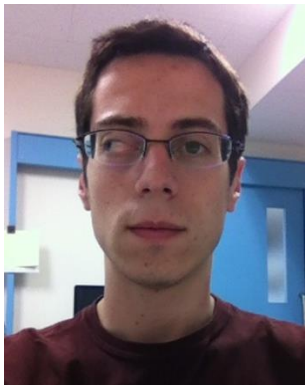

Thiago Teixeira Tasso, Taniyuki Furuyama, and Nagao Kobayashi
Graduate School of Science, Tohoku University Aoba 6-6, Aoba-ku, Sendai 980-8579, Japan.
Email: thiagott@s.tohoku.ac.jp
Key words: tetraazaporphyrin, fluorescence, aggregation induced effect

Tetraazaporphyrins (TAPs), also called porphyrazines, are porphyrin derivatives in which the four *meso*-carbon atoms are substituted by nitrogen atoms, rendering these macrocycles new properties and potential applications. Although porphyrins and phthalocyanines show moderate fluorescence, octaaryl-TAPs have very weak fluorescence. Since phthalocyanine and TAP have a common macrocyclic structure, we speculate that modification of TAP with appropriate substituent groups can allow fluorescence emission switching, which is interesting for bio-imaging purposes. Molecules such as tetraphenylethylene (TPE), which are non-emissive when monomeric but show considerable fluorescence emission enhancement in the aggregated form, has been recently discovered, and many researches has been conducted since then[1]. This aggregation-induced emission (AIE) behavior thus inspired us to design novel porphyrazine macrocycles in which the dark and emissive states can be controlled through their monomer-aggregate equilibrium in solution and solid state. In this context, we report in this work the synthesis of tetraazaporphyrins bearing TPE substituents and investigation of their photophysical properties.

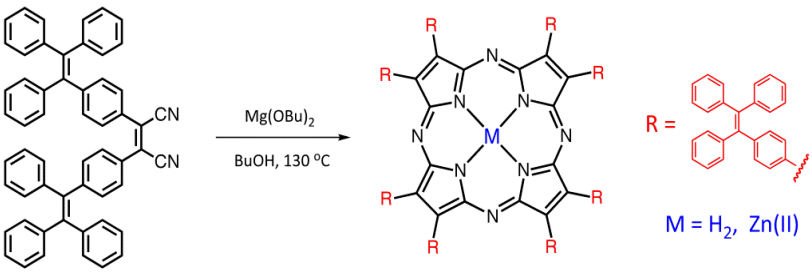

Fig. 1. Synthetic procedure of the TPE substituted porphyrazines.

The synthesis of the precursor dinitrile yielded both *cis* and *trans* isomers, which showed AIE effect and distinct fluorescence properties in solution and solid state. The photophysical studies of the directly linked TPE-TAP conjugate revealed low fluorescence quantum yields due to a charge transfer process occurring from the TPE groups to the macrocycle. We are now synthesizing heteroatom-linked conjugates to prevent energy transfer processes.

Ref. [1] Y. Hong; J. W. Y. Lam; B. Z. Tang. *Chem. Soc. Rev.* **2011**, *40*, 5361-5388.

Poster 66

Control of Alignment of Fullerenes Using Highly Deformed Phthalocyanines

Akito Miura,[1] Soji Shimizu,[1] Nagao Kobayashi[1]
[1]Department of Chemistry, Graduate School of Science, Tohoku University, 6-3 Aza-Aoba, Aoba-ku, Sendai 980-8578, Japan
E-mail: miuraakito@s.tohoku.ac.jp
Key words: phthalocyanine, fullerene, co-crystallate

Phthalocyanines (Pcs) show interesting optical properties due to the intense π-π* bands associated with the planar heteroaromatic π-conjugated system. As a result, Pcs have been used as dyes and pigments, optical discs, nonlinear optics, solar cells, and so on. In recent years, donor-acceptor pairs based on Pcs and fullerenes have been investigated for applications in the fields of molecular electronics and optoelectronics such as organic transistors and photovoltaic cells. Although porphyrins which have a similar structure to Pcs, have been often utilized for co-crystallization with fullerene, there is no phthalocyanine-fullerene co-crystallates probably due to their smaller π-π interaction compared to porphyrins. Based on this point, we focused on *α*-octaphenylphthalocyanine (*α*-Ph_8H_2Pc). *α*-Ph_8H_2Pc exhibits a saddle-like distorted structure due to the steric hindrance of adjacent phenyl substituents at the *α*-positions. Its deformed structure can provide concave surfaces so that co-crystallization of Pcs and fullerenes can be expected. Recently, we succeeded in co-crystallization of fullerene C_{60} and C_{70} molecules with *α*-Ph_8H_2Pc as expected. These co-crystallates formed one dimensional array structure by convex-concave interaction using its distorted π-conjugation surface. The structures and properties of these co-crystallates will be reported.

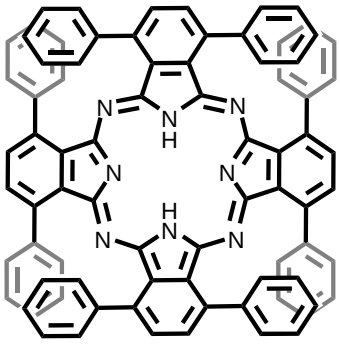

Figure 1. Deformed structure of *α*-Ph_8H_2Pc.

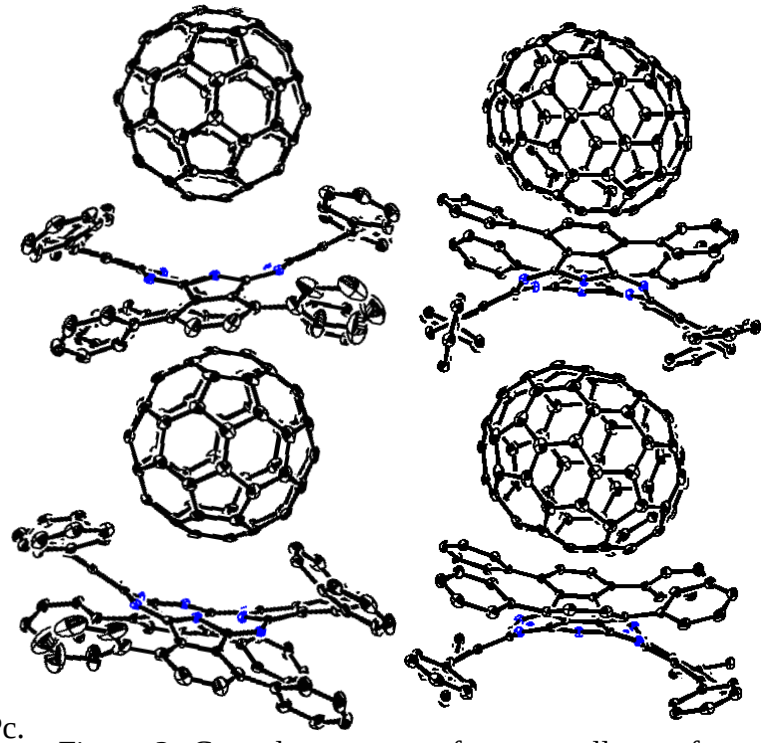

Figure 2. Crystal structures of co-crystallates of *α*-Ph_8H_2Pc and fullerene (C_{60}: right, C_{70}: left).

Poster 67

Push-Pull Subporphyrazines with Red-Shifted Absorptions

Xu Liang,[1] Soji Shimizu,[1] and Nagao Kobayashi[1]

[1]Department of Chemistry, Graduate School of Science, Tohoku University, Sendai 980-8578, Japan.

Email: B2SD5703@s.tohoku.ac.jp

Key words: subporphyrazine, push-pull effect, red-shifted absorption

Porphyrinic chromophores with electron-donating (push) and electron-withdrawing (pull) substituents generally exhibit main absorption bands at longer wavelength region due to the smaller HOMO-LUMO gap arising from destabilization of the HOMO by push-substituents and stabilization of the LUMO by pull-substituents. Introduction of push-pull substituents to chromophores has thus been one of the effective strategies for achieving red-shift of the main absorption bands. Subporphyrazines (SubPzs), 14π heteroaromatic chromophores comprising of three pyrrole rings, is known to exhibit main absorption band (Q-band) at around 500 nm.[1]

In this study, the "push-pull strategy" was tested for SubPzs, in which push- and pull-substituents were directly introduced to the *β*-positions of pyrrole moieties. From a reaction of 2-aryl-1,1',2-tricyanoethylene and BCl_3, *C*3 symmetric *β*-*p*-tolyl-*β*'-CN SubPz **1** and *C*3 symmetric *β*-*p*-methoxyphenyl-*β*'-CN SubPz **2** were obtained and characterized. Electronic absorption spectra exhibited red-shift of the main absorption bands at 589 nm for **1** and 628 nm for **2** as compared to those of regular SubPzs, and an additional band appeared at around 400 nm. Theoretical calculations were performed to give in-depth insight into the push-pull effect on the red-shift of the main absorption bands. In this poster presentation, the synthesis and properties of push-pull SubPzs with red-shifted absorptions will be discussed.

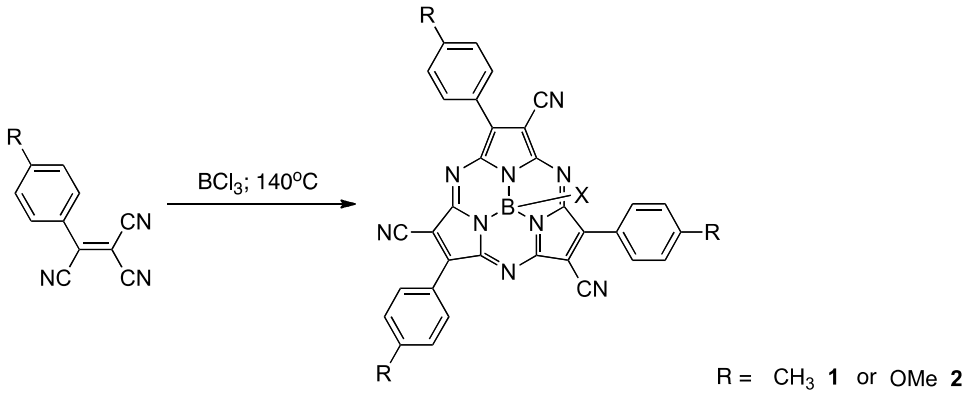

Scheme 1 Synthesis of push-pull subporphyrazines **1** and **2**.

Ref. [1] N. Kobayashi et al., *J. Am. Chem. Soc.*, **1999**, *121*, 9096; *Inorg. Chem.*, **2006**, *45*, 6148; T. Torres and et al., *Chem. Eur. J.*, **2005**, *11*, 354.

Poster 68

Optimal control simulation of laser isotope separation utilizing molecular alignment

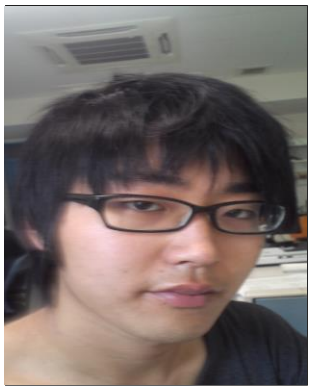

Kaoru Nakashima, Yukiyoshi Ohtsuki, and Hirohiko Kono
Graduate School of Science, Tohoku University Aoba 6-3, Aoba-ku, Sendai 980-8578, Japan.
Email: tohoku_naka@yahoo.co.jp
Key words: isotope separation, molecular alignment, optimal control, laser pulse

[Introduction] Molecular laser isotope separation is attractive methods due to its higher selectivity. Recently, Averbukh et al. proposed laser isotope separation using quantum interference[1]. In this method, the isotope selectivity originates from difference in time evolution of vibrational wave packets which are induced by short laser pulse. But this method is difficult to apply for molecules including by heavy isotope because of difference in vibrational period decreases as the atomic mass increases. Although molecular laser isotope separation utilizing alignment control of molecular rotational wave packet can be carried out without tunable laser (because of non-resonant raman rotational transition) and the isotope selectivity is not lowered for heavy isotopes in contrast to conventional methods. As the first step toward this isotope separation, here we study the design of laser pulses that achieve isotope-selective molecular alignment in the case of $C^{16}O/C^{18}O$ mixture.

[Results and Discussions] Assume that the wavelength of the laser pulse is around 800 nm. A rotational wave packet is created by an induced dipole interaction averaged over fast optical oscillations. We numerically design laser pulse to align $C^{16}O$ parallel to the laser polarization vector (called alignment state) and align $C^{18}O$ vertically to laser polarization vector (called anti alignment state) by means of optimal control simulation. An Optimal control designs a laser pulse to manipulate molecular dynamics for a defined purpose utilizing the calculus of variations. Fig1(a) shows the envelope function of optimal pulse as a function of time and Fig1(b) shows time evolution of the degree of alignment of each isotopologues (θ means an angle between the polarization vector and molecular axis. See Fig2.) For the temperatures T = 10K. $T_{rot} \cong 9\,\mathrm{ps}$ is a rotational period of $C^{16}O$. The optimal pulse in Fig1(a) is almost consists of one sub-pulse which is located on $t/T_{rot} = 1.0$. Moreover, we analyze the mechanism of control with δ pulse. It indicates that the selectivity takes the maximum when pulse is irradiated at t/T_{rot} =1.0 and selectivity is independent to temperature.

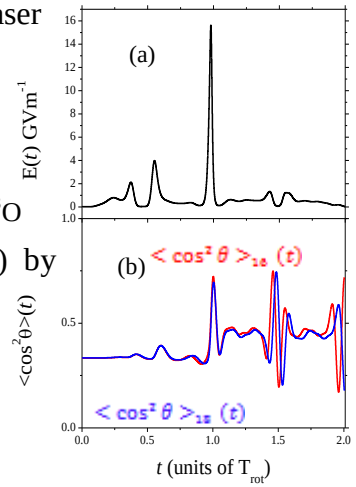

Fig1. (a) Envelope function of optimal pulse (b)Degree of alignment (red:$C^{16}O$ blue:$C^{18}O$)

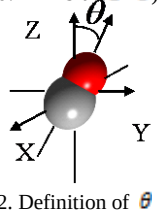

Fig2. Definition of θ

[1]I.Sh.Averbukh *et al., Phys. Rev. Lett.* **77,** 3518 (1996)

Poster 69

Theoretical analysis of ion transport through soft interfaces

Nobuaki Kikkawa,[1] and Akihiro Morita[1]

[1]Graduate School of Science, Tohoku University Aoba 6-3, Aoba-ku, Sendai 980-8578, Japan

Email: kikkawa@s.tohoku.ac.jp

Key words: molecular dynamics, free energy, water finger, counter ion

Ion transport through soft interfaces is often discussed in many fields such as interfacial chemistry, reaction engineering, electrochemistry, atomospheric chemistry, and biochemistry. Ion transfer can be investigated with electrochemical and thermodynamical measures, but it is very difficult to connect these results with the microscopic pictures. To fill the gap between them, Molecular dynamics (MD) simulation is one of the valid methods.

The first important insight of ion transport from MD simulation is that the interfacial fluctuation has a great effect of ion transport.[1] This characteristic fluctuation is called water finger. This finding inspired the following theoretical and calculational studies. In these researches, it was shown theoretically that the water finger making may slow down the rate of ion transport.[2, 3] It was also implied that there is the free energy barrier in water finger broken.[4]

Recently we studied the effect of hydrophobic counter ion on the ion transport through water-chloroform interface by using free energy calculation.[5] As a result, we found that the existence of hydrophobic counter ion decreases the transfer free energy of ion through the interface and shortens the water finger (Fig. 1). We consider these two phenomena are related to each other and they create the acceleration of ion transport. The details will be shown in the poster presentation.

[1] I. Benjamin, *Science* **1993**, 261, 1558.

[2] R. A. Marcus, *J. Chem. Phys.* **2000**, 113, 22.

[3] A. A. Kornyshev, M. Urbakh, *et al.*, *J. Chem. Phys.* **2002**,117, 8.

[4] K. J. Schweighofer, I. Benjamin, *J. Phys. Chem.* **1995**, 99, 9974.

[5] N. Kikkawa, *et al.*, *Chem. Phys. Lett.* **2012**, 534, 19.

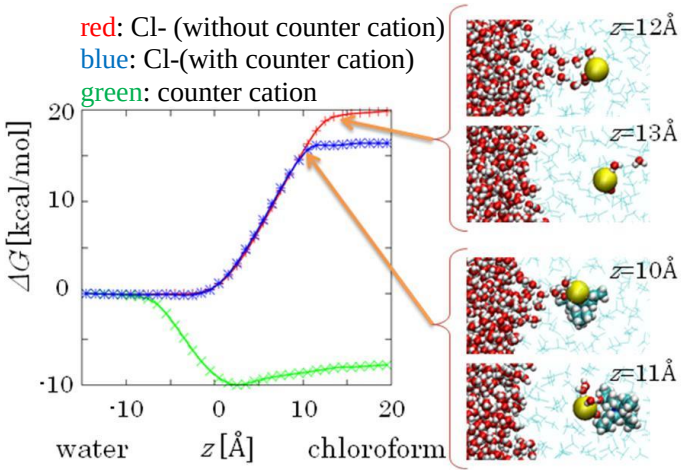

Fig. 1. Free energy profiles and snapshots of water finger. z = 0 in this graph means the interface. The red and white balls are oxygen and hydrogen of water molecules respectively. The yellow balls are the observed ions and the neighbor molecules composed of blue and white balls are the hydrophobic counter ion. The blue-line molecules are the chloroforms.

Poster 70

Free energy analyses for ATP hydrolysis using quantum mechanical /molecular mechanical simulations combined with a theory of solutions.

Yuji Miki, Hideaki Takahashi*, and Akihiro Morita
Graduate School of Science, Tohoku University Aoba 6-3, Aoba-ku, Sendai 980-8578, Japan.
Email: mikiyuji@s.tohoku.ac.jp
Key words: ATP hydrolysis, DFT, QM/MM, Theory of solutions

Adenosine-tri-phosphate (ATP) hydrolysis is one of the most important biological reactions. However, the computation of the free energy of ATP hydrolysis on the basis of the molecular theory is still a challenge. Major difficulty arises from the fact that the excess charges of the solutes will significantly fluctuate in response to the electrostatics field due to water solvent. To address this issue, we adopt the quantum mechanical and molecular mechanical (QM/MM) approach combined with the theory of energy representation (QM/MM-ER[1]) to the hydrolysis of pyrophosphoric acid (PPi) regarded as a prototype reaction of ATP.

Within the framework of QM/MM-ER method, the total solvation free energy $\Delta\mu$ of the QM solute is decomposed into two contributions, the two-body interaction energy $\Delta\bar{\mu}$ and the many-body interaction energy $\delta\mu$, thus $\Delta\mu = \Delta\bar{\mu} + \delta\mu$. $\Delta\bar{\mu}$ is the solvation free energy of a solute of which electron density is fixed at an arbitrary distribution. Then it is possible to apply a theory of energy representation[2] to compute $\Delta\bar{\mu}$. $\delta\mu$ is the residual free energy associated with the electron density fluctuation of the solute in solution which can be exactly formulated by adopting the energy shift of the whole system due to the solute polarization as a new energy coordinate η in the method of energy representation.

Computed free energies ΔG for the hydrolysis of PPi are summarized in Table 1. For the solutes ($H_4P_2O_7$, $H_3P_2O_7^-$) with 0 and 1 excess electron, the free energies given by the present approach are in good agreement with the experimental values[3] with deviations less than 1.0 kcal/mol. For the solute ($H_2P_2O_7^{2-}$) with 2 excess charges, we re-optimized the size parameters to realize the two-body interaction between the solute and solvent water molecules. Then, it was found that the computed free energy reasonably agrees with an experimental value[3]. The free energy calculations for the solute with 3 excess charges are now in progress.

[1] H. Takahashi, et al. *J. Chem. Phys.* **2004**, 136, 214503.
[2] N. Matubayasi, et al. *J. Chem. Phys.* **2000**,113, 6070.
[3] P. George, et al. *Biochim Biophys. Acta,* **1970**, 223,1.

Reaction	ΔG	ΔG (expt)[3]
$H_4P_2O_7 + H_2O \rightarrow 2\ H_3PO_4$	–10.1	–9.5
$H_3P_2O_7^- + H_2O \rightarrow H_3PO_4 + H_2PO_4^-$	–6.7	–7.5
$H_2P_2O_7^{2-} + H_2O \rightarrow 2\ H_2PO_4^-$	–9.1	–7.7

Table.1 Reaction of the hydrolysis of pyrophosphoric acid and the free energy change associated with the reactions (units : kcal/mol)

Poster 71

Development of software “CALNOS” for Nonlinear spectroscopy calculation and its application to surface of water/methanol mixture

Takashi Ishihara,[1] Tatsuya Ishiyama,[1] and Akihiro Morita[1]
[1]Graduate School of Science, Tohoku University
Aoba 6-3, Aoba-ku, Sendai 980-8578, Japan.
Email: shacho@s.tohoku.ac.jp
Key words: surface spectroscopy, molecular dynamics, aqueous surface

The vibrational sum frequency generation (SFG) spectroscopy is one of the most powerful tools to probe molecular orientational structure and hydrogen bonding (H-bonding) network at aqueous interfaces in monolayer sensitivity. However, it is sometimes difficult to interpret SFG spectra in terms of interfacial structure uniquely, since the spectra are often complicated by overlap or interference of vibrational bands, extensive inhomogeneous broadening sensitive to local environment, etc.

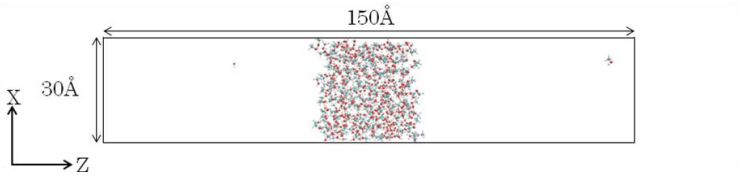

Fig.1. Snapshot of 0.4 mole fraction

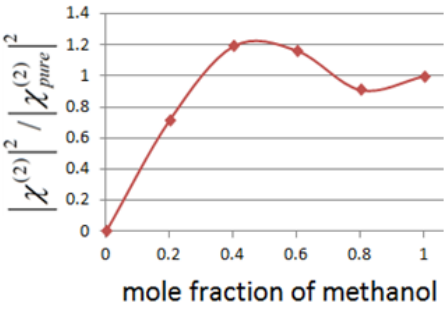

Fig.2. SFG intensity of CH symmetric stretching mode in MD simulation

The software “CALNOS” (Calculation of Nonlinear Optical Spectrum) is a computer program to calculate interfacial structure and SFG spectra with molecular dynamics (MD) simulation, and has been developed by our group to overcome the difficulties in spectral assignments mentioned above.

Recently, the program code was optimized for massively parallel computing, and applied it to surfaces of water-methanol mixture. The experimental study [1] reported that the SFG intensity of methanol C-H symmetric stretching mode increases with increasing methanol concentration in low concentration range, whereas it decreases over 0.5 mole fraction. This non-monotonic behavior of the SFG intensity was difficult to explain only from the experimental analysis. Here we address this issue by employing CALNOS, in which a MD simulation containing a liquid slab of water-methanol mixture (Fig.1) was carried out.

The present MD simulation can successfully reproduce the experimentally reported result (Fig.2). It was found that the increasing of the SFG intensity in the low concentration range can be explained by the increasing of surface methanol concentration, and the decreasing in the high concentration range is due to the randomized orientation of surface methanol molecules.

Ref. [1] J. Sung, K. Park, and D. Kim, *J. Phys. Chem. B* **2005**, *109*, 18507-18514

Denka Memo Pad　184 (w) x 270 (h) mm ／方眼のサイズ 10mm ／色：BW

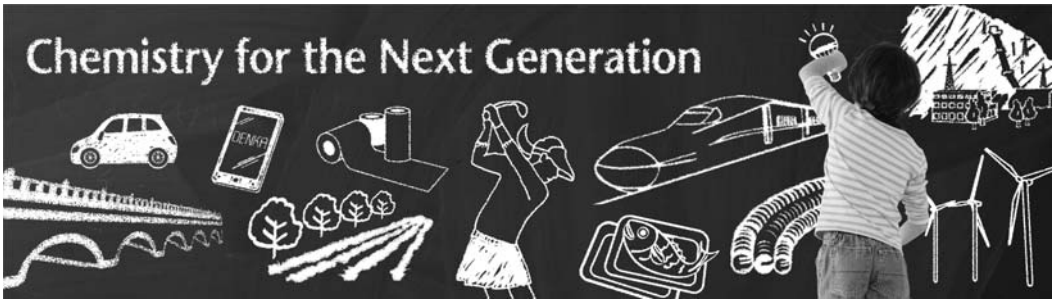

MEMO

DENKA
DENKI KAGAKU KOGYO KABUSHIKI KAISHA
www.denka.co.jp

SEC-N100 series

㈱堀場エステック
マスフローコントローラ
制御ユニットセットのご紹介



- ***新機能　マルチガス・マルチレンジ機能搭載※1***
- ***高速応答　全流量域1秒以内***
- ***高精度±1.0%S.P.***

※1、デジタルアクセサリを用いて
ユーザーサイドで仕様変更可能です。

HORIBASTEC

マルチレンジ・マルチガス機能

専用ソフト・アクセサリ※1を用い研究現場でMFCのガス種・流量を変更できます。

緊急時対応用に在庫しているMFCも装置仕様に合わせる必要はありません。保守時に必要なガス種・流量を設定していただくだけです。

マルチレンジ・マルチガス機能付きのデジタルマスフローコントローラは予備在庫を最小限にとどめ大学での研究を支援いたします。

専用ソフトウェアを用い、簡単操作で仕様変更が可能

お客様ご自身でマスフローコントローラ(MFC)の流量レンジ・使用ガスを変更できます。

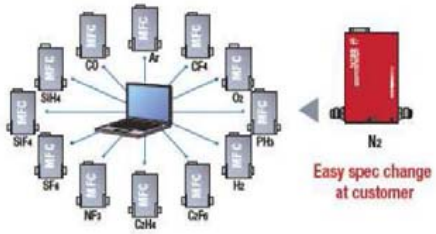

マルチガス対応

使用ガスの変更が行えます。

例：SEC-N100 MR-MG-02　N2 100 SCCM ▶ Ar 110 SCCM

マルチレンジ対応

流量レンジの変更が行えます。

例：SEC-N100 MR-MG-04　N2 1000 SCCM（流量制御範囲 20~1000 SCCM） ▶ N2 250 SCCM（流量制御範囲 5~250 SCCM）

▶マルチガス・マルチレンジ　フルスケール流量の一例

ガス種 / MR-MG型号	N_2	Ar	H_2	He	CO_2	CH_4
SEC-N112(W), SEC-N114(W), SEC-N116						
R01	3-10	4-11	—	4-12	3-8	2-7
R1.5						
01	10-30	11-35	8-30	10-38	7-25	6-22
1.5						
02	25-100	35-110	25-100	33-120	21-83	19-75
2.5						
03	75-300	110-350	75-300	99-380	64-250	57-220
3.5						
04	250-1000	350-1100	250-1000	330-1300	210-830	190-750
4.5						
05	750-3000	1100-3500	750-3000	1100-4100	610-2400	590-2300
5.5						
06	2500-10000	3500-11000	2500-10000	3900-13000	2000-8000	2000-7800
SEC-N122(W), SEC-N124(W), SEC-N126						
6.5						
07	10000-30000	10000-30000	10000-30000	12000-30000	7300-21000	5800-22000
08	30000-50000	30000-50000	30000-50000	30000-50000	21000-35000	—
SEC-N132, SEC-N134, SEC-N136						
09	50000-100000	—	—	—	35000-75000	—
SEC-N1142, SEC-N144, SEC-N146						
10	100000-200000	—	—	—	—	—

お問合せご用命は
右記まで

株式会社　旭商会仙台店
〒980-0011　仙台市青葉区上杉一丁目9-38
Tel:022-221-7501　/　Fax:022-225-8456
Email ; sales2@asahi-syokai.co.jp

㈱堀場エステック
ポータブル水素発生器のご紹介

- ■各種分析機器の燃料ガスやキャリアガスに便利！
- ■物理・化学実験室用　水素源にも有効！
- ■発生状態の監視と、外部信号による停止も可能！

HORIBA STEC

水素発生器はコンパクトな卓上設計だから安全！

水素発生器の原料は純水いつでもガス発生はOK！

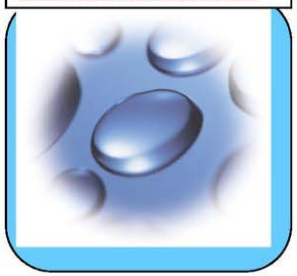

水素ボンベの管理は必要なし！

仕様

型式	OPGU-7100	OPGU-7200	OPGU-2100	OPGU-2200
発生ガス	H_2 99.999%以上（露点-65℃　実績値）		H_2 99.99%以上（水分含まず）	
発生流量	100mL/min（at 25℃ 1013hPa）	225mL/min（at 25℃ 1013hPa）	100mL/min（at 25℃ 1013hPa）	225mL/min（at 25℃ 1013hPa）
発生圧力	20～400kPa（可変）			
使用温度	5～40℃			
純水タンク	2L			
使用純水	比抵抗5～10MΩ･cm 25℃（イオン交換水）			
純水消費量	約5.5mL/h（100mL/min発生時）	約12mL/h（225mL/min発生時）	約5.5mL/h（100mL/min発生時）	約12mL/h（225mL/min発生時）
電源	AC100V　50/60Hz　100VA	AC100V　50/60Hz　200VA	AC100V　50/60Hz　100VA	AC100V　50/60Hz　200VA
水素ガス出口	本体Rc1/8メネジ、φ3用パイプ継手			
重量	10kg（水を含まず）			

※到達露点温度は、使用条件により若干異なります。その他 詳細仕様についてはお問い合わせください。
※発生ガス純度について、N_2,O_2は含んでいません。

外形寸法　（単位:mm）

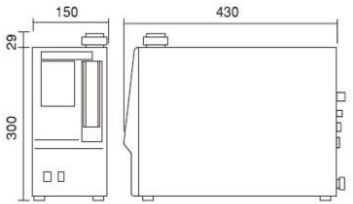

（突起物を除く）

フローシート

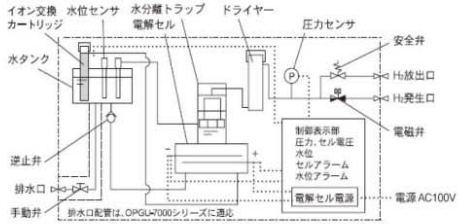

イオン交換カートリッジ付き

お問合せは
右記担当者まで

株式会社　旭商会仙台店
〒980-0011　仙台市青葉区上杉一丁目9-38
Tel:022-221-7501　/　Fax:022-225-8456
Email ; sales2@asahi-syokai.co.jp

TII Group UNISOKU Co., Ltd.

UNISOKU Scientific Instruments — TII Group

UHV Ultra Low Temperature STM System with Dilution Refrigerator

USM1600

High-End Model STM in Ultra Low Temperature and High Magnetic Field.

Application

- ☑ High energy resolution IETS on single molecule
- ☑ Atom manipulation
- ☑ Spin polarized STM
- ☑ Spin resonance STM on single atom and molecule
- ☑ High-resolution spectroscopy on super conductor

Specification of STM

Max Scan Size	→	800nm x 800nm x 100nm at 100mK (2.5 x 2.5 x 0.4μm@RT)
Resolution	→	Spatial; <0.01nm, Energy; <1meV
Base Temperature	→	40mK (Target 30mK)
Magnetic field	→	11T, 15T Vertical or 9-2-2T Vector Magnet

Continuous Cooling Lower Than 40mK (Target 30mK).

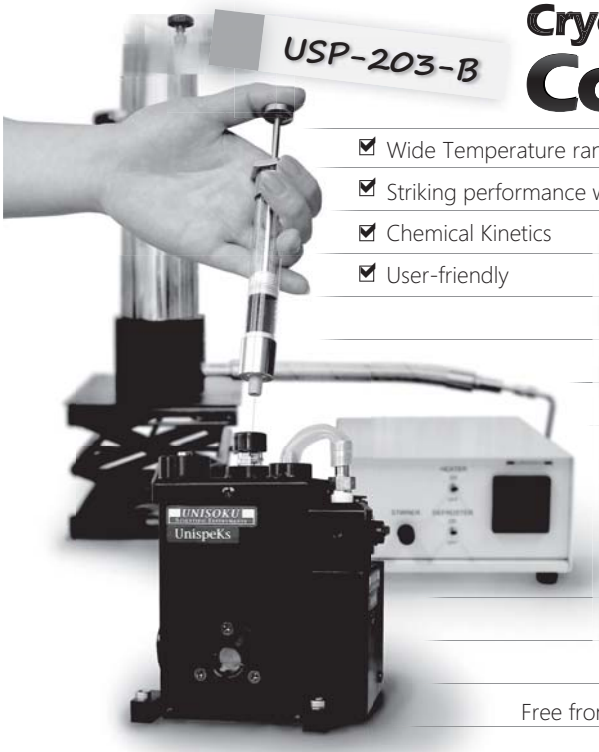

USP-203-B

Cryostat for Spectrophotometer

CoolSpeK UV/CD

- ☑ Wide Temperature range
- ☑ Striking performance with liquid sample
- ☑ Chemical Kinetics
- ☑ User-friendly

Time-dependent UV-vis spectra

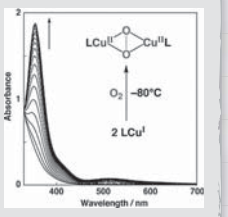

Spectral changes for the reaction of O_2 and a Cu(I) complex at -80℃. Formation of a m- peroxo dinuclear copper(II) complex can be easily monitored by the time-dependent UV-vis spectrum at low temperature.
(Courtesy of Prof. Shinobu Itoh of Osaka University)

Variable-temperature UV-vis, CD, and fluorescence spectra

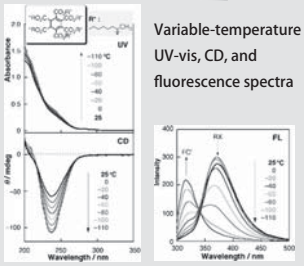

Variable-temperature UV-vis, circular dichroism, and fluorescence spectra of (R)-1-methylheptyl mellitate (0.03 mM) in pentane at 25℃ to –110℃. FL; Excitation at 270 nm.
(Courtesy of Prof. Yoshihisa Inoue of Osaka University and Prof. Takehiko Wada of Tohoku University)

- Compact and lightweight ☑
- Compatible with many spectrophotometers ☑
- Free from vacuum pumps and surprisingly low dew condensation ☑

CoolSpeK can be placed inside a sample compartment of commercial UV-Vis / fluorescence / CD spectrophotometers.
Measurement in a temperature range from –80℃ to +100℃ is realized by regulating the flow of liquid N2.

UNISOKU Scientific Instruments — TII Group

UNISOKU Co., Ltd.
www.unisoku.com

2-4-3 Kasugano Hirakata, Osaka 573-0131, Japan
TEL +81-72-858-6456 FAX +81-72-859-5655
e-mail info@unisoku.co.jp

Provide consistent support of research and development with extensive experience

Kitano Seiki's high flexible and high-quality finished vacuum equipments for research and developments. High quality products, experimental environments of good quality research and development are supported by our technical strength and know-how fostered with our extensive experience and actual performance. We pursue the goal of "We don't compete, but we create through competition." First, based on the communication with our clients, we set our rule of conduct of "We deal with it because of difficult task." This is our basic stance we definitely reflect a desire up to even the single part. It is our pleasure to have the achievements and success by customers' research and developments.

- Design
- Machine processing
- Welding processing
- Leak test
- Surface processing
- Cleaning
- Assembling
- Vacuum start up

Line of business

- Instruments and equipments for research and development
- Instruments and equipments for ultrahigh vacuum
- Thin film production equipments (MBE, CVD, EB, Spattering, etc.)
- Surface analysis equipments (FIM, STM, TEM, CMA, etc.)
- Cryogenic-cooling equipments, instruments, parts
- Multi-spindle manipulators
- Various linear and rotation introduction machines (single axle, biaxial)
- Transfer rod
- Ultrahigh vacuum chamber
- Various repairs, maintenances, retrofit, relocation operations

KITANO SEIKI CO.,LTD.
7-17-3 Chuo Ohtaku, Tokyo Zip Code143-0024 Tel: 03-3773-3956 Fax:03-3778-0379
E-mail: info@kitano-seiki.co.jp http://www.kitano-seiki.co.jp

All for Researchers.
KITANO

Reagents

BioChemicals

FineChemicals

OrganicChemicals

脱水溶媒シリーズに、水分含量を10ppm以下まで抑えた「超脱水」グレード溶媒、手軽に取り扱える9Lのキャニスター缶包装、いつでもフレッシュな脱水溶媒を使用できる100ml包装の品目を追加しました。是非ご利用下さい！！

フレキシブルマイクロプレートリーダー

インフィニット M1000PRO

Instruments

Equipment

ClinicalChemicals

Medical Appliances

仙台和光純薬株式会社
Sendai WAKO PureChemical.ltd
Tel ; 022(239)2700 Fax ; 022(239)2705
Email ; 1nfo@sendaiwako.com
http://www.sendaiwako.com

中圧接触還元装置

YAZAWA

Medium-Pressure Catalytic Hydrogenators

中圧接触還元装置

YS-11型

中圧下(0.5MPa以下)で接触還元反応を行う装置で，常圧下における接触還元に比べて反応を速やかに行うことが出来ます．マグネチックスターラによる攪拌方式ですので，反応ボトルを静止した状態で反応が行えます．

形式名	YS−11型
サイズ	W500×D450×H500 mm
重量	29 kg
タンク	内容積約4.4 L　SUS316製
バルブ類	SUS316製
圧力計	0〜0.5 Mpa
ガス導入アダプター	SUS316製(焼結フィルター付)
攪拌装置	強力マグネチックスターラー
価格(￥)	1,040,000

YAZAWA 理化学汎用機器　共通摺合せ硝子器具
理化学医療用硝子器具

矢澤科学器械株式会社

〒981-0951　仙台市青葉区滝道42番12号
ＴＥＬ．022（278）7531㈹
ＦＡＸ．022（279）7390

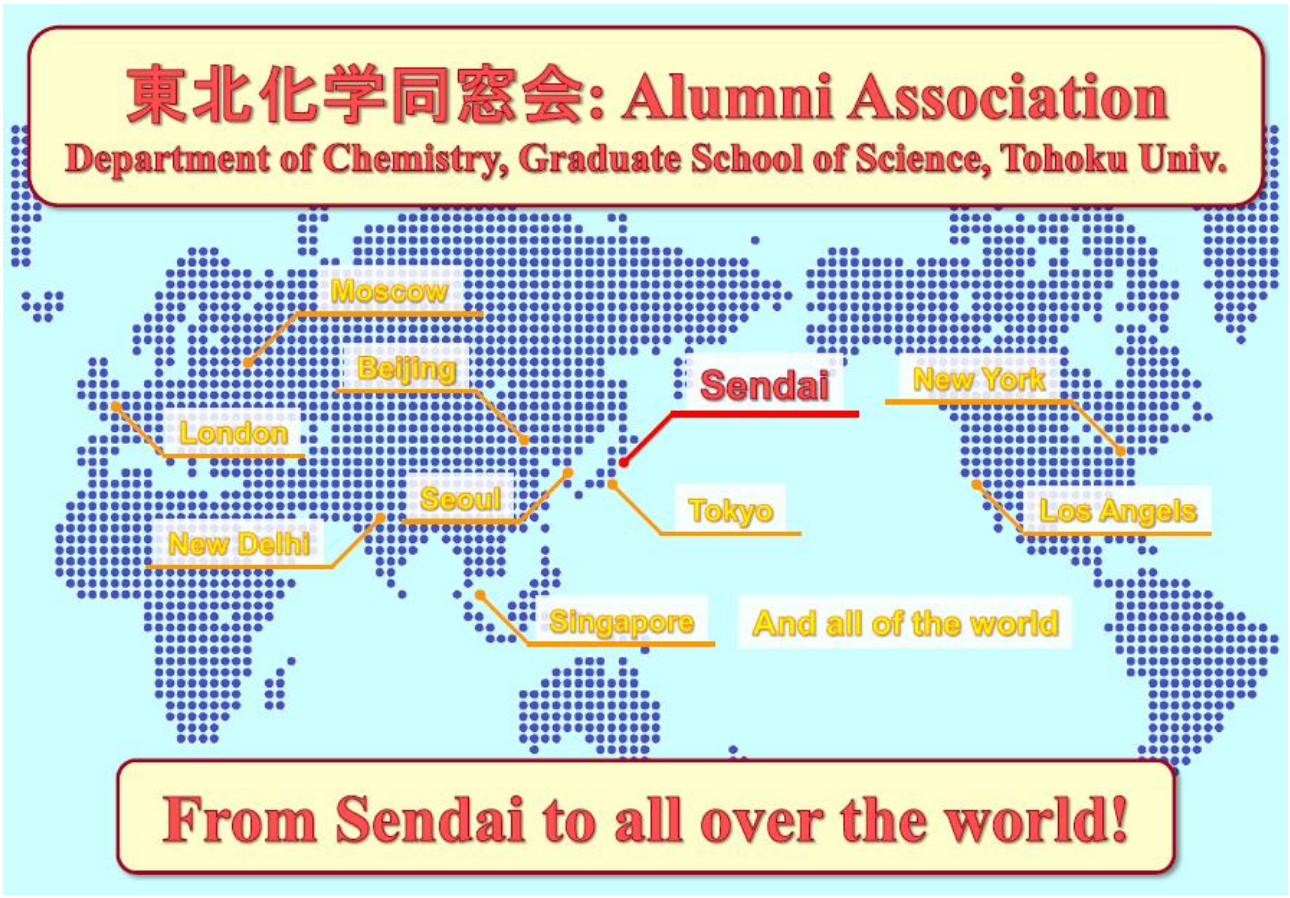
東北化学同窓会: Alumni Association
Department of Chemistry, Graduate School of Science, Tohoku Univ.
Moscow
Beijing
Sendai
New York
London
Seoul
Tokyo
Los Angels
New Delhi
Singapore
And all of the world
From Sendai to all over the world!

Student Organizers

Yuta Kudo (Yamashita Lab.)	b3ad1305@s.tohoku.ac.jp
Yosuke Sano (Kino Lab.)	y.sano@s.tohoku.ac.jp
Yuya Yoshii (Akutagawa Lab.)	yuuya.y@mail.tagen.tohoku.ac.jp
Norioki Abe (Hoshino Lab.)	fy11013@mail.kankyo.tohoku.ac.jp
Yo Kushida (Yamaguchi Lab.)	b3yd1002@s.tohoku.ac.jp
Yuto Naruse (Arimoto Lab.)	y.naruse@biochem.tohoku.ac.jp
Yuto Kanno (Tobita Lab.)	b2sd5009@s.tohoku.ac.jp
Hiroki Saito (Nishizawa Lab.)	b2sm5031@s.tohoku.ac.jp
Shohei Kumagai (Yamashita Lab.)	s-kumagai@s.tohoku.ac.jp
Thiago Teixeira Tasso (Kobayashi Lab.)	thiagotasso@hotmail.com
Shusuke Egoshi (Ueda Lab.)	b2sd5005@s.tohoku.ac.jp
Fumiya Hirakawa (Iwamoto Lab.)	f-hirakawa@s.tohoku.ac.jp
Shigenobu Umemiya (Hayashi Lab.)	sumemiya0398@gmail.com
Hironobu Kono (Toyota Lab.)	b3sm5034@s.tohoku.ac.jp
Narumi Tomohiro (Terada Lab.)	b3sd5014@s.tohoku.ac.jp
Taisuke Matsuno (Isobe Lab.)	t.matsuno@s.tohoku.ac.jp
Mary Richardson (Sogawa Lab.)	b2sm5704@s.tohoku.ac.jp
Ryoichi Moriyama (Misaizu Lab.)	r-mrym@s.tohoku.ac.jp
XIE Min (Fujii Lab.)	xiemin821@163.com
Hikaru Sotome (Fukumura Lab.)	b2sd5012@s.tohoku.ac.jp
Hajime Imai (Kono Lab.)	imhajime@gmail.com
Nobuaki kikkawa (Morita Lab.)	kikkawa@s.tohoku.ac.jp
Qiang Chen (Asao Lab.)	chenqiang_ripp@yahoo.com.cn
Jie Liu (Komeda Lab.)	suit_911@hotmail.com
Yuta Ito (Ueda Lab.)	y-ito@mail.tagen.tohoku.ac.jp
Ryohei Uematsu (Wada Lab.)	uematsu@mail.tagen.tohoku.ac.jp
Shunichi Kawasaki (Kinbara Lab.)	s-kawa@mail.tagen.tohoku.ac.jp
Yoshikazu Ikuta (Oikawa Lab.)	y.ikuta@mail.tagen.tohoku.ac.jp
Takuya Akisawa (Nagatsugu Lab.)	aki_07301001@yahoo.co.jp
Aya Yoshida (Takahashi Lab.)	yoshida@mail.tagen.tohoku.ac.jp
Takatoshi Kasukabe (Kyotani Lab.)	kasukabe@mail.tagen.tohoku.ac.jp
Yuki Kobayashi (Muramatsu Lab.)	wwbaba@mail.tagen.tohoku.ac.jp
Huie Zhu (Mitsuishi Lab.)	zhuhuie@mail.tagen.tohoku.ac.jp
Yu Gao (Mitsuishi Lab.)	gaoyu@mail.tagen.tohoku.ac.jp
Shunya Ito (Nakagawa Lab.)	ito.sh@mail.tagen.tohoku.ac.jp
Asuka Sakai (Kurihara Lab.)	asuka@mail.tagen.tohoku.ac.jp
Fukuma Sato (Yokoyama Lab.)	fukuma@mail.tagen.tohoku.ac.jp
Jun Kamei (Shimomura Lab.)	jules17@mail.tagen.tohoku.ac.jp
Xiaoyong Wu (Sato Lab.)	wxy521@mail.tagen.tohoku.ac.jp

Yasuyuki Takeda (Tomishige Lab.)	momomo_7531@yahoo.co.jp
Kenta Sugawara (Takizawa Lab.)	sugawara@aim.che.tohoku.ac.jp
Kei Watanabe (Asai Lab.)	a9tb3121@gmail.com
Nao kamezawa (Konno Lab.)	Nao.Kamezawa@mickey.che.tohoku.ac.jp
Shinji Sakai (Tsukada Lab.)	s.sakai@pcel.che.tohoku.ac.jp
Taichi Shimizu (Inomata Lab.)	t-shimizu@scf.che.tohoku.ac.jp
Erika Huruhashi (Nakayama Lab.)	furuhashi@seika.che.tohoku.ac.jp
Fei Ge (Shoda Lab.)	gefei@poly.che.tohoku.ac.jp
Ikuko Miyoshi (Hattori Lab.)	miyoshi@orgsynth.che.tohoku.ac.jp
Hayato Toyoda (Uozumi Lab.)	toyoda@biophy.che.tohoku.ac.jp
Masataka Kubouchi (Miyazaki Lab.)	kubo@crystal.apph.tohoku.ac.jp
Xiongwe Wang (Mastue Lab.)	ouyuui@bioinfo.che.tohoku.ac.jp
Norifumi Takahashi (Yoshioka Lab.)	takahashi@env.che.tohoku.ac.jp
Ryoma Maruta (Smith Lab.)	ryoma-m@scf.che.tohoku.ac.jp
Atsushi Umehara (Tokuyama Lab.)	b2yd1019@s.tohoku.ac.jp
Ryusuke Doi (Iwabuchi Lab.)	r-doi@s.tohoku.ac.jp
Aki Kohyama (Iwabuchi Lab.)	a-kohyama@s.tohoku.ac.jp
Koichi Fujiwara (Doi Lab.)	k.fujiwara@s.tohoku.ac.jp
Misato Kobayashi (Kondo Lab.)	b1yd1013@s.tohoku.ac.jp
Takashi Yamamoto (Oshima Lab.)	b3yd1010@s.tohoku.ac.jp
Wataru Igarashi (Kuwahara Lab.)	pcf09804@yahoo.co.jp
Ryo Hukazawa (Sasaki Lab.)	b2bm1021@s.tohoku.ac.jp

Staff Assitants

Professor Masahiro Yamashita	yamasita@agnus.chem.tohoku.ac.jp
Associate Professor Ilya Gridnev	igridnev@m.tohoku.ac.jp
Campus Asia Secretary Satoko Onodera	chem-coe@m.tohoku.ac.jp
Campus Asia Secretary Touko Takahashi	t-taka@m.tohoku.ac.jp

Useful Telephone and FAX Numbers

Facilitator

Yamashita Lab.	phone	022-795-6547

Hotel

UNIZO INN Sendai	phone	022-262-3211
Police	phone	110
Fire and Ambulance	phone	119

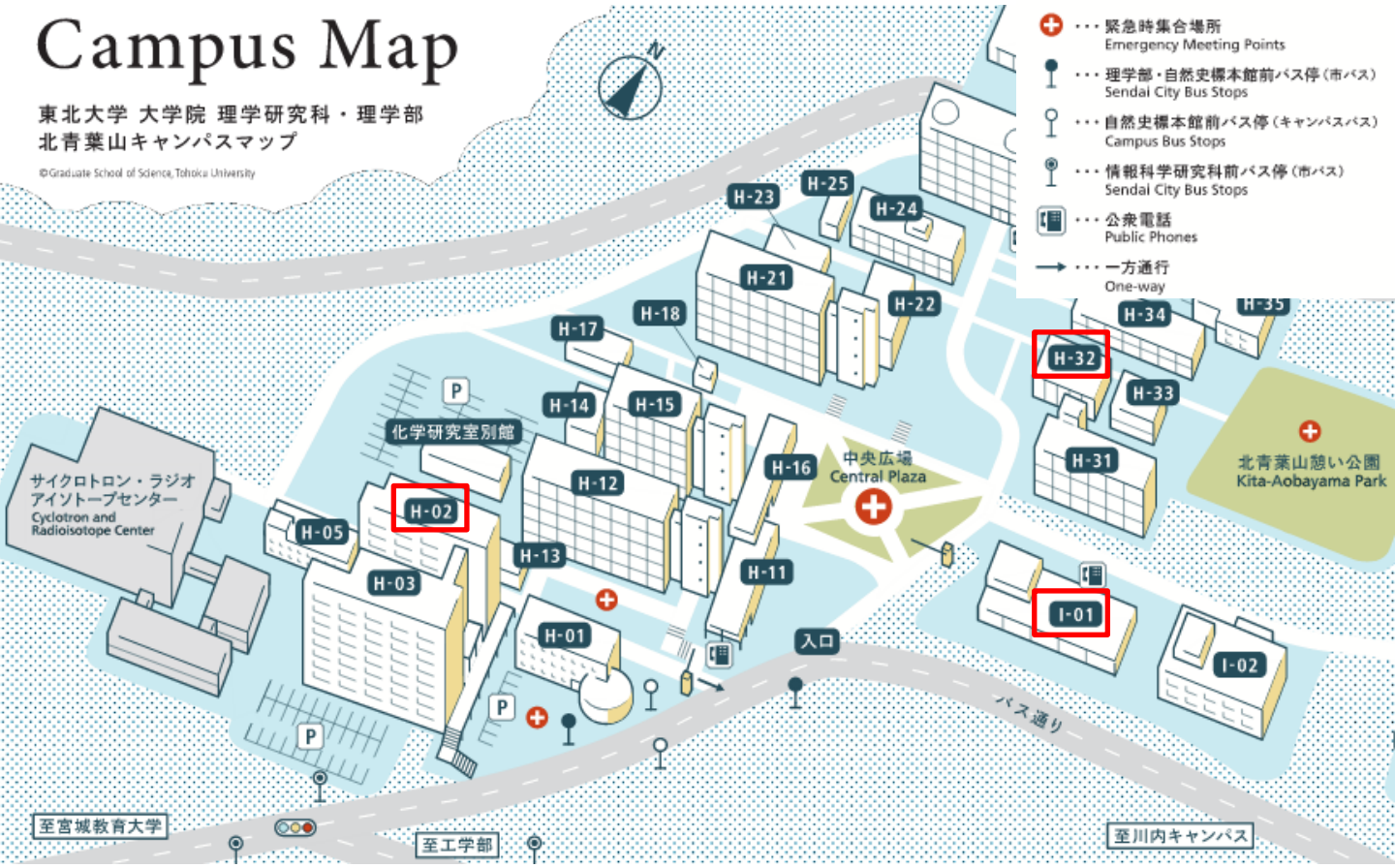

Oral Session : H-32 (Science Lecture Hall)
Poster Session : H-02 (Science Complex A 2F: entrance hall, 201-205)
Banquet : I-01 (Cafeteria)

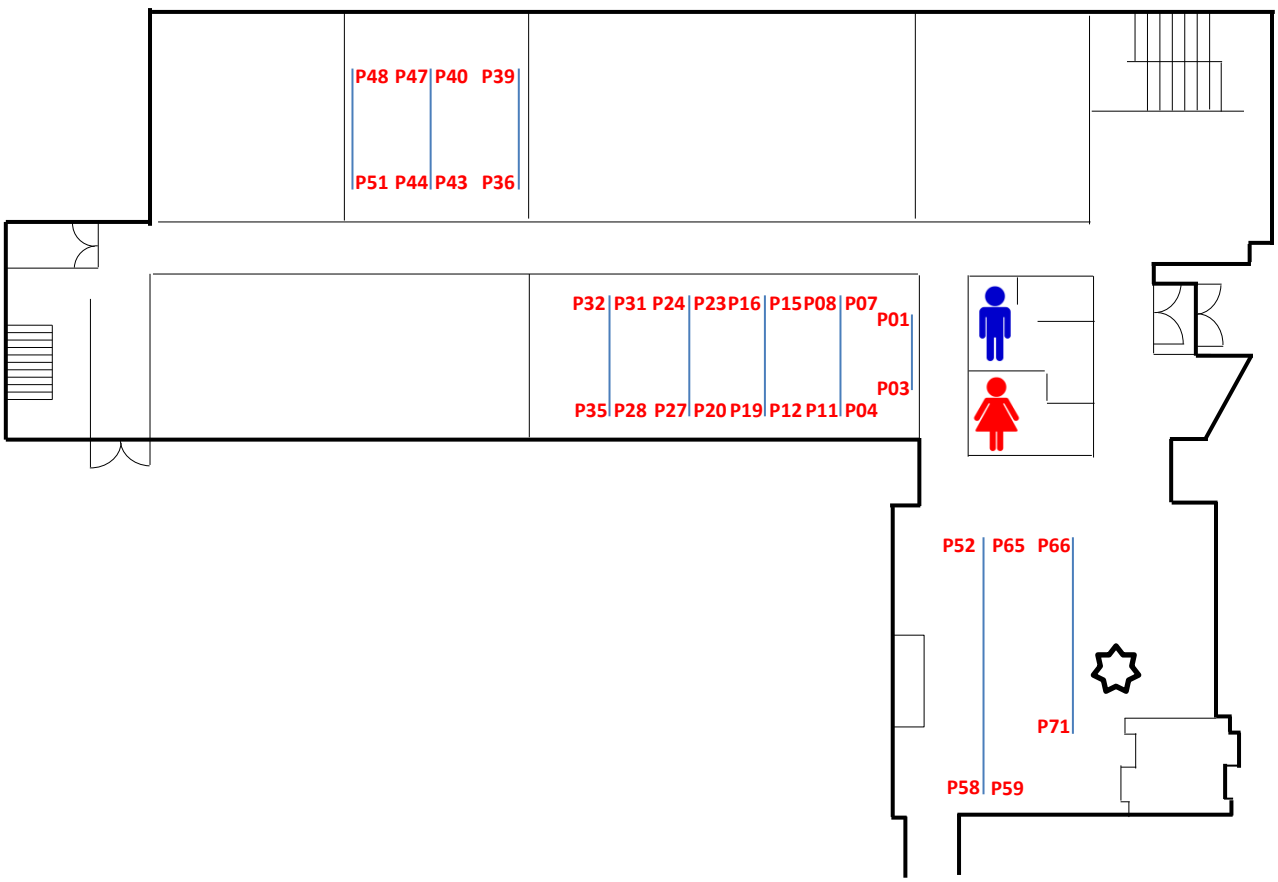

① Aoba Castle

② Osaki Hachimangu Shrine

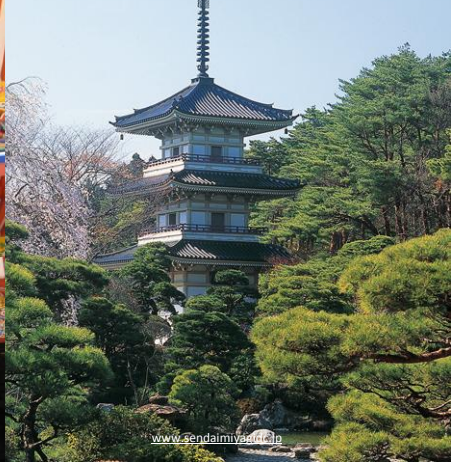

③ Rinnoji Temple

④ Zuiho-den

⑤ Sendai Mediatheque

⑥ Jyozenji St.